

https://dspace.org/

Crystallographic investigation of n-Aminopyridinium perhalometallates

Lawrence, Estee

2012-02-06
http://hdl.handle.net/10539/11247

Downloaded from a DSpace repository. https://dspace.org/

Crystallographic Investigation of *n*-Aminopyridinium Perhalometallates

Esteē Lawrence

A Dissertation Submitted to the Faculty of Science

University of the Witwatersrand, Johannesburg

For the Degree of Master of Science

October 2011

Abstract

This dissertation presents the results of a crystallographic investigation into nineteen novel *n*-aminopyridinium perhalometallates of the general formula $(C_5H_7N_2^+)_2MX_4^{2-}$ where n = 2, 3 or 4, M = Zn, Cd or Hg and X = Cl, Br or I. The aim was to identify positional effects of the cation hydrogen bonding donor groups on the structures and to possibly identify robust synthons. Overall structural trends were also studied. The hybrid crystals were synthesized using temperature controlled crystallization methods and were characterized using X- ray diffraction techniques. Eighteen of the nineteen hybrid crystals displayed isolated tetrahedral perhalometallate anions. The results were classified into six different classes of isostructural compounds. Eight of the nineteen hybrid structures (42%) contained water. The 42% include two 3-ammoniopyridinium structures and all cadmium and mercury containing 4-aminopyridinium structures. The effect of a change in metal and/ or halide on the structure was investigated, and the overall structural trends in each *n*-aminopyridinium family were identified. Four different synthons were observed in the 2-aminopyridinium series while one synthon was observed throughout the 4-aminopyridinium series. A common synthon was observed in both the 3-aminopyridinium and 3-ammoniopyridinium series.

Acknowledgments

Prof. Dave Billing and Dr. Melanie Rademeyer- words cannot express my gratitude and appreciation for post graduate supervisors whose support, understanding and encouragement went far beyond the call of duty not to mention all the proof-reading and deadlines!

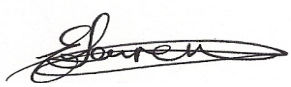
Dr. Manuel Fernandez, Robert Black and Dr. Andreas Lemmerer- thank you for all the time that you have spent teaching me how to operate the XRD, without your help I would never have managed to characterize the volume of crystal structures that appear in this dissertation.

My family especially my sister Delania who has always been my rock, you are one in a million sister!

My Jesus. I can do all things through Christ who strengthens me.

Declaration

I declare that this dissertation is my own, unaided work. It is being submitted for the Degree of Master of Science at the University of the Witwatersrand, Johannesburg. It has not been submitted before for any degree or examination at any other University.



Esteē Lawrence

7th day of October 2011

Table of Contents

Title Page		i
Abstract		ii
Acknowledgements		iii
Declaration		iv
Contents Page		v
List of Figures		x
List of Tables		xiv
Chapter 1: Introduction		**1**
1.1	Organic-Inorganic Hybrids In Nature	1
1.2	Applications of Organic-Inorganic Hybrids	2
1.3	What is Crystal Engineering?	2
1.4	Supermolecular Interactions	4
	1.4.1 Hydrogen bonding	5
	1.4.2 Aromatic Interactions	7
1.5	Current Study	8
	1.5.1 Protonation of *n*-aminopyridines	10
1.6	Literature Survey	13
	1.6.1 Case Study	13
	1.6.2 *n*-Aminopyridinium perhalometallate structures reported in the literature	19
Chapter 2: Experimental Methods		**31**
2.1	Starting materials	31
	2.1.1 Inorganic components selected for this study	31
	2.1.2 Organic Components Selected for this study	32
2.2	Synthetic Methodology	33
	2.2.1 Temperature Controlled Crystallization of Organic-Inorganic Hybrids	34
2.3	Instrumental Techniques	36

2.3.1 Theory of X-ray diffraction 36
2.3.2 Single crystal X-ray diffraction 37
2.3.3 SCXRD data collection 40
2.4 Structural Analysis Software 41

Chapter 3: Results 42
3.1 Bis(2-aminopyridinium) tetrachlorozincate(II) 45
3.2 Bis(2-aminopyridinium) tetrabromozincate(II) 47
3.3 Bis(2-aminopyridinium) tetrachloromercurate(II) 48
3.4 Bis(2-aminopyridinium) tetraiodozincate(II) 49
3.5 Bis(2-aminopyridinium) tetraiodocadmate(II) 51
3.6 Bis(2-aminopyridinium) tetraiodomercurate(II) 53
3.7 Bis(2-aminopyridinium) tetrabromomercurate(II) 54
3.8 Bis(3-aminopyridinium) tetrachlorozincate(II) 56
3.9 Bis(3-ammoniopyridinium) tetrabromozincate(II) monohydrate 58
3.10 Bis(3-ammoniopyridinium) tetraiodomercurate(II) monohydrate 60
3.11 Bis(4-aminopyridinium) tetrachlorozincate(II) 62
3.12 Bis(4-aminopyridinium) tetrabromozincate(II) 64
3.13 Bis(4-aminopyridinium) tetraiodozincate(II) 65
3.14 Catena-(bis(4-aminopyridinium) bis(μ_2-chloro) dichlorocadmium(II) monohydrate) 66
3.15 Bis(4-aminopyridinium) tetrabromocadmate(II) 68
3.16 Bis(4-aminopyridinium) tetraiodocadmate(II) monohydrate 70
3.17 Bis(4-aminopyridinium) tetrachloromercurate(II) monohydrate 71
3.18 Bis(4-aminopyridinium) tetrabromomercurate(II) monohydrate 72
3.19 Bis(4-aminopyridinium) tetraiodomercurate(II) monohydrate 73

Chapter 4: Discussion 78
4.1 Keeping the Cation Constant 78
4.1.1 2-Aminopyridinium Series 78
4.1.1.1 Trends in 2-aminopyridinium Series 78
4.1.1.2 Class 2A 78

4.1.1.3 Class 2B 81
4.1.1.4 Class 2C 81
4.1.1.5 Class 2D 81
4.1.1.6 Class 2E 81
4.1.1.7 2-Aminopyridinium Crystal Packing Trends 81
4.1.1.8 2-Aminopyridinium Cation Pair Packing 83
4.1.1.9 2-Aminopyridinium Synthons 86
4.1.2 3-Aminopyridinium and 3-Ammoniopyridinium Series 89
4.1.2.1 Trends in 3-Aminopyridinium and 3-Ammoniopyridinium Series 89
4.1.2.2 Class 3A 89
4.1.2.3 Class 3B 89
4.1.2.4 Class 3C 90
4.1.2.5 3-Aminopyridinium and 3-Ammoniopyridinium Crystal Packing Trends 90
4.1.2.6 3-Aminopyridinium and 3-Ammoniopyridinium Cation Pair Packing 91
4.1.2.7 3-Aminopyridinium and 3-Ammoniopyridinium Synthons 93
4.1.3 4-Aminopyridinium Series 94
4.1.3.1 Trends in 4-aminopyridinium Series 94
4.1.3.2 Class 4A 94
4.1.3.3 Class 4B 94
4.1.3.4 Class 4C 95
4.1.3.5 4-Aminopyridinium Crystal Packing Trends 95
4.1.3.6 4-Aminopyridinium Cation Pair Packing 96
4.1.3.7 4-Aminopyridinium Synthons 99
4.2 Comparison Across Cation Families 101
4.2.1 Cation Protonation 101
4.2.2 Water Incorporation 101
4.2.3 Anions and Cations 102
4.2.4 Crystal Packing Comparison 103

4.2.4.1 2-Aminopyridinium and 4-Aminopyridinium Families 103
4.2.4.2 Packing Trends Across Families 107
4.3 Effect of a Change in Metal Atom 108
4.3.1 2-Aminopyridinium Family 108
4.3.1.1 2-Aminopyridinium Chlorometallate Structures 108
4.3.1.2 2-Aminopyridinium Bromometallate Structures 109
4.3.1.3 2-Aminopyridinium Iodometallate Structures 110
4.3.2 3-Aminopyridinium and 3-Ammoniopyridinium Family 111
4.3.2.1 3-Aminopyridinium Chlorometallate Structures 111
4.3.2.2 3-Ammoniopyridinium Bromometallate Structures 111
4.3.3 4-Aminopyridinium Family 112
4.3.3.1 4-Aminopyridinium Chlorometallate Structures 112
4.3.3.2 4-Aminopyridinium Bromometallate Structures 113
4.3.3.3 4-Aminopyridinium Iodometallate Structures 114
4.4 Effect of a Change in Halogeno Ligand 115
4.4.1 2-Aminopyridinium Family 115
4.4.1.1 2-Aminopyridinium Perhalozincate Structures 115
4.4.1.2 2-Aminopyridinium Perhalomercurate Structures 116
4.4.1.3 2-Aminopyridinium Perhalocuprate Structures 116
4.4.2 3-Aminopyridinium and 3-Ammoniopyridinium Family 117
4.4.2.1 3-Aminopyridinium and 3-Ammoniopyridinium Perhalozincate Structures 117
4.4.2.2 3-Ammoniopyridinium Perhalomercurate Structures 117
4.4.3 4-Aminopyridinium Family 118
4.4.3.1 4-Aminopyridinium Perhalozincate Structures 118
4.4.3.2 4-Aminopyridinium Perhalocadmate Structures 118
4.4.3.3 4-Aminopyridinium Perhalomercurate Structures 119
4.4.3.4 4-Aminopyridinium Perhalocuprate Structures 119
4.5. Effect of Halogeno Ligands on Hydrogen Bonding Interactions 120
4.5.1 Hydrogen Bonding Interactions in Chloro Ligand containing Structures 120

4.5.2 Hydrogen Bonding Interactions in Bromo Ligand containing Structures 121

4.5.3 Hydrogen Bonding Interactions in Iodo Ligand containing Structures 121

4.5.4 Trends, When Keeping the Halogeno Ligand constant 122

Chapter 5: Conclusion and Recommendations for Future Work 124

5.1 Conclusion 124

5.2 Recommendations for Future Work 126

Chapter 6: References 127

Appendix A: Crystallographic Codes a132

Appendix B: Detailed Crystallographic and Structural Data compact disc

List of Figures

Figure 1:	Illustration of aromatic interactions, at which significant aromatic interactions can occur (Janiak, 2000).	7
Figure 2:	Examples of stacking of aromatic rings.	8
Figure 3:	Electron donating effect of $-NH_2$ in *n*-aminopyridines.	10
Figure 4:	Location of additional negative charge at the ortho and para positions of *n*-aminopyridines.	11
Figure 5:	Resonance structures of 4-aminopyridinium. Adapted from Bordwell *et al*, 1992	11
Figure 6:	Resonance structures of 2-aminopyridinium. Adapted from Bordwell *et al*, 1992	12
Figure 7:	A layer of the crystal structure [4,4'-H_2bipy][$PbCl_4$], [4,4'-H_2bipy] and [$ZnCl_4$],[4,4'-H_2bipy][$CdCl_4$].	15
Figure 8:	Ribbon packing in [4,4'-H_2bipy][$PtCl_4$], [1,2-bis-4-pyridinium-ethene][$PtCl_4$] and [4,4'-H_2bipiperidyl][$PtCl_4$]	17
Figure 9:	Crystal structures from the literature in the space group $P\bar{1}$.	20
Figure 10:	Crystal structures from the literature in the space group $C2/c$.	20
Figure 11:	Crystal structures from literature the in the space group $P21/c$.	21
Figure 12:	Crystal structure from the literature in the space group Cc.	22
Figure 13:	Crystal structure from the literature in the space group $P4_2/n$.	22
Figure 14:	Crystal structure from the literature in the space group P_2/n.	22
Figure 15:	Crystal structure from the literature in the space group $P2_1/n$.	23
Figure 16:	Crystal structure from the literature in the space group $Pbcm$.	23
Figure 17:	Crystal structure from the literature in the space group $P2_12_12_1$.	23
Figure 18:	Organic cations selected for this study.	32
Figure 19:	Apparatus for temperature controlled crystallization.	34
Figure 20:	Asymmetric unit and other structural characteristics of **2ampZnCl.**	46

Figure 21:	Asymmetric unit and other structural characteristics of **2ampZnBr.**	47
Figure 22:	Asymmetric unit and other structural characteristics of **2ampHgCl.**	48
Figure 23:	Asymmetric unit and other structural characteristics of **2ampZnI**.	50
Figure 24:	Asymmetric unit and other structural characteristics of **2ampCdI.**	52
Figure 25:	Asymmetric unit and other structural characteristics of **2ampHgI.**	53
Figure 26:	Asymmetric unit and other structural characteristics of **2ampHgBr**.	55
Figure 27:	Asymmetric unit and other structural characteristics of **3ampZnCl.**	57
Figure 28:	Asymmetric unit and other structural characteristics of **3ampZnBr·H_2O.**	59
Figure 29:	Asymmetric unit and other structural characteristics of **3ampHgI·H_2O.**	61
Figure 30:	Asymmetric unit and other structural characteristics of **4ampZnCl.**	63
Figure 31:	Asymmetric unit and other structural characteristics of **4ampZnBr.**	64
Figure 32:	Asymmetric unit and other structural characteristics of **4ampZnI.**	65
Figure 33:	Asymmetric unit and other structural characteristics of **4ampCdCl·H_2O.**	67
Figure 34:	Asymmetric unit and other structural characteristics of **4ampCdBr·H_2O.**	69
Figure 35:	Asymmetric unit and other structural characteristics of **4ampCdI·H_2O.**	70
Figure 36:	Asymmetric unit and other structural characteristics of **4ampHgCl·H_2O.**	71

Figure 37:	Asymmetric unit and other structural characteristics of **4ampHgBr·H_2O.**	72
Figure 38:	Asymmetric unit and other structural characteristics of **4ampHgI·H_2O.**	73
Figure 39:	Structure of **2ampZnCl** and **2ampyZnBr.**	79
Figure 40:	Packing trends in the 2-aminopyridinium family.	82
Figure 41:	Cation pair orientation in the 2-aminopyridinium family**.**	84-85
Figure 42:	Identified synthons in the 2-aminopyridinium family.	87-88
Figure 43:	Layered structures observed for the 3-aminopyridinium and 3-ammoniopyridinium family.	90
Figure 44:	Cation pair orientation in the 3-aminopyridinium and 3-ammoniopyridinium family.	92
Figure 45:	Identified synthons in the 3-aminopyridinium and 3-ammoniopyridinium family.	93
Figure 46:	Layered structures observed for the 4-aminopyridinium family.	95
Figure 47:	Cation pair orientation in the 4-aminopyridinium family.	97-98
Figure 48:	Identified synthons in the 4-aminopyridinium family.	99-100
Figure 49:	Polymeric anion observed for **4ampCdCl·H_2O**.	102
Figure 50:	Crystal structure of **2ampZnCl, 2ampCoCl** (Jebas *et al*, 2006; DELPOA) and **4ampCuCl·H_2O** (Halvorson *et al*, 1990; SEZLEO).	103
Figure 51:	Unit cell parameters of isostructural compounds in the 2-aminopyridinium and 4-aminopyridinium family.	104
Figure 52:	Anions packing in channel formed by 2-aminopyridinium cations in the structure **2ampZnBr**.	104
Figure 53:	Packing trends across families of *n*-aminopyridinium perhalometallates.	107
Figure 54:	Packing in 2-aminopyridinium chlorometallate structures.	108
Figure 55:	Packing in 2-aminopyridinium bromometallate structures.	109
Figure 56:	Packing in 2-aminopyridinium iodometallate structures.	110
Figure 57:	Packing in 3-aminopyridinium chlorometallate structures.	111
Figure 58:	Packing in 3-ammoniopyridinium bromometallate structures.	111

Figure 59:	Packing in 4-aminopyridinium chlorometallate structures.	112
Figure 60:	Packing in 4-aminopyridinium bromometallate structures.	113
Figure 61:	Packing in 4-aminopyridinium iodometallate structures.	114
Figure 62:	Packing in 2-aminopyridinium perhalozincate structures.	115
Figure 63:	Packing in 2-aminopyridinium perhalmercurate structures.	116
Figure 64:	Packing in 2-aminopyridinium perhalocuprate structures.	116
Figure 65:	Packing in 3-aminopyridinium and 3-ammoniopyridinium perhalozincate structures.	117
Figure 66:	Packing in 3-ammoniopyridinium perhalomercurate structures.	117
Figure 67:	Packing in 4-aminopyridinium perhalozincate structures.	118
Figure 68:	Packing in 4-aminopyridinium perhalocadmate structures.	118
Figure 69:	Packing in 4-aminopyridinium perhalomercurate structures.	119
Figure 70:	Packing in 4-aminopyridinium perhalocuprate structures.	119
Scheme 1:	Comparison between covalent and supermolecular synthesis (Aakeröy *et al*, 2001).	3
Scheme 2:	Illustration of hydrogen bonds using donor and acceptor notation.	5
Scheme 3:	Flowchart of Crystal structure determination (Clegg, 2005).	39

List of Tables

Table 1:	pK_a values for n-aminopyridines. Adapted from Gaballero, 2006.	12
Table 2:	Case study where the changing variable is the metal.	14
Table 3:	Case study where the inorganic part is kept constant and the organic cation varied.	16
Table 4:	Main Structural Characteristics of *n*-aminopyridinium perhalometallates reported in literature.	24-26
Table 5:	Structural and Experimental Parameters for *n*-aminopyridinium perhalometallates in the literature.	27
Table 6:	Selected Cg-Cg and Non-Covalent Intermolecular Distances of the type d(H···A) for 2-aminopyridinium hybrids reported in the literature.	28
Table 7:	Selected Cg-Cg and Non-Covalent Intermolecular Distances of the type d(H···A) for 3-aminopyridinium hybrids reported in the literature.	29
Table 8:	Selected Cg-Cg and Non-Covalent Intermolecular Distances of the type d(H···A) for 4-aminopyridinium hybrid reported in the literature.	30
Table 9:	Masses of amines and metal halides used in temperature controlled experiments.	35
Table 10:	Summary of results.	42
Table 11:	Structural and Experimental Parameters determined for characterized hybrids.	44
Table 12:	Selected Cg-Cg and Non-Covalent Intermolecular Distances of the type d(H···A) for 2-aminopyridinium hybrids.	74
Table 13:	Selected Cg-Cg and Non-Covalent Intermolecular Distances of the type d(H···A) for 3-aminopyridinium and 3-ammoniopyridinium hybrids.	75
Table 14:	Selected Cg-Cg and Non-Covalent Intermolecular Distances of the type d(H···A) for anhydrous 4-aminopyridinium hybrids.	76

Table 15:	Selected Cg-Cg and Non-Covalent Intermolecular Distances of the type d(H···A) for hydrated 4-aminopyridinium hybrids.	77
Table 16:	Unit cell parameters of selected 2-aminopyridinium containing structures.	80
Table 17:	Unit cell parameters of selected 2-aminopyridinium and 4-aminopyridinium containing structures.	106
Table 18:	Ionic Radii of selected halogens (Brown, 2003).	120
Table 19:	Summary of effect of halogeno ligands on hydrogen bonding interactions.	123

1. Introduction

The current crystallographic project focuses on the structural investigation of organic-inorganic hybrid materials and the identification of packing trends and motifs using the concept of crystal engineering. Crystal engineering aims to control the structure and properties of crystalline solids. The concept of crystal engineering is relevant to the current project because it allows structural design and control of organic-inorganic hybrids that combine the physical properties of both organic and inorganic components. The inorganic components offer a wide range of electronic properties, mechanical hardness and thermal stability, while the organic moieties have plastic mechanical properties, structural diversity and can provide high fluorescence efficiency (Mitzi *et al*, 2001). However, the choice of each component affects the crystal structure of the hybrid and thus alters the physical properties of the material. As a matter of fact, the same occurs in nature. For example shells, mammalian teeth and bone are all examples of organic-inorganic hybrids.

1.1 Organic-Inorganic Hybrids In Nature

Shells contain $CaCO_3$ and organic matter that is high in protein. However the packing of the $CaCO_3$ and the organic matter differ in the mollusk shell and seashell, which in turn result in distinct properties for each. In the mollusk shell, the layered packing increases fracture resistance and in seashells the organic matter encircles the $CaCO_3$ thus controlling elasticity (Mitzi *et al*, 1999).

Other examples of organic-inorganic composites are mammalian teeth and bone. Both contain calcium phosphate and protein. However teeth contain much more calcium phosphate than bone (Mitzi *et al*, 1999). That is why bone can bend to a certain extent before it breaks but teeth on the other hand can chip quite easily.

1.2 Applications of Organic-Inorganic Hybrids

Over the last decade numerous applications of organic-inorganic hybrids have been discovered and are now being used commercially. Bio-active sol-gel derived hybrid materials have applications in biotechnology and are used as biosensors (Sanchez *et al*, 2005). Hybrid materials are also being used in paint and function as protective coatings and corrosion resistant primers and offer scratch resistant surfaces (Sanchez *et al*, 2005). Hybrid materials also have dental applications in that they are used as fillings that are non-toxic and have a feature that prevents them from shrinking (Sanchez *et al*, 2005). These materials also show interesting electronic and luminescent properties and applications like LEDs and semi-conductors have been proposed (Mitzi *et al*, 2001).

1.3 What is Crystal Engineering?

Thus leading us back to the concept of crystal engineering, in which we are interested in the factors that control the crystal structures of these hybrids. Crystal engineering has been defined by Desiraju as "the understanding of intermolecular interactions in the context of crystal packing, and in applying that knowledge and understanding to design new solids, with desired physical and chemical properties" (Desiraju, 1997).

Crystals are supermolecules, and their structural features are best described in terms of supermolecular descriptors that is, patterns of interactions as opposed to molecular descriptors like functional groups (Desiraju, 1997). A supermolecule as defined by Turro is "an assembly of molecules that is held together by relatively weak intramolecular bonds" (Turro, 2005). The terminology supermolecule and supramolecule are used interchangeably but for consistency supermolecule will be used throughout this investigation. In covalent synthesis one focuses on C-C bond formation, to produce single molecules, where the quantitative yield is a measure of success (Aakeröy *et al*, 2001). In supermolecular synthesis one focuses on intermolecular interactions (between molecules), where reliability of motifs is a measure of success (Aakeröy *et al*, 2001). Both supermolecular and covalent synthesis require in-depth analysis of the structure and properties of the final product (Aakeröy *et al*, 2001). Nevertheless, covalent and supermolecular (non-covalent) synthesis can be seen as

having considerable overlap in terms of both methods and focus (Aakeröy *et al*, 2001). See **Scheme 1** below.

Supermolecular Synthesis	**Covalent Synthesis**
↓	↓
Assemblies of Molecules	**Single Molecules**
↓	↓
Reliability of Motifs	**Quantitative Yields**
↓	↓
Structure and Properties	**Structure and Properties**

Scheme 1: Comparison between covalent and supermolecular synthesis (Aakeröy *et al*, 2001).

After solving the crystal structure of an Organic-Inorganic hybrid, a pattern of alternating charged inorganic and organic parts linked by non-covalent interactions can be identified, and this pattern is known as a "motif". From the motif, a single repeat unit can be identified and the repeat unit is known as a "synthon". Supermolecular synthons were defined by Desiraju as "structural units within supermolecules which can be formed and/or assembled by known or conceivable synthetic operations involving intermolecular interactions" (Desiraju, 1995). Desiraju also distinguished between the concepts of "intermolecular interaction" and "synthon", stating that an intermolecular interaction is based on recognition between parts, for example functional groups, but a synthon encompasses both recognition between parts as well as taking the geometry of the interaction into account (Desiraju, 1995). In some cases the synthon consists of a number of intermolecular interactions between functional groups, but often no distinction can be made between an intermolecular interaction and a synthon. Synthons may be categorized as either homosynthons or heterosynthons. Homosynthons have the same donor and acceptor groups, for example the carboxylic acid dimer, while heterosynthons are formed between different donor and acceptor groups.

It was stated by Desiraju that: "The major challenge in crystal engineering is that a one-to-one correspondence does not exist between functional groups and patterns of interactions and so questions relating to the prediction of supermolecular (crystal)

structure from molecular structure (i) are difficult to answer, (ii) may have multiple answers, and (iii) may not even be the most relevant questions one might ask." (Desiraju, 1997). Generally two factors have to be taken into account when considering the packing of units in a crystal structure, namely the shape of the molecule/ion (close packing) as well as the non-covalent interactions (hydrogen bonding, aromatic interactions etc.) present in the structure. According to the concept of close packing, which was described in detail by Kitaigorodskii (Pidcock and Motherwell, 2004) the units in a crystal aim to pack as efficiently as possible, with as little unoccupied space as possible. Due to this requirement, it is found that a relatively small number of space groups are often encountered.

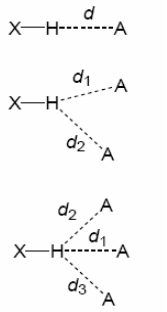
It is important to keep in mind that the crystal structure obtained in the end, is the result of a delicate balance between all the intermolecular forces and the shape effect. The field of crystal engineering has passed its infancy, but there is not yet enough information to be certain of all parameters that may possibly control supermolecular crystal formation.

1.4 Supermolecular Interactions

Supermolecular interactions act between molecules, hence intermolecular or any non-covalent bonding. Hydrogen bonding, for example is one of the most common attractive intermolecular interactions, if not the most important of the supermolecular interactions. Other examples of supermolecular interactions include van der Waals forces, π-π stacking and ionic interactions. A result of supermolecular interactions is that each component, whether a molecule or molecular ion, retains its physical and chemical **identity** once evaporated or dissolved (Braga and Grepioni, 2005). This is not characteristic of covalent bond formation in which certain bonds are broken in order for new bonds to form, thus changing the chemical identity of a component. An interesting aspect of supermolecular crystals is that different compounds may have the same or similar supermolecular structure (Desiraju, 1997). When two crystals have the same structure, but not necessarily the same cell dimensions or composition then they are said to be isostructural to each other (Online Dictionary of Crystallography).

1.4.1 Hydrogen bonding

A hydrogen bonding interaction typically consists of a donor atom D to which a hydrogen atom is covalently bonded, as well as an acceptor atom A, with the hydrogen atom acting as a bridge between atoms A and D. A number of definitions of a hydrogen bond have been put forward, with Steiner defining a hydrogen bond as follows: "A D-H···A interaction is called a "hydrogen bond", if firstly it constitutes a local bond and second, X-H acts as proton donor to A" (Steiner, 2002). More than one accepter atom may be present, resulting in bifurcated (two acceptor atoms) or trifurcated (three acceptor atoms) hydrogen bonds, as illustrated in **Scheme 2** below. The hydrogen bonding interaction is directional and its nature is mainly electrostatic.



Scheme 2: Illustration of hydrogen bonds using donor and acceptor notation. **Top**: typical hydrogen bond. **Centre**: bifurcated hydrogen bond. **Bottom**: trifurcated hydrogen bond.

Hydrogen bond strength can vary depending on the nature of atoms D and A, and it can be viewed as an interaction without clearly defined borders, as suggested by Desiraju (Desiraju, 2002). Hydrogen bonds can be classified as weak, strong or very strong, with energies ranging from 0.25 to 40 kcal mol^{-1} (Desiraju, 2002). Weaker hydrogen bonds may have more van der Waals character (in addition to its electrostatic nature) while very strong hydrogen bonds have more covalent character combined with electrostatic character (Desiraju, 2002). In a strong, classical interaction D–H···A, the DHA angle, θ, is typically close to linear and the distance between atoms D and A are smaller than the van der Waals radii (Desiraju, 2002).

Due to its strength and directionality the hydrogen bond plays an important role in the

supermolecular organization of molecules or ions in a crystal, and the stronger the hydrogen bond, the more effective it is in affecting the structural outcome of the crystal. A rule of thumb when it comes to hydrogen bonding is that when there is a multitude of hydrogen-bonding functionalities, the best hydrogen-bond donor and the best hydrogen-bond acceptor will preferentially form hydrogen bonds (Aakeröy *et al*, 2001). It follows that the second best hydrogen-donor will preferentially form hydrogen bonds with the second best hydrogen-acceptor and so on. Also important to note is that a small number of specific molecular interactions can substantially stabilize molecular crystals (Aakeröy *et al*, 2001). On the other hand electrostatic interactions may outweigh hydrogen bonding, that is if it results in a more stable crystal structure.

Charge assisted hydrogen bond interactions are formed when the donor or acceptor atom (or both) in a hydrogen bond carry a charge. There may also be a conjugation of positive and negative charge that is energetically favourable (Janiak, 2000). This type of hydrogen bond is typically stronger than the neutral equivalent due to an enhancement of the electrostatic component of the interaction. The majority of hydrogen bonds observed in the current study fall in this category. In the perhalometallate anion of the compounds investigated here, the metal atom (M) is covalently bonded to a halogen atom (X) resulting in a partially positive metal and a partially negative halogen, $X^{\delta-}M^{\delta+}$. It has been reported that halide ligands bonded to metal atoms are good hydrogen bond acceptors (Alluo'n *et al, 1998*). In the perhalometallate anion the negative charge on the anion enhances the partial negative charge on the halide ligands. The partially negative halogen is then readily available to act as a hydrogen bond acceptor. In this study the high electronegativity of the nitrogen donor as well as the positive charge on the cation enhances the partial positive charge on the hydrogen atom. Thus the overall interaction will be cation-N^{+}-H$\cdots X^{-}$-M-anion.

Water molecules also play an important role in supermolecular interactions because of its small size and high polarity and the fact that it can form strong hydrogen bonds to other polar molecules (Ostojić *et al*, 2008). So if water is present in a hybrid crystal structure, it would be expected to participate in hydrogen bonding.

1.4.2 Aromatic Interactions

Aromatic interactions may occur whenever there are π-bonds in a system. These interactions can be considered as electrostatic, with repulsion occurring between π-electrons of two aromatic rings and attraction between the π-electrons of one ring and the σ-framework of another ring (Janiak, 2000). Two common orientations are observed, namely an edge-to-face interaction (also called T-shaped) or a face-to-face stacking interaction as illustrated in **Scheme 2** on page 5 (Janiak, 2000). When face-to-face stacking is present, it may be eclipsed where the aromatic parts overlap perpendicularly or offset where the aromatic parts are slipped relative to one another. See **Figure 1** below. Aromatic interactions are relevant to the current study since the cation component contains an aromatic ring with a pyridine nitrogen atom as well as an amine (or ammonium) substituent. Heteroatoms included in or substituents on the aromatic system affects the π-π interactions, in that an electron donating substituent will increase the π-electron density of the ring, thereby increasing π-π repulsion and weakening the interaction (Janiak, 2000). The opposite occurs for an electron withdrawing substituent (Janiak, 2000).

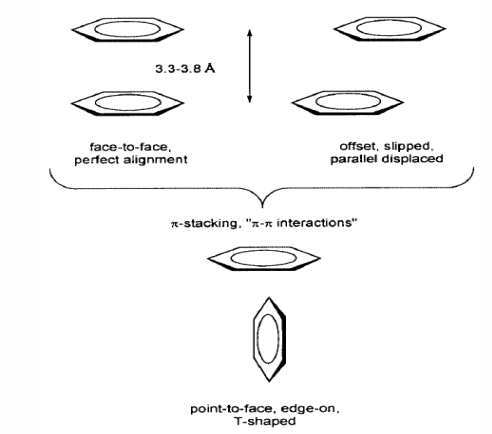


Figure 1: Illustration of aromatic interactions, depicting the centroid-to-centroid distance (3.3-3.8Å) at which significant aromatic interactions can occur (Janiak, 2000).

The Cg-Cg distance is the distance from the centroid (centre) of one π-stacking ring to the centroid of the second π-stacking ring. The distance that the centroids of slipped rings differ from that of perfect alignment is known as the slippage distance.

It has been reported that nitrogen hetero atoms in aromatic rings favour slipped stacking of rings in the overall crystal structure due to the reduction of the π-electron density reducing the repulsion between stacked rings (Janiak, 2000). In the *n*-aminopyridinium cation both the pyridine nitrogen atom as well as the amine substituent decrease the π-electron density of the ring, favouring the stacking of rings. When hetero atoms are present stacking may occur in a head to tail fashion or a rotated arrangement to maximize the electrostatic dipole interactions. See **Figure 2** below.

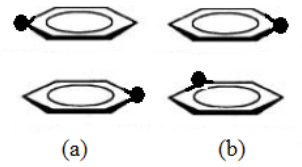


Figure 2: (a.) Head to tail stacking. **(b.)** Rotated stacking (Janiak, 2000).

1.5 Current Study

At present we do not have the ability to predict a crystal structure or any structural characteristics if the only starting information available are the chemical components in the structure. One way of gaining some information on the structural behaviour of a specific type of compound is to systematically introduce small changes to one of the moieties comprising the compound, and notice the effect of the change on the overall structure.

This approach is followed in the current study which focuses on novel organic-inorganic hybrid compounds. The *n*-aminopyridinium moiety, where *n* ranges from 2 to 4, were selected as organic parts of the hybrid in this study. These cations were selected due to their similarity to other cations in structures reported in the literature, for example the 4,4'-bipyridinium cation. The reasons for choosing the *n*-aminopyridinium series specifically relate to the design aspects of the cation part of the hybrid. The neutral starting materials *n*-aminopyridine may be protonated at either the pyridine nitrogen or the amine nitrogen, the pK_a values of the different nitrogen atoms are listed in **Table 1** on page 12 in section **1.5.1** below. From these pK_a values it is expected that

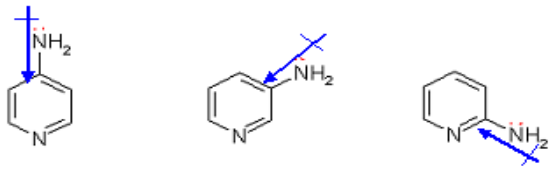
the pyridine nitrogen will be protonated first, and that the amine nitrogen will be protonated only where an excess of acid is available. Two functional groups occur on this cation – a pyridinium functional group, as well as an amine group (or ammonium when the amine group is protonated), meaning that this cation can be considered to be a hybrid between pyridinium and aniline (or anilinium when the amine group is protonated). This provides additional complexity to the structures when compared to a structure containing only anilinium or only pyridinium cations. It is suspected that the dimensionality of the structure may change when the orientation of the functional groups relative to one another is varied along the *n*-aminopyridinium series, due to the hydrogen bonding donor capability of the cation changing from one side of the cation in 2-aminopyridinium to opposite sides of the cation in 4-aminopyridinium. Other reasons for the cation selection include the fact that all the cations are rigid and have a flat geometry thereby excluding complicating factors like conformational flexibility, and the presence of the aromatic ring part which may result in the formation of aromatic interactions.

The perhalometallate anion was selected as the inorganic part of the hybrid in this study. These anions have been reported to be good hydrogen bonding acceptors (Brammer *et al*, 2002) due to their ability to form charge assisted hydrogen bonds. Perhalometallate anions with d^{10} metals Zn, Cd and Hg, and the halide ligands Cl, Br and I were selected. In theory, the perhalometallate anions may adopt different geometries, and may be isolated, or the halide ligands may bridge different metals, resulting in the formation of inorganic polymers.

Different permutations of *n*-aminopyridinium cations and perhalometallate anions result in composite structures in which the organic and the inorganic components are associated at the nano scale level. The current study aims to investigate the positional effects of cation hydrogen bonding donor groups on the structures, to possibly identify robust synthons. In addition the identification of overall structural trends in the matrix of compounds will be attempted. These results will provide a better understanding of the structural characteristics of the compounds under investigation, and provide information helpful in the design of other related novel hybrid compounds.

1.5.1 Protonation of *n*-aminopyridines

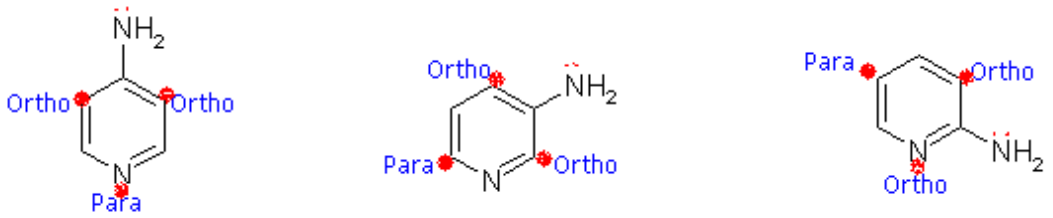
n-Aminopyridines are Lewis bases with two potential protonation sites (Smith, 2006). The deciding factor as to which site gets protonated (or whether both sites get protonated) depends on inductive and resonance effects. The amine substituent adds electron density into the ring because it has a lone pair of electrons, so it adds electron density into the ring via the resonance effect (Smith, 2006). However the amine group also has an electron withdrawing inductive effect because nitrogen is more electronegative than carbon, therefore it pulls electron density towards itself and away from the ring (Smith, 2006). If the inductive and resonance effects work against each other, then the effect of resonance (delocalised electrons) typically wins over the inductive effect. The net effect is therefore electron donation into the ring via resonance which is stabilization by the delocalisation of electrons. See **Figure 3** below.



(a.) **(b.)** **(c.)**

Figure 3: Illustration of the electron donating effect of $-NH_2$ in **(a.)** 4-aminopyridine, **(b.)** 3-aminopyridine and **(c.)** 2-aminopyridine.

The amine group activates the ortho and para positions on the ring, making it electronegative by introducing electron density (Smith, 2006). Therefore 2-aminopyridine has additional negative charge at the ortho position (where the pyridine nitrogen is present) and 4-aminopyridine has additional negative charge at the para position (where the pyridine nitrogen is present). So the pyridine nitrogen atoms of the 2-aminopyridine and 4-aminopyridine prefer to be protonated, making them good bases (Fossey *et al*, 1980). Therefore in most cases, it would be expected that the pyridine N on both 2-aminopyridine and 4-aminopyridine will be protonated. This leaves 3-aminopyridine having no additional negative charge on the pyridine N, making it the weakest base. See **Figure 4** on page 11.



(a.) **(b.)** **(c.)**

Figure 4: Additional negative charge at the ortho and para positions of **(a.)** 4-aminopyridine, **(b.)** 3-aminopyridine and **(c.)** 2-aminopyridine, indicated by red dots.

With 4-aminopyridine the delocalisation of electrons occurs over a larger part of the molecule (on average) (see **Figure 5** below) as compared to the delocalisation of electrons in the 2-aminopyridine molecule (see **Figure 6** on page 12) (Bordwell *et al*, 1992). Therefore the conjugate acid of 4-aminopyridine which is 4-aminopyridinium is more stable than the conjugate acid of 2-aminopyridine (2-aminopyridinium). This is important because when a stable conjugate acid is formed, the base prefers to be protonated to form the very stable conjugate acid. This means that 4-aminopyridine is a stronger base than 2-aminopyridine (Fossey *et al*, 1980).

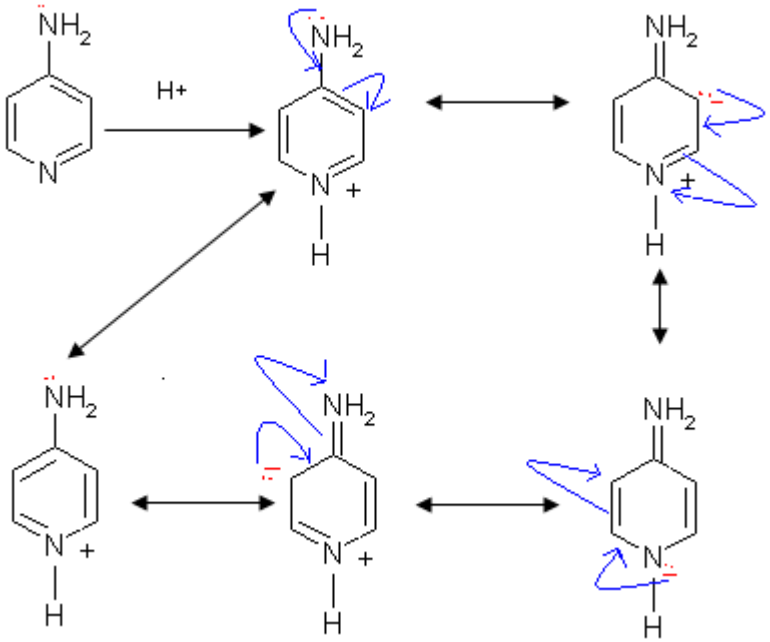


Figure 5: Resonance structures of 4-aminopyridinium. Adapted from Bordwell *et al*, 1992.

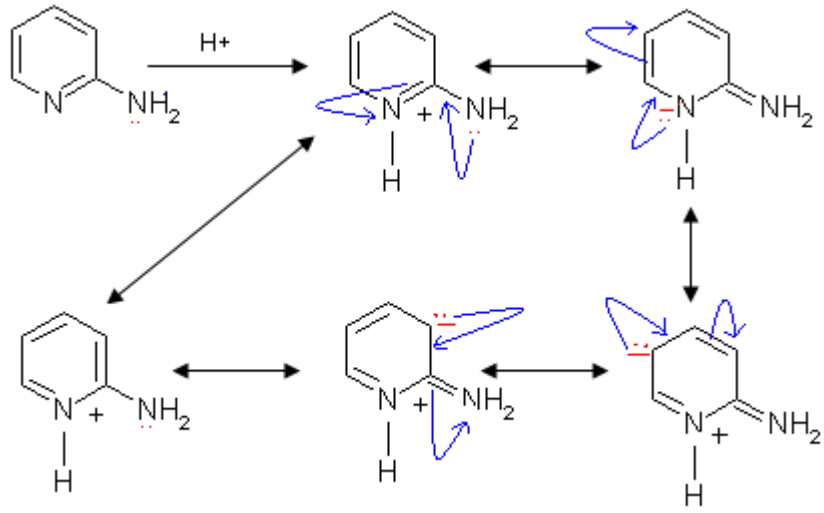


Figure 6: Resonance structures of 2-aminopyridinium. Adapted from Bordwell *et al*, 1992.

The protonated forms (2-aminopyridinium cation and 4-aminopyridinium cation) have successfully delocalised the lone pair of electrons from the amine nitrogen into the ring (and have several resonance structures) so that they are no longer available (Bordwell *et al*, 1992). This makes the amine in 2-aminopyridinium and 4-aminopyridinium weak bases that are difficult to protonate hence they are typically not protonated further at the amine nitrogen atom (Fossey *et al*, 1980). See **Table 1** below for protonation constants.

In 3-aminopyridinium the delocalisation of electrons is poor, so the lone pair of electrons on the amine is more available to act as a base (Bordwell *et al*, 1992). As a result it is possible for the amine nitrogen to be protonated together with the pyridine nitrogen. See **Table 1** below for protonation constants.

Table 1: pK_a values for *n*-aminopyridines. pK_a1 refers to the first protonation constant and pK_a2 refers to the second protonation constant. Adapted from Caballero, 2006.

n-aminopyridine	**pK_a1**	**pK_a2**
2-aminopyridine	6.86	-7.65
3-aminopyridine	5.98	-1.36
4-aminopyridine	9.17	-6.60

1.6 Literature Survey

In the literature a number of structures containing arylammonium cations and perhalometallate anions have been reported. The focus will, however, only be on those that are of direct relevance to the current investigation so only structures with divalent metal atoms and tetrahedral anions will be considered, even though more structures are listed in the literature.

1.6.1 Case Study

Orpen's group has performed number of intensive investigations focusing on the 4,4' bipyridinium cation (and similar cations) with different perhalometallate anions (Adams and Orpen *et al*, 2006; Gillon and Orpen *et al,* 1999; Gillon and Orpen *et al*, 2000; Lewis and Orpen, 1998). (Note 4,4'-H_2bipy = 4,4' bipyridinium). These studies are relevant to the current investigation since the authors did not only report the crystal structures, but also analyzed them in terms of crystal engineering principles. What follows is a summary of the results obtained from relevant case studies.

In general a hybrid consists of three different components or variables. These are the organic cation, the metal and the halogen, with the last two forming the perhalometallate anion. In the studies of the 4,4'-bipyridinium (H_2bipy) perhalometallate hybrids, reported in the literature, two parameters were varied systematically, namely the metal and halogen, while the cation (H_2bipy) was kept constant (Gillon and Orpen *et al*, 1999; Gillon & Orpen *et al*, 2000; Lewis and Orpen, 1998). Other investigations focused on the effects of introducing a different, related cation into the hybrid structure while keeping the metal and halogen constant (Adams and Orpen *et al*, 2006; Gillon and Orpen *et al*, 2000; Lewis and Orpen *et al,* 1998).

The crystal structures of:

A. [4,4'-H_2bipy][**Pt**Cl_4] (Gillon and Orpen *et al*, 2000; Lewis and Orpen, 1998) (Reference compound).

B. [4,4'-H_2bipy][**Pb**Cl_4] (Gillon and Orpen *et al*, 2000)

C. [4,4'-H_2bipy][**Zn**Cl_4] (Gillon and Orpen *et al*, 1999; Gillon and Orpen *et al*, 2000)

D. [4,4'-H_2bipy][**Cd**Cl_4] (Gillon and Orpen *et al*, 1999; Gillon and Orpen *et al*, 2000)

E. [4,4'-H_2bipy][**Hg**Cl_4] (Gillon and Orpen *et al*, 2000)

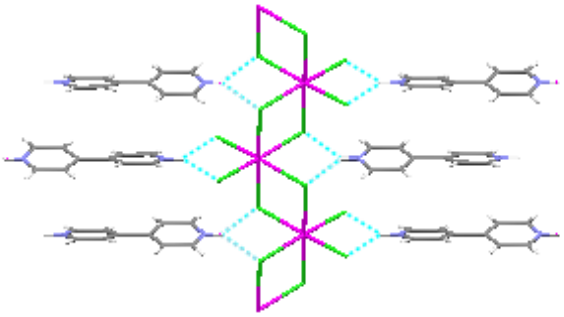
F. [4,4'-H_2bipy][**Co**Cl_4] (Gillon and Orpen *et al*, 2000)

G. [4,4'-H_2bipy][**Mn**Cl_4] (Gillon and Orpen *et al*, 1999; Gillon and Orpen *et al*, 2000)

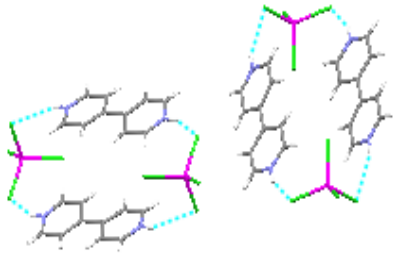
have been determined and it was found that the use of different metals, while keeping the halide (Cl atom) and cation constant (4,4'-H_2bipy), resulted in very different crystal structures, due to the change in geometry of the perhalometallate anion (see **Table 2** below and **Figure 7** on page 15). However, all seven crystal structures displayed NH···Cl charge assisted hydrogen-bonds, in which the nitrogen atom acted as the hydrogen bond donor, and the halogen ligand acted as the hydrogen bond acceptor (Gillon and Orpen *et al*, 2000).

Table 2: Summary of structural observations for case study where the changing variable is the metal. The organic cation and the halogen are constant.

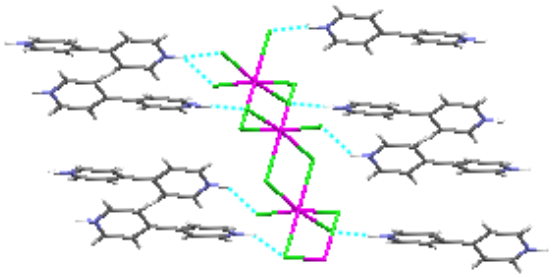
Hybrid	Perhalometallate Anion Geometry	Shortest NH···$Cl_{terminal}$ distance (Å)	Isostructural Hybrids
A	Isolated $PtCl_4^{2-}$, square planar	2.40	None
B	$\{[PbCl_4]^{2-}\}_n$ chains, octahedral $PbCl_6$ units linked by cis edge-sharing into chains	2.56	None (similar to **D**, differ in H-bonding)
C	Isolated $ZnCl_4^{2-}$, tetrahedral	2.30	**E** and **F**
D	$\{[CdCl_4]^{2-}\}_n$ chains, octahedral $CdCl_6$ units linked by cis edge-sharing into chains	2.54	**G**
E	Isolated $HgCl_4^{2-}$, tetrahedral	2.28	**C** and **F**



(a.)



(b.)



(c.)

Figure 7: (a.) A layer of the crystal structure **B** showing $\{[PbCl_4]^{2-}\}_n$ chains cross-linked by hydrogen bonding to $[4,4'\text{-}H_2\text{-bipy}]^{2+}$ (Gillon and Orpen *et al*, 2000). **(b.)** Crystal structure of **C** showing crystallographically independent tetrahedral $ZnCl_4^{2-}$ anions. Isostructural to **E** (Gillon and Orpen *et al*, 1999; Gillon and Orpen *et al*, 2000). **(c.)** Crystal structure of **D** showing $\{[CdCl_4]^{2-}\}_n$ chains cross-linked by hydrogen bonding to $[4,4'\text{-}H_2\text{-bipy}]^{2+}$. Isostructural to **G** (Gillon and Orpen *et al*, 2000; Gillon and Orpen *et al*, 1999).

In addition to varying the metal parameter, studies (Gillon and Orpen *et al*, 2000; Adams and Orpen *et al*, 2006) also focused on the effect that subtle changes to the cation, may have on the crystal structure obtained. The following crystal structures were investigated, while keeping the metal and halide parts ($PtCl_4^{2-}$) constant.

A. [4,4'-H_2bipy][$PtCl_4$] (Gillon and Orpen *et al*, 2000; Lewis and Orpen, 1998) (Reference compound as above).

H. [1,2-bis-4-pyridinium-ethene][$PtCl_4$] (Adams and Orpen *et al*, 2006) (ethene bridge between aromatic moieties therefore longer cation).

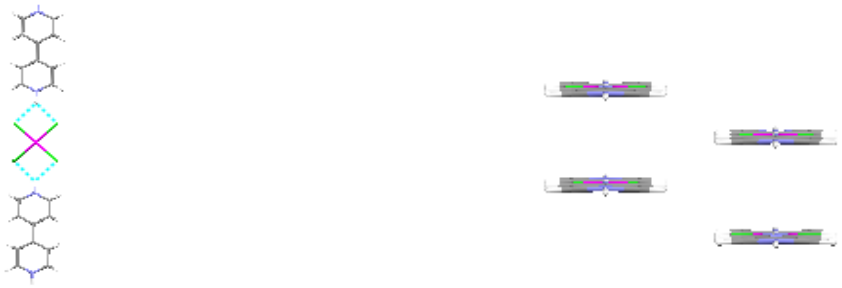
I. [1,3-bis-4-pyridinium-ethane][$PtCl_4$] (Adams and Orpen *et al*, 2006) (ethane bridge between aromatic moieties therefore longer cation).

J. [4,4'-H_2bipiperidyl][$PtCl_4$] (Adams and Orpen *et al*, 2006) (saturated version of 4,4'-H_2bipyridinium).

It was reported (Adams and Orpen *et al*, 2006; Gillon and Orpen *et al*, 2000; Lewis and Orpen, 1998) that ribbon motifs were observed for all four structures, irrespective of the cation. These ribbons are illustrated in **Figure 8 (left)**, and the packing is shown in **Figure 8 (right)** on page 17. See **Table 3** below for Pt···Pt distances observed for these structures.

Table 3: Summary of Pt···Pt distances for case study where the inorganic part is kept constant and the organic cation varied.

Hybrid	Pt···Pt distance along the ribbon (Å)	Pt···Pt inter-ribbon distance (Å) (packing distance of ribbons)
A	15.76	3.5
H	18.14	3.5
I	18.23	3.5
J	15.87	4.0



(a.)



(b.)



(c.)

Figure 8: (a.) left: NH···Cl hydrogen-bonded ribbon in **A**, right: ribbon packing in crystalline **A**. (Gillon and Orpen, 2000; Lewis and Orpen, 1998) **(b.)** left: NH···Cl hydrogen-bonded ribbon in **H**, right: ribbon packing in crystalline **H**. Isostructural to **I**. (Adams and Orpen, 2006) **(c.)** left: NH···Cl hydrogen-bonded ribbon in **J**, right: ribbon packing in crystalline **J**. (Adams and Orpen, 2006).

Conclusions Drawn from Case Study:

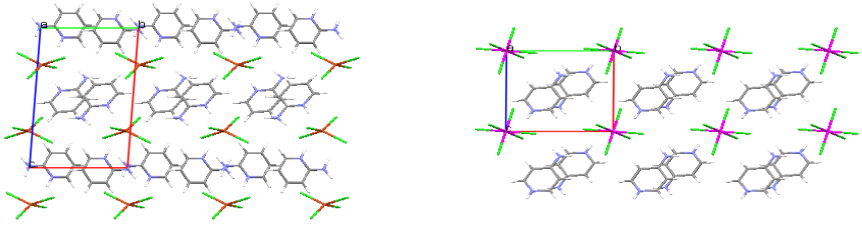
- Changing the metal ion results in the most dramatic change in crystal structure. (**Table 2** on page 14).
- Ring saturation affects Pt···Pt inter-ribbon distance. The greater the ring saturation the greater the Pt···Pt inter-ribbon distance. (**Table 3: A, H, I** vs **J** on page 16).
- Bridging between aromatic moieties increases Pt···Pt distance along the ribbon. (**Table 3: H, I** vs **A, J** on page 16).
- Saturation of bridge between aromatic moieties has little effect on crystal structure. (**Table 3: H vs I** on page 16).

1.6.2 *n*-Aminopyridinium perhalometallate structures reported in the literature

The crystal structures of seventeen organic-inorganic hybrids were selected from the Cambridge Structural Database (CSD), on the condition that they contained either the 2, 3 or 4-aminopyridinium cation, thus making them comparable with the results in the current crystallographic investigation. Poor or disordered structures were excluded from the comparison. These included structures where the cif files were incomplete and anion or cation geometries were significantly distorted thus eliminating the possibility for comparison. The list below indicates the names of the seventeen structures reported in the literature, which are numbered accordingly in the figures that follow on pages 20 to 23 and the tables that follow on pages 24 to 30.

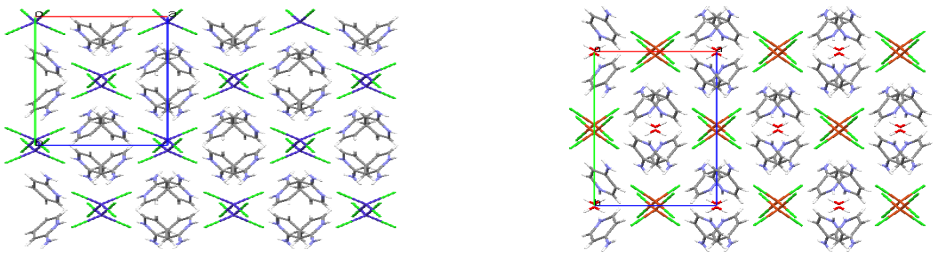
1. Bis(2-aminopyridinium) tetrachlorocuprate(II) (Kumar *et al*, 2005)
2. Bis(2-aminopyridinium) tetrabromocuprate(II) (Luque *et al*, 1997)
3. Bis(2-aminopyridinium) tetrachlorocobolt(II) (Jebas *et al*, 2006)
4. 2-Aminopyridinium tetrachloroantimony(III) (Kulicka *et al*, 2004)
5. 2-Aminopyridinium tetrabromoantimony(III) (Kulicka *et al*, 2004)
6. Bis(3-aminopyridinium) tetrachlorocuprate(II) (Kumar *et al*, 2005)
7. 3-Ammoniopyridinium tetrabromidomercurate(II) monohydrate (Ali *et al*, 2008)
8. Bis(4-aminopyridinium) tetrabromocadmium(II) monohydrate (Hatano *et al*, 2008)
9. Bis(4-aminopyridinium) tetrachlorocuprate(II) monohydrate (Halvorson *et al*, 1990)
10. 4-Aminopyridinium tetrabromocopper(II) monohydrate (Román *et al*, 1996)
11. Catena(tetrakis(4-aminopyridinium) tetrabromo-copper(ii) bis(bis(m~2~-bromo)-copper(i))) (Sertucha *et al*, 1998)
12. 4-Aminopyridinium tetrachloroantimony(III) (Jakubas *et al*, 2003)
13. 4-Aminopyridinium hexachloroantimonate(V) (Kulicka *et al*, 2006)
14. Catena-(4-aminopyridinium bis(m~2~-bromo)-dibromo-antimony(III)) (Hashimoto *et al*, 2003)
15. Bis(4-aminopyridinium) tetrachloropalladate(II) (Ivanova *et al*, 2005)
16. Bis(4-aminopyridinium) hexachloridostannate(IV) (Rademeyer *et al*, 2007)
17. Bis(4-aminopyridinium) tetrachloridocobaltate(II) (Jebas *et al*, 2009)

Packing characteristics and packing similarities between different literature structures are shown in **Figure 9 to Figure 17** on pages 20-23. **Table 4** on pages 24-26 contains the abbreviated names as well as the selected structural characteristics. The unit cell parameters and space groups are listed in **Table 5** on page 27. **Tables 6 to 8** on pages 28 to 30 list non-covalent interaction distances for *n*-aminopyridinium structures in the literature. Note that colour coding in tables indicate isostructural hybrids. In the case that structures from both the literature and this study were isostructural then the same colours were used throughout the report for consistency. So all structures highlighted in yellow are isostructural throughout this report and so forth.



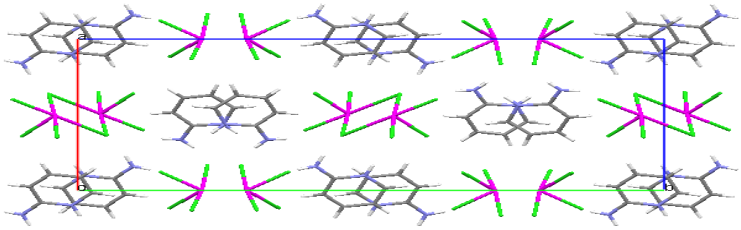
(a.) **(b.)**

Figure 9: Crystal structures from literature in the space group $P\bar{1}$. **(a.)** Crystal structure of **2ampCuCl (1)** (Kumar *et al*, 2005; YAPNAS01), viewed down the *a*-axis. Isostructural to **2ampCuBr (2)** (Luque *et al*, 1997; RIPWIW) and **3ampCuCl (6)** (Kumar *et al*, 2005; PATMUT). **(b.)** Crystal structure of **4ampSnCl (16)** (Rademeyer *et al*, 2007; RIGDER), viewed down the a-axis.

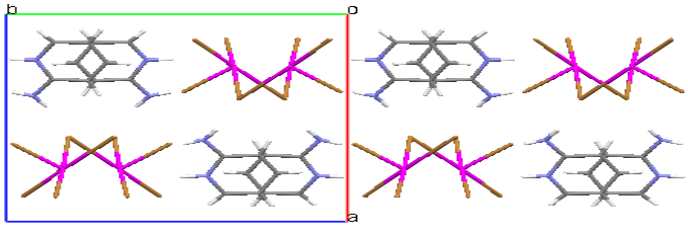


(a.) **(b.)**

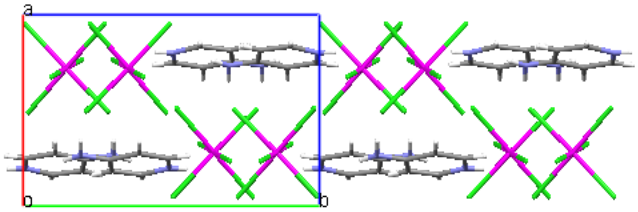
Figure 10: Crystal structures from literature in the space group *C*2/*c*. **(a.)** Crystal structure of **2ampCoCl (3)** (Jebas *et al*, 2006; DELPOA), viewed down the *c*-axis. **(b.)** Crystal structure of **4ampCuCl·H_2O (9)** (Halvorson *et al*, 1990; SEZLEO), viewed down the *c*-axis. Isostructural to **4ampCuBr·H_2O (10)** (Román *et al*, 1996; ZUDKUE).



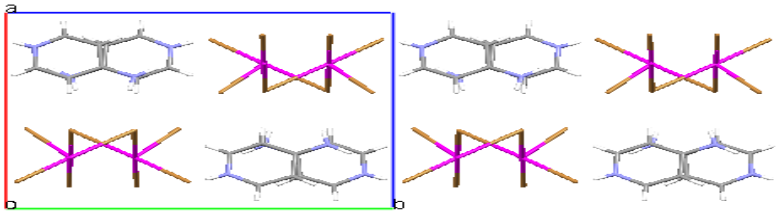
(a.)



(b.)



(c.)



(d.)

Figure 11: Crystal structures from literature in the space group $P2_1/c$, all viewed down the c-axis. **(a.)** Crystal structure of **2ampSbCl (4)** (Kulicka *et al*, 2004; NAKLIV)**. (b.)** Crystal structure of **2ampSbBr (5)** (Kulicka *et al*, 2004; NAKLER). **(c.)** Crystal structure of **4ampSbCl (octahedron) (13)** (Kulicka *et al*, 2006; ECAPUU). **(d.)** Crystal structure of **4ampSbBr (14)** (Hashimoto *et al*, 2003; ENIKIV).

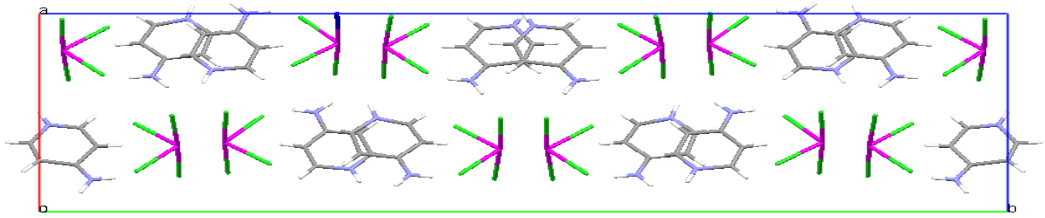


Figure 12: Crystal structure of **4ampSbCl (see-saw) (12)** (Jakubas *et al*, 2003; XUQQAB), space group *Cc*, viewed down the *c*-axis. Similar to structures in **Figure 11**, of space group $P2_1/c$.

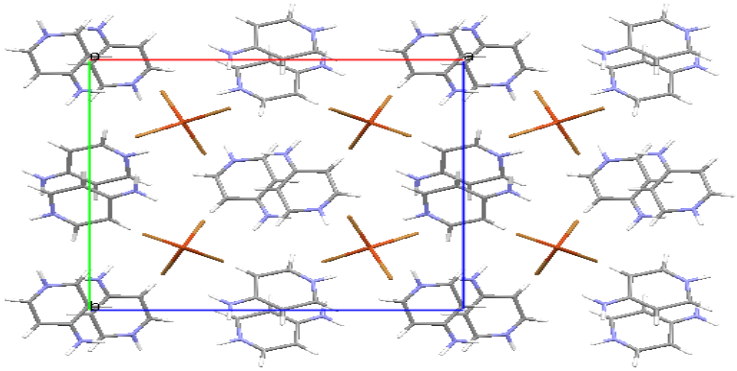


Figure 13: Crystal structure of **4ampCuBr (1)** (Sertucha *et al*, 1998; LAHYAU), space group $P4_2/n$, viewed down the *c*-axis.

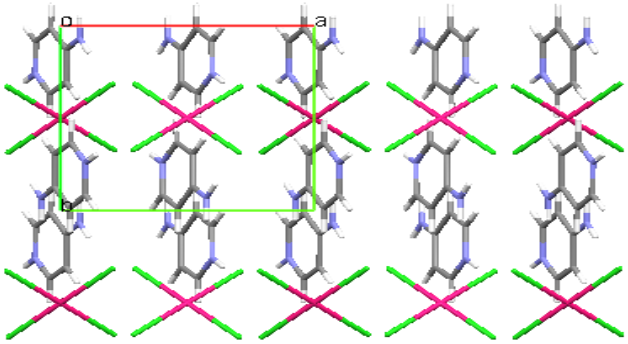


Figure 14: Crystal structure of **4ampPdCl (15)** (Ivanova *et al*, 2005; KAYKAX), space group P_2/n, viewed down the *c*-axis.

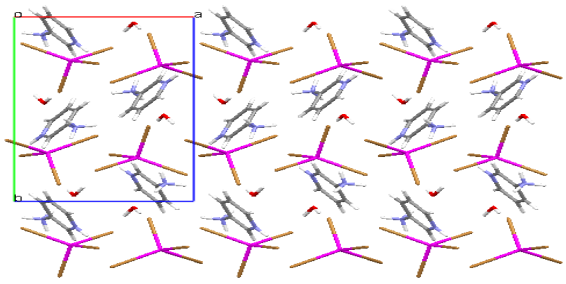


Figure 15: Crystal structure of **3ampHgBr·H_2O (7)** (Ali *et al*, 2008; TOBCOD), space group $P2_1/n$, viewed down the *c*-axis.

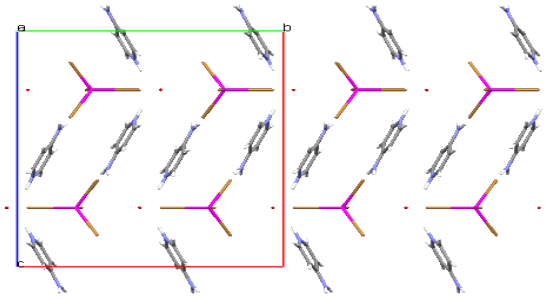


Figure 16: Crystal structure of **4ampCdBr·H_2O (8)** (Hatano *et al*, 2008; POGHEZ), space group *Pbcm*, viewed down the *a*-axis.

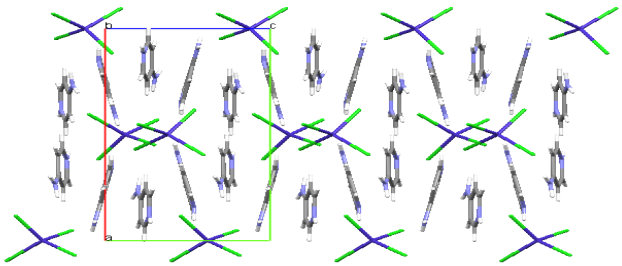


Figure 17: Crystal structure of **4ampCoCl (17)** (Jebas *et al*, 2009; HOSVIV), space group $P2_12_12_1$, viewed down the *b*-axis.

Table 4: Main Structural Characteristics of *n*-aminopyridinium perhalometallates reported in literature. Isostructurality is indicated by colour. White blocks indicate no isostructural equivalent.

Hybrid	Abbreviated Name	Formula	CSD Refcode	N protonated	Asymmetric Unit	Anion Geometry
1	2ampCuCl	$2(C_5H_7N_2^+)$, $CuCl_4^{2-}$	YAPNAS01	Pyridine	Two cations, one $CuCl_4^{2-}$unit	Isolated tetrahedral
2	2ampCuBr	$2(C_5H_7N_2^+)$, $CuBr_4^{2-}$	RIPWIW	Pyridine	Two cations, one $CuBr_4^{2-}$ unit	Isolated tetrahedral
3	2ampCoCl	$2(C_5H_7N_2^+)$, $CoCl_4^{2-}$	DELPOA	Pyridine	One cation, half an anion	Isolated tetrahedral
4	2ampSbCl	$2(C_5H_7N_2^+)$, $SbCl_4^{2-}$	NAKLIV	Pyridine	Two cations, two SbCl units	Isolated see-saw unit and edge sharing distorted octahedral unit
5	2ampSbBr	$2(C_5H_7N_2^+)$, $SbBr_4^{2-}$	NAKLER	Pyridine	One cation, one SbBr unit	Edge sharing distorted octahedral unit
6	3ampCuCl	$2(C_5H_7N_2^+)$, $CuCl_4^{2-}$	PATMUT	Pyridine	Two cations, one $CuCl_4^{2-}$ unit	Isolated distorted tetrahedron

Table 4: Main Structural Characteristics of *n*-aminopyridinium perhalometallates reported in literature. (continued). Isostructurality is indicated by colour. White blocks indicate no isostructural equivalent.

Hybrid	Abbreviated Name	Formula	CSD Refcode	N protonated	Asymmetric Unit	Anion Geometry
7	3ampHgBr·H_2O	2($C_5H_7N_2^+$), $HgBr_4^{2-}$, H_2O	TOBCOD	Pyridine and Amine	One cation, one anion, one water molecule	Isolated tetrahedral
8	4ampCdBr·H_2O	2($C_5H_7N_2^+$), $CdBr_4^{2-}$, H_2O	POGHEZ	Pyridine	One cation, one $CdBr_3^-$ unit, one water molecule	Isolated tetrahedral
9	4ampCuCl·H_2O	2($C_5H_7N_2^+$), $CuCl_4^{2-}$, H_2O	SEZLEO	Pyridine	One cation, one anion, one water molecule	Isolated distorted tetrahedron
10	4ampCuBr·H_2O	2($C_5H_7N_2^+$), $CuBr_4^{2-}$, H_2O	ZUDKUE	Pyridine	One cation, half an anion, half water molecule	Isolated distorted tetrahedron
11	4ampCuBr	$(C_5H_7N_2^+)_{4n}$ n($CuBr_4^{2-}$) 2n($CuBr_2^-$)	LAHYAU	Pyridine	One cation, two CuBr unit	Isolated distorted tetrahedron and edge sharing tetrahedron forming one-dimensional chain
12	4ampSbCl(see-saw)	$C_5H_7N_2^+$ $SbCl_4^-$	XUQQAB	Pyridine	Three cations, one $SbCl_3$ unit	Isolated see-saw geometry

Table 4: Main Structural Characteristics of *n*-aminopyridinium perhalometallates reported in literature. (continued). Isostructurality is indicated by colour. White blocks indicate no isostructural equivalent.

Hybrid	Abbreviated Name	Formula	CSD Refcode	N protonated	Asymmetric Unit	Anion Geometry
13	4ampSbCl(octahedron)	$C_5H_7N_2^+$ $SbCl_6^-$	ECAPUU	Pyridine	One cation, one anion	Isolated octahedron
14	4ampSbBr	$(C_5H_7N_2^+)_n$ $n(SbBr_4^-)$	ENIKIV	Pyridine	One cation, one $SbBr_4$ unit	Face sharing octahedrons form one-dimensional chain
15	4ampPdCl	$2(C_5H_7N_2^+)$, $PdCl_4^{2-}$	KAYKAX	Pyridine	One cation, half an anion	Isolated square planar cation
16	4ampSnCl	$2(C_5H_7N_2^+)$ $SnCl_6^{2-}$	RIGDER	Pyridine	One cation, one $SnCl_3^-$ unit	Isolated octahedron
17	4ampCoCl	$2(C_5H_7N_2^+)$, $CoCl_4^{2-}$	HOSVIV	Pyridine	Two cations, one anion	Isolated tetrahedron

Table 5: Structural and Experimental Parameters for *n*-aminopyridinium perhalometallates in the literature. Isostructurality is indicated by colour. White blocks indicate no isostructural equivalent.

Hybrid	Abbreviated Name	Space Group	a(Å)	b(Å)	c(Å)	α(°)	β(°)	γ(°)	R
1	2ampCuCl	$P\bar{1}$	7.929(4)	8.115(3)	13.667(4)	91.21(3)	94.71(3)	114.55(4)	0.0559
2	2ampCuBr	$P\bar{1}$	8.090(1)	8.366(1)	14.020(1)	91.23(1)	95.22(1)	113.82(1)	0.042
3	2ampCoCl	$C2/c$	8.2152(3)	14.0713(5)	13.5731(5)	90	95.190(2)	90	0.032
4	2ampSbCl	$P2_1/c$	11.3199(7)	25.6398(16)	7.5446(6)	90	91.833(6)	90	0.0389
5	2ampSbBr	$P2_1/c$	12.4841(12)	13.1056(12)	7.4915(10)	90	105.843(10)	90	0.0301
6	3ampCuCl	$P\bar{1}$	7.974(1)	8.133(1)	13.63(3)	91.23(2)	94.73(2)	115.00(1)	0.0437
7	3ampHgBr·H_2O	$P2_1/n$	8.1896(7)	14.0245(12)	11.5711(10)	90	94.730(2)	90	0.035
8	4ampCdBr·H_2O	$Pbcm$	6.876(2)	14.089(2)	18.845(2)	90	90	90	0.0485
9	4ampCuCl·H_2O	$C2/c$	8.457(2)	14.318(2)	14.382(2)	90	95.82(1)	90	0.035
10	4ampCuBr·H_2O	$C2/c$	8.797(1)	14.860(1)	14.216(1)	90	96.94(2)	90	0.051
11	4ampCuBr	$P4_2/n$	15.608(3)	15.608(3)	6.882(2)	90	90	90	0.059
12	4ampSbCl(see-saw)	Cc	13.322(2)	38.001(5)	7.888(1)	90	123.87(1)	90	0.0428
13	4ampSbCl(octahedron)	$P2_1/c$	7.3180(10)	12.013(2)	15.561(3)	90	98.40(3)	90	0.0399
14	4ampSbBr	$P2_1/c$	11.548(3)	14.029(5)	7.432(2)	90	93.19(2)	90	0.0312
15	4ampPdCl	P_2/n	7.8440(16)	7.5450(15)	13.608(3)	90	96.23(3)	90	0.0451
16	4ampSnCl	$P\bar{1}$	7.2248(6)	8.3273(7)	8.3403(8)	89.100(6)	87.002(6)	65.225(5)	0.020
17	4ampCoCl	$P2_12_12_1$	15.0051(12)	14.9751(12)	7.1723(6)	90	90	90	0.0214

Table 6: Selected Cg-Cg and Non-Covalent Intermolecular Distances of the type d(H···A) for 2-aminopyridinium hybrids reported in the literature. Isostructurality is indicated by colour. White blocks indicate no isostructural equivalent.

Hybrid	Abbreviated Name	Cg-Cg Distance (Å)	Shortest Cation-N-H···X-M-Anion Distance (Å)	
			pyrNH···X	amineNH···X
1	2ampCuCl	3.767	2.193; 2.415 and 2.864 are bifurcated	2.325; 2.354 and 2.940 are bifurcated
2	2ampCuBr	3.852	2.305	2.422
3	2ampCoCl	4.228	2.581	2.420
4	2ampSbCl	4.209	2.592	2.546
5	2ampSbBr	4.058	2.717	2.893

Table 7: Selected Cg-Cg and Non-Covalent Intermolecular Distances of the the type d(H···A) for 3-aminopyridinium and 3-ammoniopyridinium hybrids reported in the literature. Isostructurality is indicated by colour.

Hybrid	Abbreviated Name	Cg-Cg Distance (Å)	Shortest Cation-N-H···X-M-Anion Distance (Å)		Shortest Water-H···X-M-Anion Distance (Å)	Shortest Cation-N-H···O-Water Distance (Å)	
			pyrNH···X	amineNH···X		pyrNH···O	amineNH···O
6	3ampCuCl	4.224	none	2.288; 2.356 and 2.906 are bifurcated	No water	No water	No water
7	3ampHgBr·H$_2$O	5.193	2.731	2.627	2.651	none	1.799

Table 8: Selected Cg-Cg and Non-Covalent Intermolecular Distances of the the type d(H···A) for 4-aminopyridinium hybrids reported in the literature. Isostructurality is indicated by colour. White blocks indicate no isostructural equivalent.

Hybrid	Perhallometallate Anion Geometry	Cg-Cg Distance (Å)	Shortest Cation-N-H···X-M-Anion Distance (Å)		Shortest Water-H···X-M-Anion Distance (Å)	Shortest Cation-N-H···O-Water Distance (Å)	
			pyrNH···X	amineNH···X		pyrNH···O	amineNH···O
8	4ampCdBr·H_2O	3.799	none	2.694	Hydrogen atoms not placed on Oxygen atom	Not available	Not available
9	4ampCuCl·H_2O	4.200	none	2.582	2.456	2.040	none
10	4ampCuBr·H_2O	4.302	none	2.561	2.582	1.840	none
11	4ampCuBr	3.594	2.539	2.515	No water	No water	No water
12	4ampSbCl(see-saw)	4.325	2.419	2.554	No water	No water	No water
13	4ampSbCl(octahedron)	5.559	2.664	2.895	No water	No water	No water
14	4ampSbBr	4.504	2.717	2.726	No water	No water	No water
15	4ampPdCl	3.553	2.354	2.512	No water	No water	No water
16	4ampSnCl	4.245	2.676	2.536	No water	No water	No water
17	4ampCoCl	4.565	2.523	2.418	No water	No water	No water

2. Experimental Methods

2.1 Starting materials

The starting materials listed in section **2.1.1** and **2.1.2** as well as the acids HCl, HBr and HI were employed to synthesize the different *n*-aminopyridinium perhalometallates. All starting materials were available commercially and were used without further purification. Due to the toxic nature of the *n*-aminopyridines and cadmium and mercury halides used, relevant safety precautions were taken.

2.1.1 Inorganic components selected for this study

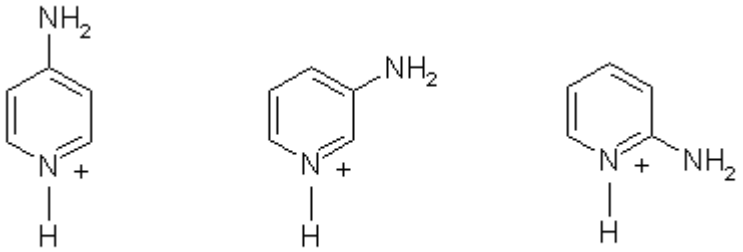
- Zinc(II) Chloride
- Zinc(II) Bromide
- Zinc(II) Iodide
- Cadmium(II) Chloride
- Cadmium(II) Bromide
- Cadmium(II) Iodide
- Mercury(II) Chloride or Mercuric Chloride
- Mercury(II) Bromide or Mercuric Bromide
- Mercury(II) Iodide or Mercuric Iodide

The nine metal halides chosen are different combinations of three d^{10} metals (zinc, cadmium and mercury) and three halogens (chlorine, bromine and iodine). Zinc halides were chosen on the basis that all three (zinc(II) chloride, zinc(II) bromide and zinc(II) iodide) almost always form tetrahedral complexes. In addition to the tetrahedral geometry, perhalocadmate and perhalomercurate anions often display complex polymerized geometries including one-dimensional chains and two- dimensional sheets.

2.1.2 Organic Components Selected for this study

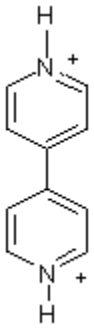
These organic cations were selected because of their similarity to each other and 4,4'-bipyridinium (NB. From the case study). See **Figure 18** below. For consistency it will be assumed that the pyridine N is protonated.

1. 4-aminopyridinium
2. 3-aminopyridinium
3. 2-aminopyridinium



1. **2.** **3.**

(a.)



(b.)

Figure 18: (a.) Organic cations selected for this study. The labeling of the cations corresponds to the above list. **(b.)** 4,4-bipyridinium cation.

2.2 Synthetic Methodology

Two possible synthetic routes were available to prepare the *n*-aminopyridinium perhalometallate hybrids:

Route 1: A two-step reaction involved the protonation of the amine using the relevant acid (note that the same halide was used in the acid (HX) and the metal halide (MX_2)). In this step the *n*-aminopyridine was dissolved in chloroform, and a slight stoichiometric excess of acid was added dropwise. The concentration of each acid was as follows: HCl (37%, 12.8M), HBr (48%, 8.84M) and HI (47%, 5.5M). Evaporation of the solvent left the *n*-aminopyridinium halide as a powder. In the second step the *n*-aminopyridinium halide was dissolved in distilled water, and the metal halide was added in the ratio 2:1 (*n*-aminopyridinium halide: metal halide). Heating of the solution in a fume cupboard assisted in solvation of the starting materials. The solution was left open to the air, at room temperature, and evaporation of the solvent allowed for the crystallization of the hybrid. This process took a couple of weeks.

Route 2: The hybrids were also prepared in a one step reaction. Using a 2:1 excess ratio of *n*-aminopyridinium, metal halide and acid, all combined in the same vial, giving a saturated solution at room temperature. The vial was sealed and heated slowly in an oil bath. After dissolution occurred (typically around 80°C) the oil bath was cooled slowly over a couple of days. This allowed for the slow crystallization of the hybrid. Regular inspection of the crystals allowed for the identification of the best time to harvest the crystals. This route is illustrated in **Figure 19** on page 34.

It was found that Route 2 typically yielded crystals of much better quality than Route 1, hence making it the preferred method of synthesis, as described in the next section.

2.2.1 Temperature Controlled Crystallization of Organic-Inorganic Hybrids

Approximately 0.1g of the organic component (*n*-aminopyridinium) was weighed and placed in a size 8 polytop vial. ($n_{organic}$= ($m_{oraganic}$ / $Mr_{organic}$)). The inorganic component (metal halide) was weighed in a separate polytop vial, where $n_{inorganic}$ = 0.5 x $n_{organic}$ and $m_{inorganic}$ = $n_{inorganic}$ x $Mr_{inorganic}$. The organic component was protonated using approximately 2cm^{-3} dilute acid (three parts distilled water and seven parts acid (v/v)). The halogen in the acid corresponded to the halogen in the inorganic component. The inorganic component was then added to the acidic aqueous organic component. The mixture was swirled very gently and the lid placed on the polytop vial. The covered polytop vial was then clamped and heated in an oil-bath (80ºC-89ºC) and stirred with a magnetic stirrer bar, until all the solid dissolved. The temperature of the oil bath was slowly reduced to 39ºC, at a rate of 2ºC to 5ºC per minute. On cooling the hybrid crystallized from the saturated solution. The experimental setup is illustrated in **Figure 19** below, and the masses used are given in **Table 9** on page 35.

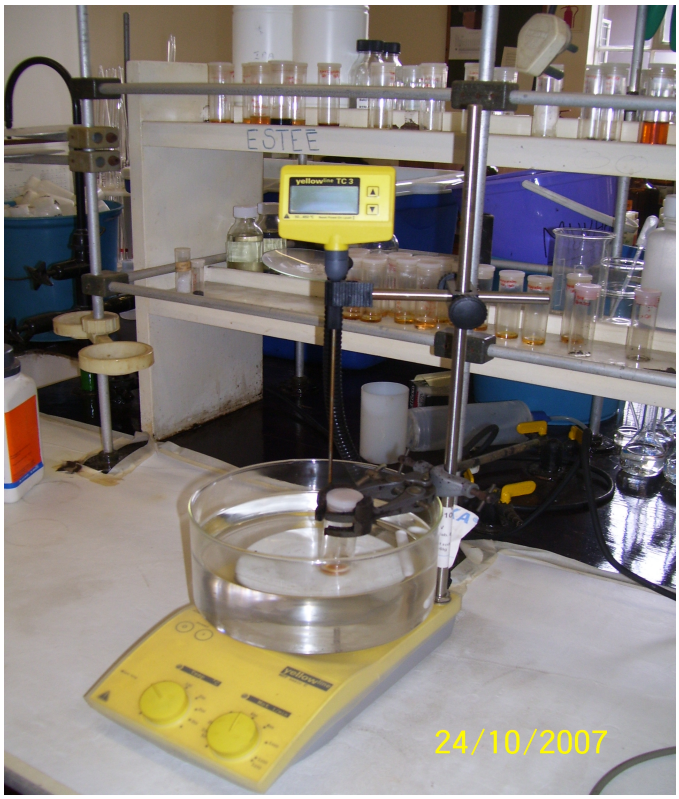


Figure 19: Apparatus for temperature controlled crystallization.

Table 9: Masses of amines (2amp, 3amp and 4amp are 2-aminopyridine, 3-aminopyridine and 4-aminopyridine respectively) and masses of metal halides used in temperature controlled experiments.

Hybrid	Mass of Amine used (g)	Moles of Amine used (mmol)	Moles of Metal Halide used (mmol)	Mass of Metal Halide used (g)	Acid used
2ampZnCl	2amp 0.1016	1.0796	0.5401	$ZnCl_2$ 0.0736	HCl
2ampZnBr	2amp 0.1014	1.0775	0.5387	$ZnBr_2$ 0.1213	HBr
2ampZnI	2amp 0.119	1.2643	0.6319	ZnI_2 0.2017	HI
2ampCdI	2amp 0.118	1.2537	0.6828	CdI_2 0.2296	HI
2ampHgCl	2amp 0.1003	1.0658	0.7076	$HgCl_2$ 0.1921	HCl
2ampHgBr	2amp 0.117	1.243	0.6221	$HgBr_2$ 0.2242	HBr
2ampHgI	2amp 0.115	1.2218	0.6109	HgI_2 0.27763	HI
3ampZnCl	3amp 0.1044	1.1093	0.5547	$ZnCl_2$ 0.0756	HCl
3ampZnBr·H₂O	3amp 0.111	1.179	0.5890	$ZnBr_2$ 0.13264	HBr
3ampHgI·H₂O	3amp 0.1013	1.0764	0.5382	HgI_2 0.2446	HI
4ampZnCl	4amp 0.1047	1.1125	0.5562	$ZnCl_2$ 0.0758	HCl
4ampZnBr	4amp 0.1064	1.1306	0.5653	$ZnBr_2$ 0.1273	HBr
4ampZnI	4amp 0.111	1.1793	0.5896	ZnI_2 0.1882	HI
4ampCdCl·H₂O	4amp 0.1054	1.1198	0.5619	$CdCl_2$ 0.1030	HCl
4ampCdBr·H₂O	4amp 0.1014	1.0775	0.5388	$CdBr_2·4H_2O$ 0.1855	HBr
4ampCdI·H₂O	4amp 0.1014	1.0775	0.5388	CdI_2 0.1973	HI
4ampHgCl·H₂O	4amp 0.1024	1.0881	0.5440	$HgCl_2$ 0.1477	HCl
4ampHgBr·H₂O	4amp 0.1001	1.0636	0.5319	$HgBr_2$ 0.1917	HBr
4ampHgI·H₂O	4amp 0.103	1.1474	0.5737	HgI_2 0.2607	HI

2.3 Instrumental Techniques

The characterization and analysis of organic-inorganic hybrids involved two main processes, where the first process was to determine the crystal structure of the ionic hybrids and the second was to locate the intermolecular hydrogen bonding networks, as well as any other non-covalent interactions. X-ray diffraction techniques were used to determine the crystal structure of the hybrids. Good quality single crystals obtained in the study were analyzed using single crystal X-ray diffraction (SCXRD).

2.3.1 Theory of X-ray diffraction

Essentially X-rays are produced by striking a metal target with electrons (Dann, 2002). This causes core electrons of the metal to be ejected, thus creating vacancies, causing electrons in higher energy levels to fall down into the now vacant orbitals (Dann, 2002). The difference in energy levels is emitted as an X-ray, where $\Delta E = h\nu$ (ΔE is the energy difference, h is Plank's constant, ν is the frequency of emitted radiation) (Dann, 2002). (Note that the electrons are generated in an X-Ray tube.)

The main principle behind X-ray diffraction is that X-rays interact with electrons (Dann, 2002). So when a beam of X-rays impinges a material, the X-rays are scattered by the electron clouds of the atoms in the material (Dann, 2002). If the wavelength of the X-rays is comparable to the separation between the atoms then interference can occur (Dann, 2002). Atoms in a crystalline solid produce an ordered array of scattering centers, thus producing interference maxima and minima according to Bragg's Law (**Equation 1**) (Dann, 2002).

$$n\lambda = 2d\sin\theta$$

Equation 1: The Bragg Equation. (Dann, 2002)

where n is the number of complete waves

λ is the X-ray wavelength

d is the lattice spacing

and θ is the angle of incidence of the X-ray beam

A single X-ray wavelength is required to carry out a diffraction experiment (Weller, 2002). A crystal monochromator is used to obtain a single wavelength. Therefore the X-ray beam emerging from the X-ray tube impinges the single crystal at a chosen, fixed orientation (Weller, 2002). Interference according to the Bragg Law (**Equation 1**), gives rise to a diffraction maximum at a specific diffraction angle. However photons are reflected from the crystal in different directions such that the overall scattering of atom contributions is determined as opposed to individual atom contributions (Read, © 1999-2009). As a result information about relative phases of diffraction is lost because the photons are counted (Read, © 1999-2009). This is known as the phase problem and is critical in crystallography.

The phase representing an overall set of scattering from a particular set of Bragg planes is known as the structure factor (**F**) (Read, © 1999-2009). These structure factors correspond to the Fourier transformation of the electron density distribution within the unit cell of the crystal (Read, © 1999-2009). So the inverse of the Fourier transform is applied to the structure factors to obtain electron densities but the phases are still not known and need to be solved (Read, © 1999-2009).

There are a few different techniques available to solve the phase problem. These include the Patterson function, molecular replacement and direct methods (Read, © 1999-2009). For this study direct methods were used to solve the phase problem as described in section **2.3.2** below. Ultimately by studying the diffraction of X-ray beams by crystalline solids structural information can be obtained (Dann, 2002).

2.3.2 Single crystal X-ray diffraction

This technique was used because it was one of the best characterization methods available to analyze crystalline materials. More over, this method of analysis was non-destructive so the crystal was intact after the analysis (Campana, 1992). The only real limitation was that the crystal had to be single, stable and optically clear or else the data would not be useful (Campana, 1992). The ideal crystal size was close to 0.3mm. After a suitable crystal was identified, the crystal was mounted onto a glass fibre attached to a brass mounting that resembled a thick pin. The brass mounting was hollow and filled

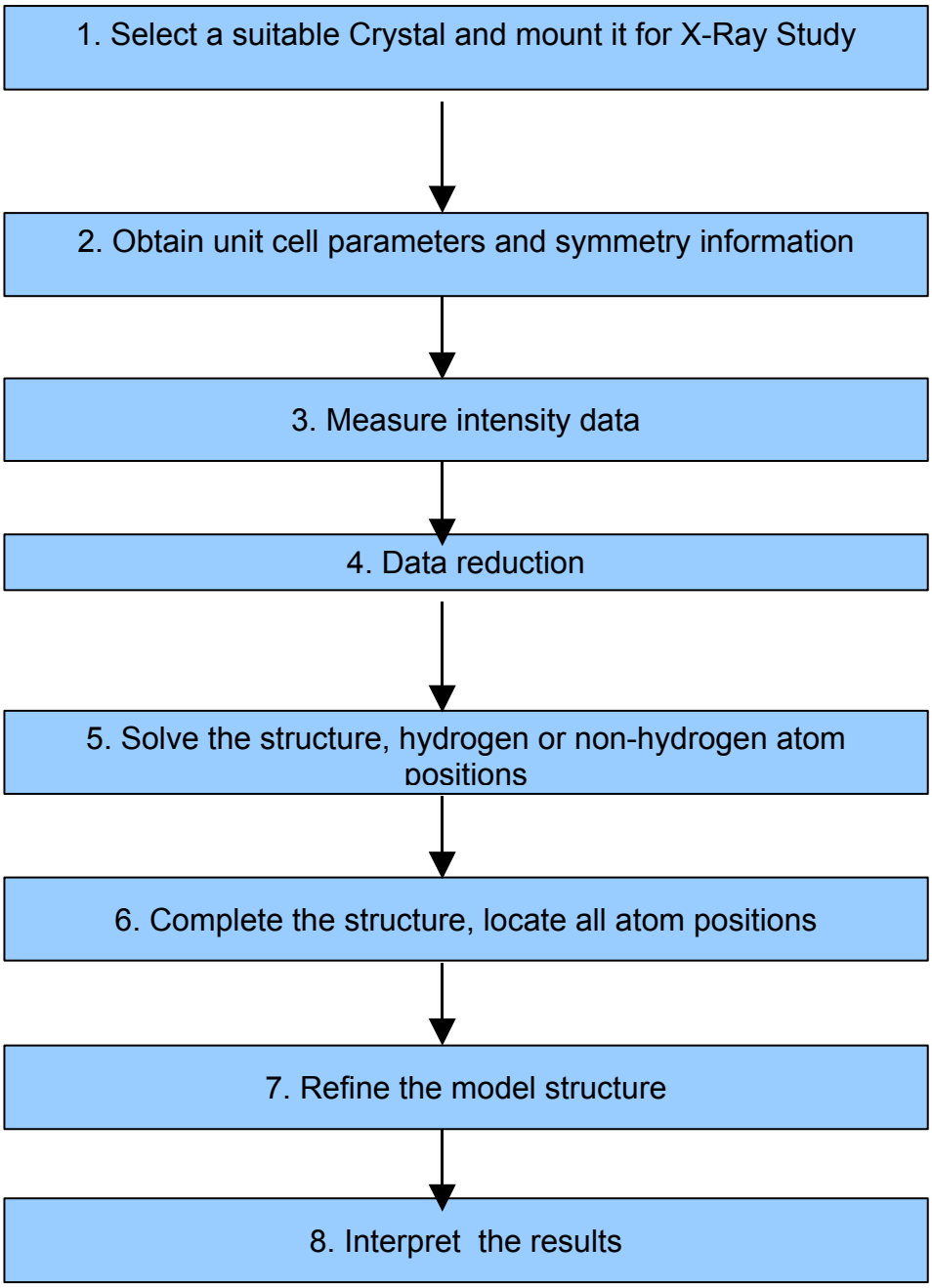
with melted candle wax. While the candle wax was still pliable, the glass fibre was inserted in to the brass mounting. The glass fibre was secured once the candle wax had hardened. The selected crystal was then attached to the tip of the glass fibre using super glue. This was done under a microscope. The tip of the glass fibre was lightly touched with super glue. Then the crystal and glass fibre were aligned and then attached. Once the glue dried and the entire assembly was fixed and secure, the brass mounting was inserted into a goniometer head. The goniometer head was then affixed to the diffractometer (Campana, 1992). The crystal was centered such the center of the crystal coinsided with the intersecting cross-hairs (Campana, 1992).

Once the crystal was centered, the quality of the crystal was determined by a preliminary 360º rotational image. The unit cell was determined by a preliminary set of frames (similar to pictures). Reflections of these frames were used to determine the reduced primitive cell and calculate the orientation matrix (Campana, 1992). The primitive unit cell was then refined twice more, using least squares (Campana, 1992). This information was converted to the appropriate crystal system and Bravias lattice (Campana, 1992). Thereafter the final orientation matrix was determined.

Intensity data was then collected, typically between 4º and 60º 2Θ for molybdenum radiation, such that a sphere or hemisphere of data was collected, by scanning at specific increments (Campana, 1992). For highly symmetric material, the data collection was manipulated to reduce data collection time (Campana, 1992). Data collections took between 6 and 24 hours, depending on the detector and the crystal (Campana, 1992). After the data collection was complete, background corrections were accounted for, most software packages that run the data collection, take this into account (Campana, 1992).

Direct methods and least squares were most often used to solve the phase problem, whereby phases were assigned to strong reflections to produce a refined fit (Campana, 1992). The last thing left to do, was solve the structure from an electron density map, using direct methods (see section **2.3.3** below) where the user assigns elements to intensity centers. The heaviest elements were assigned to the highest intensities (Campana, 1992). Once the crystal structure was solved, the structure was refined to

obtain the best possible fit between the observed crystal structure and the calculated crystal structure, represented by the *R*-value (Campana, 1992). The lower the *R*-value the better the agreement between the calculated and observed crystal structure. Software packages such as Mercury (Bruno *et al*, 2002) and Platon (Spek, 2000), allow the user to determine bond lengths and bond angles and a series of crystallographic data. See **Scheme 3** below for a summary of the steps described above.



Scheme 3: Flowchart of Crystal structure determination (Clegg, 2005).

2.3.3 SCXRD data collection, solution and refinement-Face Indexed

Three single crystal X-ray diffractometers (SCXRD) were used during the course of this study, namely the APEX2, SMART and the Oxford Xcalibur2 (only room temperature data). The above process was carried out on each crystal structure in this study.

APEX2 SCXRD (WITS):

Intensity data was collected on a Bruker APEX II CCD area detector diffractometer with graphite monochromated Mo K_α radiation (50kV, 30mA) using the APEX 2 (Bruker, 2005a) data collection software. The collection method involved ω-scans of 0.5º and 512x512 bit data frames. Data reduction was carried out using the program *SAINT+* (Bruker, 2005b) and face indexed absorption corrections were made using *XPREP* (Bruker, 2005b). The crystal structure was solved by direct methods using *SHELXTL* (Bruker, 1999b). Non-hydrogen atoms were first refined isotropically followed by anisotropic refinement by full matrix least-squares calculations based on F^2 using *SHELXTL* (Bruker, 1999b). Hydrogen atoms were first located in the difference map and then positioned geometrically and allowed to ride on their respective parent atoms. Diagrams were generated using *SHELXTL* (Bruker, 1999b).

Bruker SMART SCXRD (WITS):

Intensity data was collected on a Bruker SMART 1K CCD area detector diffractometer with graphite monochromated Mo K_α radiation (50kV, 30mA). The collection methods involved ω-scans of 0.3º. Data reduction was carried out using the program *SAINT+* (Bruker, 1999a) and face indexed absorption corrections were made using the program *XPREP* (Bruker, 1999a). The crystal structure was solved by direct methods using *SHELXTL* (Bruker, 1999b). Non-hydrogen atoms were first refined isotropically followed by anisotropic refinement by full matrix least-squares calculations based on F^2 using *SHELXTL* (Bruker, 1999b). Hydrogen atoms were first located on a difference map and then positioned geometrically and allowed to ride on their respective parent atoms. Diagrams were generated using *SHELXTL* (Bruker, 1999b).

Xcalibur2 SCXRD (UKZN):

Intensity data was collected on an Oxford Diffraction Xcalibur 2 CCD area detector diffractometer with ceramic X-Ray tube Mo K_α radiation (3kW Spellman X-Ray generator). Data reduction was carried out using the program *CrysAlis RED* (Oxford Diffraction, 2003). The crystal structure was solved by direct methods using *SHELXS97* (Sheldrick, 1997). Non-hydrogen atoms were first refined isotropically followed by anisotropic refinement by full matrix least-squares calculations based on F^2 using *SHELXS97* (Sheldrick, 1997). Hydrogen atoms were first located on a difference map and then positioned geometrically and allowed to ride on their respective parent atoms. Diagrams were generated using *SHELXS97* (Sheldrick, 1997).

2.4 Structural Analysis Software

After obtaining diffraction data from the instrument and solving the structures (as described in section **2.3.3** above) the following software packages were used to prepare material for the report:

- WinGX (Farrugia, 1999)
- Mercury (Bruno, 2002)
- Platon (Spek, 2000)

The use of these software packages enable us to carry out the following analysis:

- Describe hydrogen-bonded networks
- Identify motifs
- Verify templating effect of cations
- Compare the packing of cations and anions with other hybrids
- Identify trends in hydrogen bonding.

3. Results

The single crystal structures of nineteen novel *n*-aminopyridinium perhalometallates were determined. Seven structures contain the 2-aminopyridinium cation, one contains the 3-aminopyridinium cation, two contain the 3-ammoniopyridinium cation and nine the 4-aminopyridinium cation.

The matrix in **Table 10** below shows all the possible combinations of the organic cations and inorganic anions under investigation. Pink blocks indicate solved crystal structures of organic-inorganic hybrids, and purple blocks show that crystals were not suitable for X-Ray diffraction techniques. From this matrix it is clear that structures of all possible combinations of the 4-aminopyridinium cation with different perhalometallate anions considered in this study were obtained.

There are two outstanding structures in the 2-aminopyridinium series, and only three structures were determined for the 3-aminopyridinium and 3-ammoniopyridinium series due to the difficulty of obtaining good quality crystals of hybrids that contain 3-aminopyridine.

Table 10: Summary of results. Pink blocks indicate solved crystal structures of organic-inorganic hybrids. Purple blocks indicate that crystals were not suitable for X-Ray diffraction techniques.

Metal Halide	Organic Component		
	2-aminopyridine	3-aminopyridine	4-aminopyridine
$ZnCl_2$	☺	☺	☺
$ZnBr_2$	☺	☺	☺
ZnI_2	☺	X	☺
$CdCl_2$	X	X	☺
$CdBr_2$	X	X	☺
CdI_2	☺	X	☺
$HgCl_2$	☺	X	☺
$HgBr_2$	☺	X	☺
HgI_2	☺	☺	☺

Table 11 on page 44 lists structural and experimental data for all the single crystal structures determined in this study. Colour coding in tables indicate isostructural hybrids. In the case that structures from both the literature and this study were isostructural then the same colours were used in all tables for consistency. So all structures highlighted in yellow are isostructural throughout this report and so forth.

Detailed lists of bond distances and angles are not included here, but may be found in the appendix provided on the compact disc. Hydrogen bonding parameters are listed in **Tables 12 to 15** on pages 74 to 77. This chapter includes figures illustrating intermolecular hydrogen bonds, where red indicates an intermolecular hydrogen bond involving a pyridinium N-H (**pyrNH···X**), blue an amine N-H (**amineNH···X**) and green a water molecule and an anion (**Water-H···X-M-Anion**). A note on nomenclature employed: the abbreviation used to name the individual structures indicate the cation first followed by the metal atom and then the relevant halide in the structure. For example 2ampZnCl indicates that the structure contains a combination of 2-aminopyridinium cations and perchlorozincate anions. The most important structural aspects of individual structures determined in this investigation are discussed in the next sections.

Table 11: Structural and Experimental Parameters determined for characterized hybrids. Isostructurality is indicated by colour. White blocks indicate no isostructural equivalent.

Metal Halide	Crystal Dimensions (mm)	Crystal Colour	Collection Temp (K)	a(Å)	b(Å)	c(Å)	Alpha(°)	Beta(°)	Gamma(°)	Space Group	R data	R structure
2ampZnCl	0.4 0.4 0.6	Colourless	298	8.3104(6)	14.1150(17)	13.8427(10)	90	93.641(6)	90	$C2/c$	0.0290	0.0213
2ampZnBr	0.2 0.2 0.4	Colourless	190	15.3064(11)	7.7064(6)	14.7911(10)	90	92.313(6)	90	$C2/c$	0.0369	0.0282
2ampZnI	0.40 0.49 0.44	Colourless	173	35.2785(8)	7.6246(2)	22.6941(5)	90	108.5920(10)	90	$C2/c$	0.0621	0.0582
2ampCdI	0.28 0.42 0.40	Colourless	173	8.2597(3)	8.7807(3)	15.5171(5)	81.9790(10)	82.1140(10)	63.1230(10)	$P\bar{1}$	0.0520	0.0466
2ampHgCl	0.4 0.4 0.3	Colourless	298	15.0298(8)	7.4925(4)	14.7577(9)	90	92.229(5)	90	$C2/c$	0.0193	0.0177
2ampHgBr	0.26 0.40 0.56	Colourless	173	6.9651(5)	14.3009(10)	17.7646(13)	90	90	97.856(4)	$P2_1/c$	0.1462	0.0889
2ampHgI	0.47 0.72 0.55	Colourless	173	8.1780(4)	8.7740(4)	15.4043(7)	82.124(2)	82.261(2)	63.166(2)	$P\bar{1}$	0.0808	0.0764
3ampZnCl	0.2 0.2 0.2	Colourless	180	6.8921(5)	8.4555(6)	13.8003(9)	99.008(6)	89.573(5)	100.194(6)	$P\bar{1}$	0.0301	0.0217
3ampZnBr-H_2O	0.98 0.40 0.50	Colourless	173	7.017(2)	7.766(2)	23.380(7)	89.929(15)	89.840(18)	85.701(7)	$P2_1/c$	0.2012	0.1357
3ampHgI-H_2O	0.2 0.05 0.5	Colourless	180	8.3752(2)	14.7432(3)	12.1260(3)	90	93.663(2)	90	$P2_1/n$	0.0493	0.0408
4ampZnCl	0.3 0.4 0.4	Colourless	180	7.1525(3)	14.9902(12)	14.9993(2)	90	90	90	$P2_12_12_1$	0.0987	0.0962
4ampZnBr	0.2 0.2 0.2	Colourless	160	7.3747(7)	15.4569(13)	15.4716(13)	90	90	90	$P2_12_12_1$	0.0531	0.0263
4ampZnI	0.34 0.50 0.37	Colourless	173	7.5844(4)	16.0413(7)	16.0410	90	90	90	$P2_12_12_1$	0.0531	0.0504
4ampCdCl-H_2O	0.4 0.4 0.6	Colourless	298	7.496(5)	24.413(5)	12.453(5)	90	101.93(4)	90	$P2_1/c$	0.2077	0.1997
4ampCdBr-H_2O	0.2 0.2 0.3	Colourless	298	6.8746(12)	14.082(2)	18.842(3)	90	90	90	$Pbcm$	0.0372	0.0296
4ampCdI-H_2O	0.2 0.2 0.3	Colourless	298	7.3983(3)	14.7586(7)	18.7562(10)	90	90	90	$Pbcm$	0.0525	0.0460
4ampHgCl-H_2O	0.2 0.2 0.3	Colourless	298	6.5735(5)	13.6799(10)	18.7593(14)	90	90	90	$Pbcm$	0.0440	0.0220
4ampHgBr-H_2O	0.1 0.3 0.3	Colourless	180	6.8625(3)	14.0041(6)	18.8161(9)	90	90	90	$Pbcm$	0.0522	0.0330
4ampHgI-H_2O	0.49 0.24 0.40	Colourless	173	7.2736(4)	14.4831(7)	18.5793(8)	90	90	90	$Pbcm$	0.0315	0.0315

3.1 Bis(2-aminopyridinium) tetrachlorozincate(II)

Chemical Formula: $(C_5H_7N_2^+)_2\ ZnCl_4^{2-}$

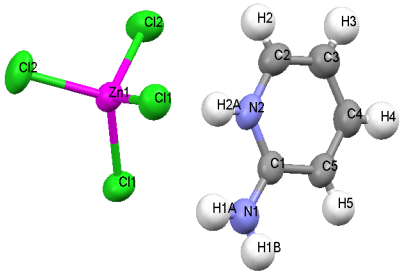
Unit cell parameters: *a*=8.3104(6)Å, *b*=14.1150(17)Å, *c*=13.8427(10)Å
Alpha(α)=90º, Beta(β)=93.641(6)º, Gamma(γ)=90º
Space Group: *C*2/*c*

The asymmetric unit contains one cation and half an anion (see **Figure 20(a.)**), with the Zn atom at the special position (0; 0.039423; 0.25). The second half of the anion is generated through symmetry operations. The 2-aminopyridinium cation is planar and protonated at N2 (pyridine N) as opposed to N1 (amine N). The anion is isolated and adopts a slightly distorted tetrahedral geometry, with Cl1-Zn1-Cl2 at 109.81° and Cl2-Zn-Cl2 at 109.41° differing from 104.5° and Cl1-Zn1-Cl2 at 104.40° and Cl2-Zn1-Cl1 at 104.40° very close to 104.5°. The unit cell of **2ampZnCl** contains eight 2-aminopyridinium cations and four $ZnCl_4^{2-}$ anions, as shown in **Figure 20(b.)**.

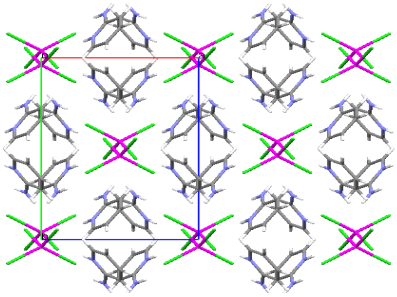
The structure is layered in that there is a layer of 2-aminopyridinium organic cations separated by a layer of isolated and distorted tetrahedral $ZnCl_4^{2-}$ anions, as illustrated in **Figure 20(c.)**. In the organic layer adjacent cations pack in pairs in a head-to-tail arrangement. When viewed down the *a*-axis it is observed that neighbouring organic layers alternate in the orientation of the cation pairs.

Interactions between the inorganic and organic parts are dominated by charge assisted hydrogen-bonds of the type **pyrNH···X** and **amineNH···X** and occur between Cl2 and H2A (2.608Å) and Cl1 and H1A (2.431Å) respectively (see **Figure 20(d.)**). The **amineNH···X** interaction is shorter, hence stronger than the **pyrNH···X** type of interaction. (See yellow highlighted sections in **Table 12.**)

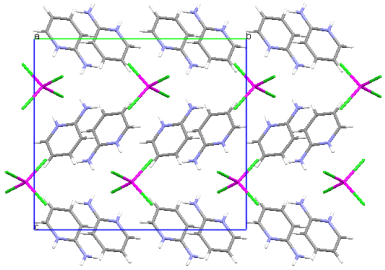
Adjacent cation pairs are oriented anti-parallel (see **Figure 20(e.)**) with a centroid-to-centroid distance of 4.250Å, greater than the accepted cut-off distance of 3.8Å for significant aromatic interactions (Janiac, 2000).



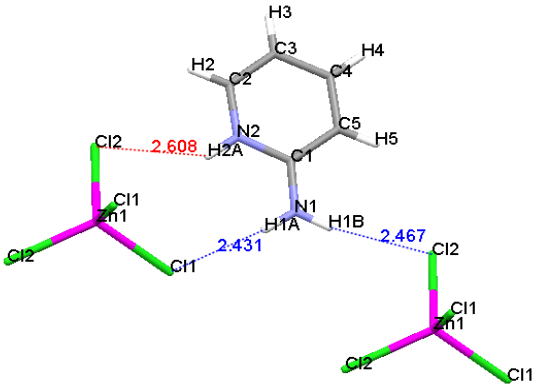
(a.)



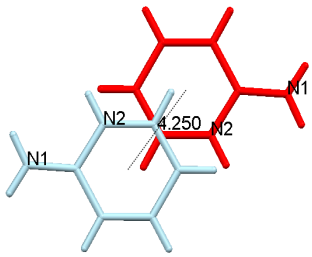
(b.)



(c.)



(d.)



(e.)

Figure 20: (a.) Asymmetric unit of **2ampZnCl** (full anion is shown for clarity). **(b.)** Crystal structure of **2ampZnCl,** viewed down the *c*-axis. Isostructural to **2ampZnBr** and **2ampHgCl. (c.)** Crystal structure of **2ampZnCl**, viewed down the *a*-axis, showing the organic and inorganic layers. **(d.)** Hydrogen bonding interactions. **(e.)** Cation orientation.

3.2 Bis(2-aminopyridinium) tetrabromozincate(II)

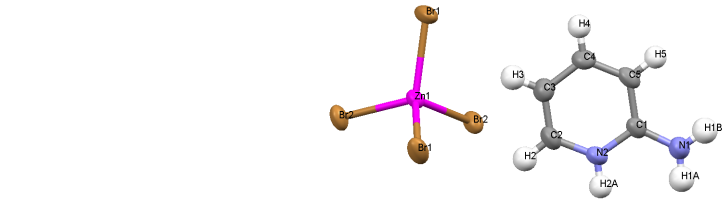
Chemical Formula: $(C_5H_7N_2^+)_2\ ZnBr_4^{2-}$

Unit cell parameters: *a*=15.3064(11), *b*=7.7064(6)Å, *c*=14.7911(10)Å

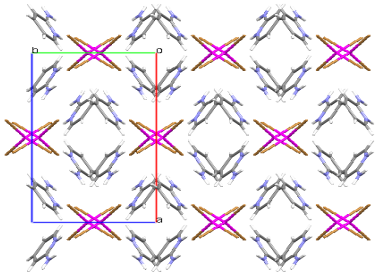
Alpha(α)=90º, Beta(β)=92.313(6)º, Gamma(γ)=90º

Space Group: *C*2/*c*

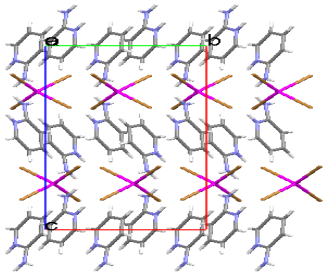
This structure is similar to that of **bis(2-aminopyridinium) tetrachlorozincate(II)** and will not be discussed in detail. The asymmetric unit and packing diagrams are shown below.



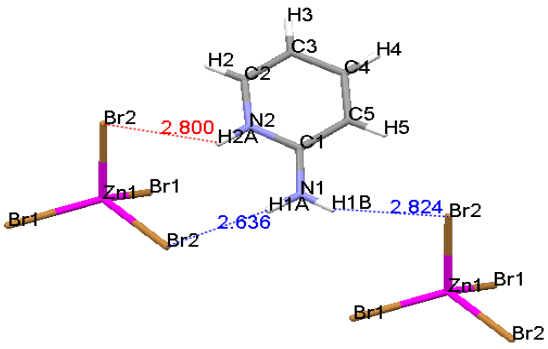
(a.)



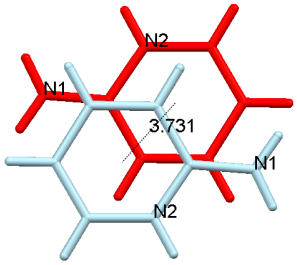
(b.)



(c.)



(d.)



(e.)

Figure 21: (a.) Asymmetric unit of **2ampZnBr** (full anion is shown for clarity). **(b.)** Crystal structure of **2ampZnBr,** viewed down the *c*-axis. Isostructural to **2ampZnCl** and **2ampHgCl. (c.)** Crystal structure of **2ampZnBr**, viewed down the *a*-axis, showing the organic and inorganic layers. **(d)** Hydrogen bonding interactions. **(e)** Cation orientation.

3.3 Bis(2-aminopyridinium) tetrachloromercurate(II)

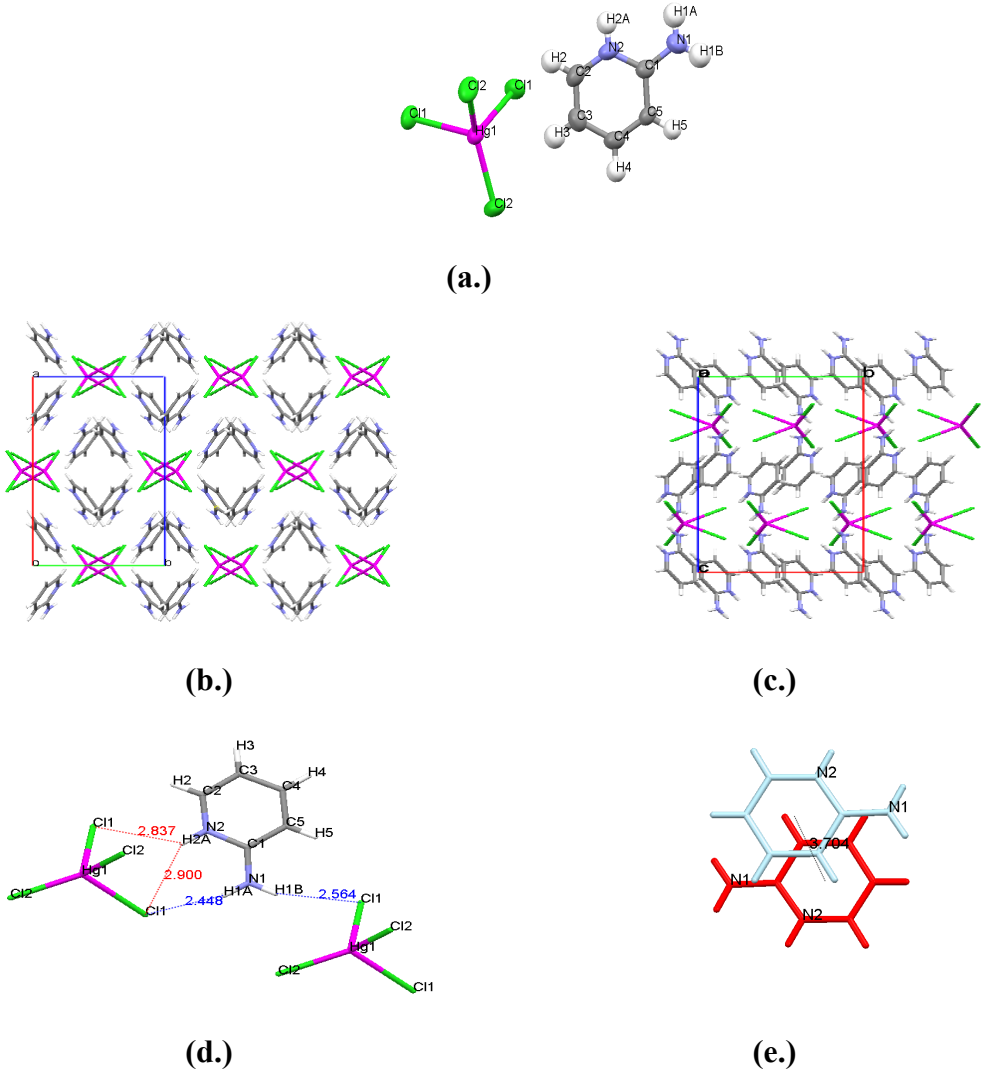
Chemical Formula: $(C_5H_7N_2^+)_2\ HgCl_4^{2-}$

Unit cell parameters: *a*=15.0298(8)Å, *b*=7.4925(4)Å, *c*=14.7577(9)Å

Alpha(α)=90º, Beta(β)=92.229(5)º, Gamma(γ)=90º

Space Group: *C*2/*c*

This structure is similar to that of **bis(2-aminopyridinium) tetrachlorozincate(II)** and will not be discussed in detail. The asymmetric unit and other structural characteristics are shown in **Figure 22.**



(a.) **(b.)** **(c.)** **(d.)** **(e.)**

Figure 22: (a.) Asymmetric unit of **2ampHgCl** (full anion is shown for clarity) **(b.)** Crystal structure of **2ampHgCl,** viewed down the *c*-axis. Isostructural to **2ampZnCl** and **2ampZnBr. (c.)** Crystal structure of **2ampHgCl**, viewed down the *a*-axis, showing the organic and inorganic layers **(d.)** Hydrogen bonding interactions. **(e.)** Cation orientation.

3.4 Bis(2-aminopyridinium) tetraiodozincate(II)

Chemical Formula: $(C_5H_7N_2^+)_2\ ZnI_4^{2-}$

Unit cell parameters: *a*=35.2785(8)Å, *b*=7.6246(2)Å, *c*=22.6941(5)Å

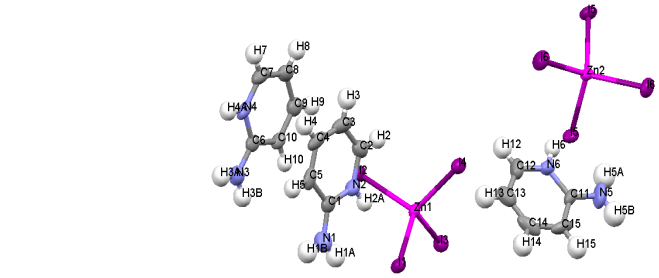
Alpha(α)=90º, Beta(β)=108.5920(10)º, Gamma(γ)=90º

Space Group: *C*2/*c*

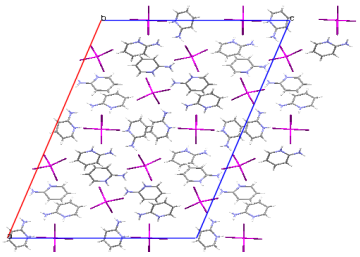
The asymmetric unit of **2ampZnI** contains three crystallographically independent 2-aminopyridinium cations and one and a half isolated zinc tetraiodide anions. Atom Zn2 occupies a special position at (0, 0.740101, 0.75), with the rest of the second anion generated by symmetry operations. The 2-aminopyridinium cations are protonated at N2, N4 and N6 (pyridine N), and display a planar geometry. Both anions are isolated with a slightly distorted tetrahedral geometry. The Zn1 anion has the following bond angles: I1-Zn1-I2 at 107.06°, I2-Zn1-I3 at 112.31°, I1-Zn1-I4 at 106.52°, I3-Zn1-I4 at 110.52° and I1-Zn1-I3 at 108.64°. The Zn2 anion, has similar bond angles with I5-Zn2-I5 at 111.38°, I5-Zn2-I6 at 109.96°, I5-Zn2-I6 at 105.73° and I6-Zn2-I6 at 114.18°. The unit cell of **2ampZnI** contains twelve asymmetric units, thus twenty-four 2-aminopyridinium cations and twelve ZnI_4^{2-} anions.

A layered structure is formed, with the 2-aminopyridinium cations packing in the organic layer, and the isolated and distorted tetrahedral ZnI_4^{2-} anions forming the inorganic layer. Interactions between the inorganic and organic parts are dominated by charge assisted hydrogen-bonds of the type **pyrNH···X** and **amineNH···X** that are relatively long as shown in See **Figure 23(d.)**. The shortest of each interaction occur between I1 and H2A (2.807Å) and I1 and H3B (3.017Å) respectively.

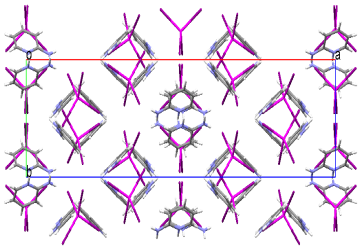
Two types of π-π stacking orientations are observed for the three types of cations in the structure. Adjacent cations are stacked head-to-tail (cations containing N6 form a pair, shown in **Figure 23(e.)**) or are slightly rotated relative to each other (cations containing N2 and N4 form a stack, shown in **Figure 23(f.)**). The shortest centroid- to-centroid distance is 3.546Å, for the head- to- tail stack and 3.689Å for the second stack, where the cations are slightly rotated relative to each other. Both are within the accepted distance for π-π interactions (<3.8Å).



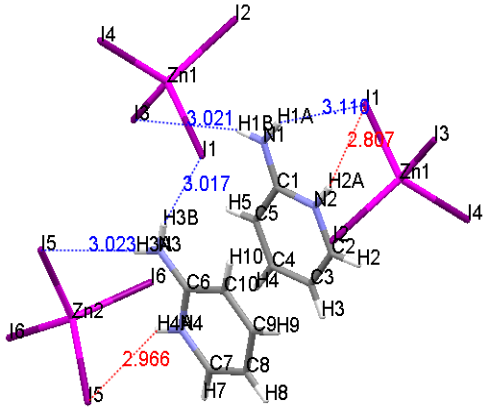
(a.)



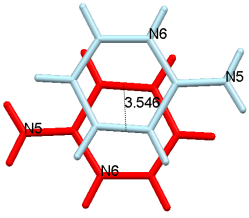
(b.)



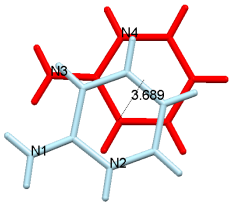
(c.)



(d.)



(e.)



(f.)

Figure 23: (a.) Asymmetric unit of **2ampZnI** (full anion is shown for clarity)**. (b.)** Crystal structure of **2ampZnI**, viewed down the *b*-axis. **(c.)** Structure viewed down the *c*-axis. **(d.)** Hydrogen bonding interactions. **(e.)** and **(f.)** Cation orientation.

3.5 Bis(2-aminopyridinium) tetraiodocadmate(II)

Chemical Formula: $(C_5H_7N_2^+)_2CdI_4^{2-}$

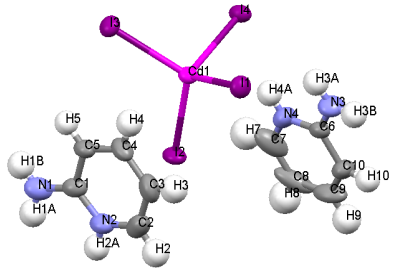
Unit cell parameters: *a*=8.2597(3)Å, *b*=8.7807(3)Å, *c*=15.5171(5)Å
Alpha(α)=81.9790(10)º, Beta(β)=82.1140(10)º,
Gamma(γ)=63.1230(10)º

Space Group: $P\bar{1}$

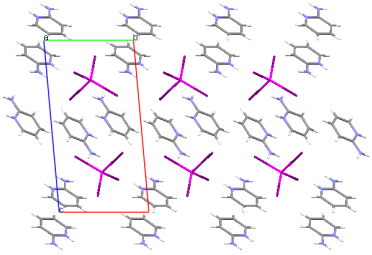
The asymmetric unit of **2ampCdI** contains two crystallographically independent 2-aminopyridinium cations and one isolated tetrahedral tetraiodocadmate anion, while the unit cell contains four cations and two anions. The 2-aminopyridinium cations are protonated at N2 and N4 (pyridine portion) as opposed to N1 and N3 (amino portion). The unit cell of **2ampCdI** contains four 2-aminopyridinium cations and two CdI_4^{2-} anions (See **Figure 24(b.)**).

The structure is layered in that there is a layer of 2-aminopyridinium organic cations separated by a layer of isolated and distorted tetrahedral CdI_4^{2-} anions. It is interesting that two different types of organic layers are formed. In the first organic layer the aromatic rings pack in a single layer, i.e. the layer is interdigitated, while the second type of organic layer contains two rows of aromatic groups, thus non-interdigitated (See **Figure 24 (b.)**). Interactions between the inorganic and organic parts are dominated by charge assisted hydrogen-bonds of the type **pyrNH···X** and **amineNH···X** and occur between I4 and H4A (2.784Å) and I1 and H1B (3.003Å) respectively (see **Figure 46**). The **pyrNH···X** is shorter, hence stronger than the **amineNH···X** type of interaction (see blue highlighted sections in **Table 12.**)

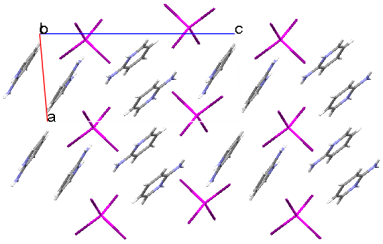
Pairs of adjacent N1 containing cations stack head-to-tail with the shortest centroid-to-centroid interaction at a distance of 3.514Å (see **Figure 24(e.)**), which is within the accepted range (3.3-3.8Å) for significant aromatic interactions (Janiac, 2000). The second pair of cations, containing N3 are slipped with a centroid-to-centroid distance of 4.188Å (see **Figure 24(f.)**).



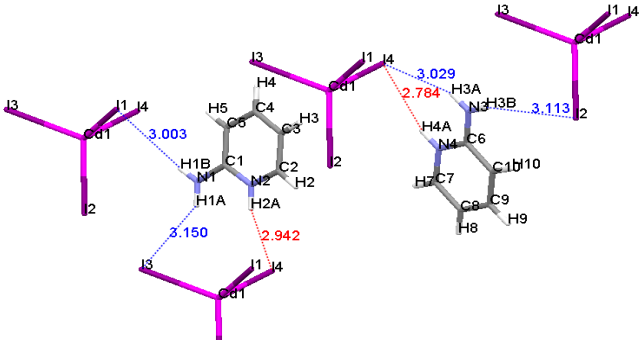
(a.)



(b.)



(c.)



(d.)



(e.) **(f.)**

Figure 24: (a.) Asymmetric unit of **2ampCdI** (full anion is shown for clarity). **(b.)** Crystal structure of **2ampCdI**, viewed down the *a*-axis. Isostructural to **2ampHgI. (c.)** Structure viewed down the *b*-axis. **(d.)** Hydrogen bonding interactions. **(e.)** and **(f.)** Cation orientation.

3.6 Bis(2-aminopyridinium) tetraiodomercurate(II)

Chemical Formula: $(C_5H_7N_2^+)_2\ HgI_4^{2-}$

Unit cell parameters: *a*=8.1780(4)Å, *b*=8.7740(4)Å, *c*=15.4043(7)Å

Alpha(α)=82.124(2)º, Beta(β)=82.261(2)º, Gamma(γ)=63.168(2)º

Space Group: $P\bar{1}$

This structure is isostructural to that of **bis(2-aminopyridinium) tetraiodocadmate(II)** and will not be discussed in detail. The asymmetric unit and other structural characteristics are shown in **Figure 25.**

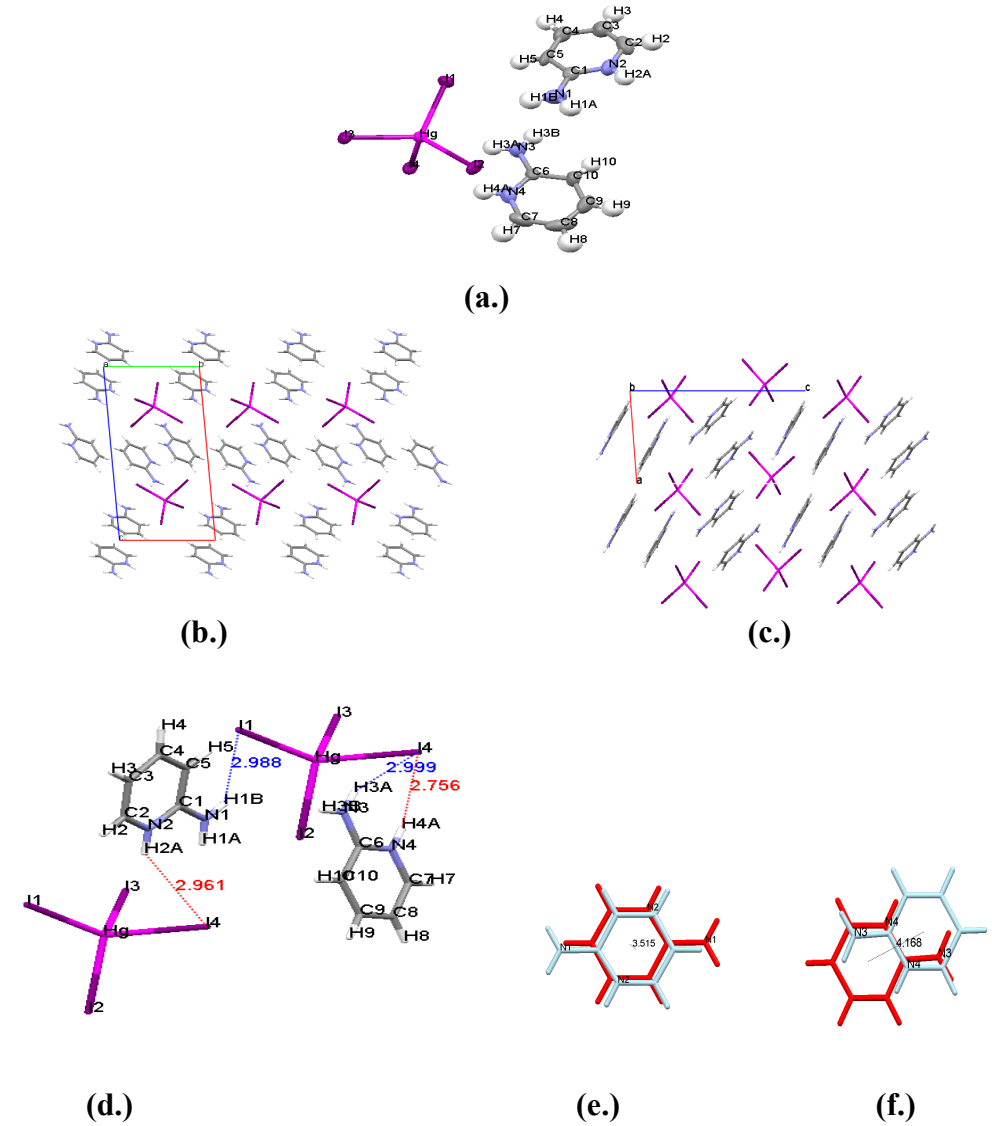


Figure 25: (a.) Asymmetric unit of **2ampHgI. (b.)** Crystal structure of **2ampHgI**, viewed down the *a*-axis. (Isostructural to **2ampCdI**). **(c.)** Structure viewed down the *b*-axis. **(d.)** Hydrogen bonding interactions. **(e.)** and **(f.)** Cation orientation.

3.7 Bis(2-aminopyridinium) tetrabromomercurate(II)

Chemical Formula: $(C_5H_7N_2^+)_2HgBr_4^{2-}$

Unit cell parameters: *a*=6.9651(5)Å, *b*=14.3009(10)Å, *c*=17.7646(13)Å

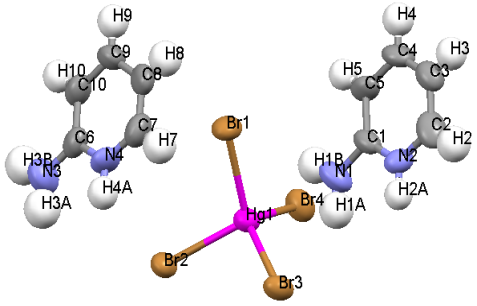
Alpha(α)=90º, Beta(β)=90º, Gamma(γ)=97.856(4)º

Space Group: $P2_1/c$

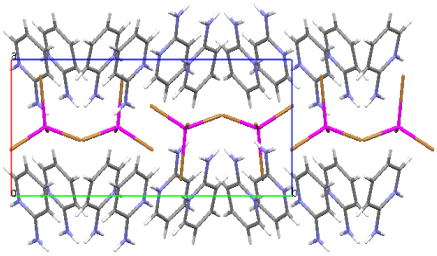
The asymmetric unit of **2ampHgBr** contains two crystallographically independent 2-aminopyridinium cations and one isolated tetrahedral tetrabromomercurate anion (see **Figure 26 (a.)**). The planar 2-aminopyridinium cations are protonated at N2 and N4 (pyridine portion) as opposed the amino portion (N1 and N3). The isolated anion displays a slightly distorted tetrahedral geometry, with Br1-Hg1-Br2 at 109.73°, Br1-Hg1-Br3 at 112.51°, Br1-Hg1-Br4 at 108.89°, Br2-Hg1-Br3 at 103.04° and Br2-Hg1-Br4 at 104.77°. The unit cell of **2ampHgBr** contains eight 2-aminopyridinium cations and four $HgBr_4^{2-}$ anions, as shown in **Figure 26 (c.)**.

The 2-aminopyridinium organic cations form the organic layers that alternate with layers containing the $HgBr_4^{2-}$ anions (see **Figure 26(b.)**). In the organic layer groups of four cations display the same orientation, but the organic layer is still interdigitated, i.e. aromatic rings pack in a single layer. Charge assisted hydrogen-bonds of the type **pyrNH···X** and **amineNH···X** occur between Br2 and H2A (2.772Å) and Br4 and H3A (2.593Å) respectively. Furthermore H1A has a bifurcated hydrogen bond with Br2 and Br3, viz 2.804Å and 3.017Å(see **Figure 26(d.)**.

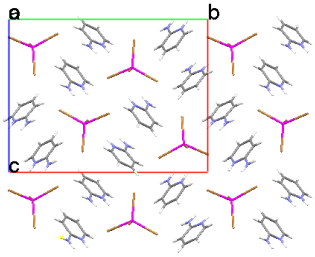
Two types of aromatic stacking interactions occur in the structure. Cations containing atoms N3 and N4, and N3 and N4 are stacked head-to-tail as shown in **Figure 26(e.)**, with a centroid-to-centroid distance of 3.876Å. A slipped interaction is formed between cations containing atoms N1 and N2, and N3 and N4 as illustrated in **Figure 26(f.)**, with a centroid-to-centroid distance of 4.132Å.



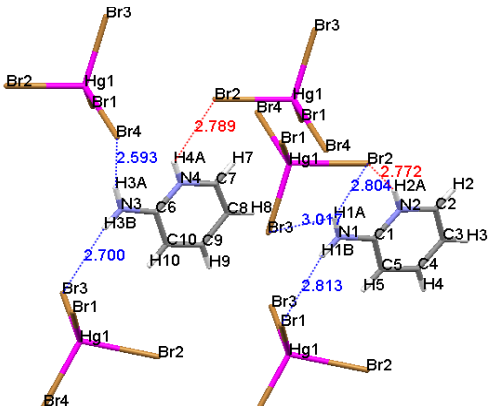
(a.)



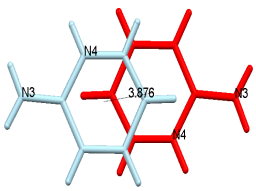
(b.)



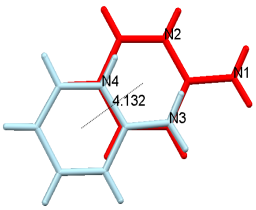
(c.)



(d.)



(e.)



(f.)

Figure 26: (a.) Asymmetric unit of **2ampHgBr**. **(b.)** Crystal structure of **2ampHgBr**, viewed down the *c*-axis. **(c.)** Structure viewed down the *a*-axis. **(d.)** Hydrogen bonding interactions. **(e.)** and **(f.)** Cation orientation.

3.8 Bis(3-aminopyridinium) tetrachlorozincate(II)

Chemical Formula: $(C_5H_7N_2^+)_2\ ZnCl_4^{2-}$

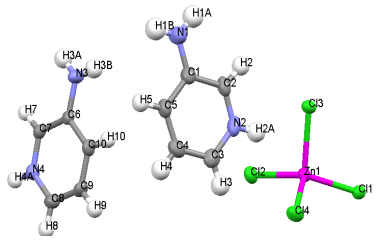
Unit cell parameters: *a*=6.8921(5)Å, *b*=8.4555(6)Å, *c*=13.8003(9)Å
Alpha(α)=99.008(6)º, Beta(β)=89.573(5)º,
Gamma(γ)=100.194(6)º

Space Group: $P\bar{1}$

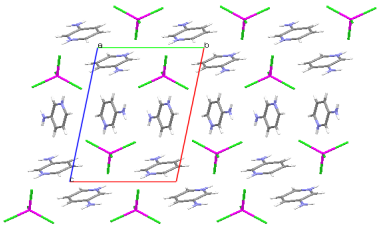
The asymmetric unit of **3ampZnCl** contains two planar, crystallographically independent 3-aminopyridinium cations and one isolated tetrahedral tetrachlorozincate anion as illustrated in **Figure 27(c.)**. The 3-aminopyridinium cations are protonated at N2 and N4 (pyridine portion) as opposed to N1 and N3 (amino portion). The unit cell of **3ampZnCl** contains four 2-aminopyridinium cations and two $ZnCl_4^{2-}$ anions as shown in **Figure 27(b.)**.

In the layered structure layers of 3-aminopyridinium organic cations alternate with layers of isolated and distorted tetrahedral $ZnCl_4^{2-}$ anions in the structure. Two types of organic layers are formed as shown in **Figure 27(b.)**, one organic layer is interdigitated, the other is non-interdigitated. Interactions between the inorganic and organic parts are dominated by charge assisted hydrogen-bonds of the type **pyrNH···X** and **amineNH···X** and occur between Cl3 and H2A (2.454Å) and Cl2 and H1A (2.553Å) respectively. Furthermore H4A has a bifurcated hydrogen bond with Cl1 and Cl1, viz 2.653Å and 2.672Å (see **Figure 27(d.).**

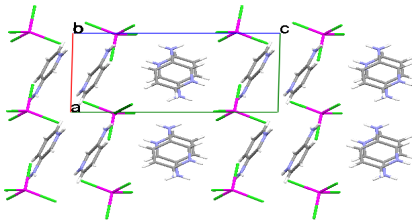
Adjacent cations are head to tail (see **Figure 27(e.)**) with a centroid-to-centroid distance of 3.672Å for the N3 and N4, and N3 and N4 pair, which is within the accepted range of 3.3-3.8Å for significant aromatic interactions (Janiac, 2000). For the N1 and N2, and N1 and N2 pair of cations, the centroid-to-centroid distance is 3.892Å.



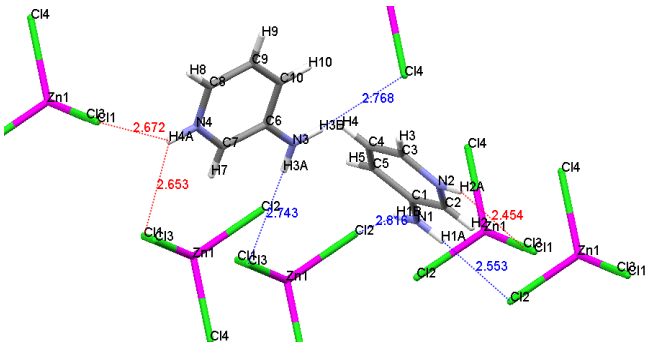
(a.)



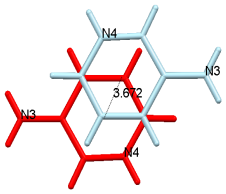
(b.)



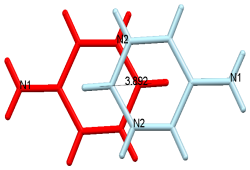
(c.)



(d.)



(e.)



(f.)

Figure 27: (a.) Asymmetric unit of **3ampZnCl. (b.)** Crystal structure of **3ampZnCl**, viewed down the *a*-axis, showing the organic and inorganic layers. **(c.)** Structure viewed down *b*-axis. **(d.)** Charge assisted intermolecular interactions in the crystal structure of **3ampZnCl**. **(e.)** and **(f.)** Cation orientation.

3.9 Bis(3-ammoniopyridinium) tetrabromozincate(II) monohydrate

Chemical Formula: $C_5H_8N_2^{2+}$ $ZnBr_4^{2-}$ ·H_2O

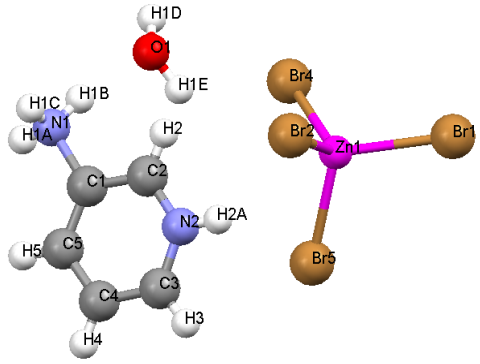
Unit cell parameters: *a*=7.017(2)Å, *b*=7.766(2)Å, *c*=23.380(7)Å
Alpha(α)=89.929(15)º, Beta(β)=89.840(18)º,
Gamma(γ)=85.701(7)º

Space Group: $P2_1/c$

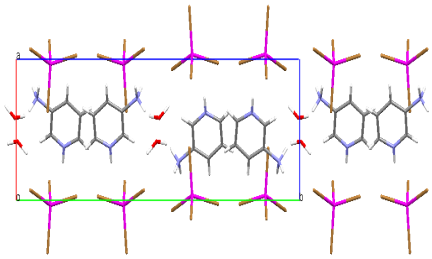
The asymmetric unit of **3ampZnBr·H_2O** contains one 3-ammoniopyridinium cation, one isolated tetrahedral tetrabromozincate anion and an isolated water molecule (**Figure 28(a.)**). The planar cation is protonated at both the N2 (pyridine portion) and N1 (amino portion). The unit cell of **3ampZnBr·H_2O** contains four 3-ammoniopyridinium cations, four $ZnBr_4^{2-}$ anions and four water molecules (see **Figure 28(b.)**).

The structure is layered in that pairs of 3-ammoniopyridinium organic cations pack with water molecules in a single layer and are separated by a layer of isolated and distorted tetrahedral $ZnBr_4^{2-}$ anions as illustrated in **Figure 28(c.)**. The anions are slightly distorted with Br1-Zn1-Br2 at 105.85°, Br2-Zn1-Br3 at 109.65°, Br1-Zn1-Br3 at 110.44°, Br3-Zn1-Br4 at 104.91° and Br1-Zn1-Br4 at 111.97°. Charge assisted hydrogen-bonds of the type **pyrNH···X** and **amineNH···X** occur between atoms Br5 and H2A (2.479Å) and Br4 and H1C (2.554Å) respectively. In addition atom H1A forms a bifurcated hydrogen bond with atoms Br1 and Br2, viz 2.964Å and 2.683Å. The water molecule acts as both a hydrogen bond donor and a hydrogen bond acceptor. **Water-H···X-M-Anion** interactions occur between Br1 and H1D (2.345Å), and **Cation-N-H···O-Water** interactions are present between the amino nitrogen and water molecule, forming an **amineNH···O** type interaction of 1.893Å between O1 and H1B (see **Figure 28(d.)**).

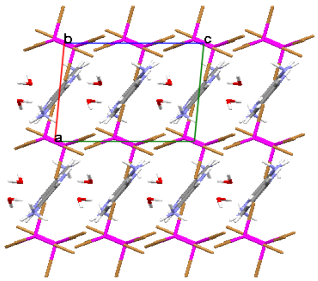
Adjacent cations pack in pairs, with the molecular ions rotated relative to each other (see **Figure 28 (e.)**) exhibiting a centroid-to-centroid distance of 5.271Å, exceeding the accepted cut-off distance of 3.8Å (Janiac, 2000) for significant aromatic interactions.



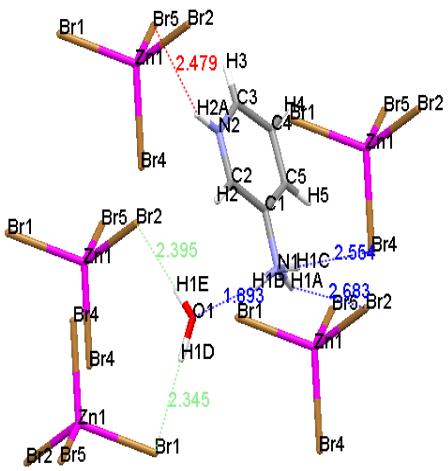
(a.)



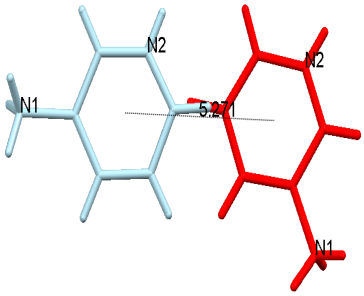
(b.)



(c.)



(d.)



(e.)

Figure 28: (a.) Asymmetric unit of **3ampZnBr·H₂O. (b.)** Crystal structure of **3ampZnBr·H₂O**, viewed down the *c*-axis **(c.)** Structure viewed down *b*-axis. **(d.)** Charge assisted intermolecular interactions in the crystal structure of **3ampZnBr·H₂O**. **(e.)** Cation orientation.

3.10 Bis(3-ammoniopyridinium) tetraiodomercurate(II) monohydrate

Chemical Formula: $C_5H_8N_2^{2+}$ $HgI_4^{2-}\cdot H_2O$

Unit cell parameters: *a*=8.3752(2)Å, *b*=14.7432(3)Å, *c*=12.1260(3)Å

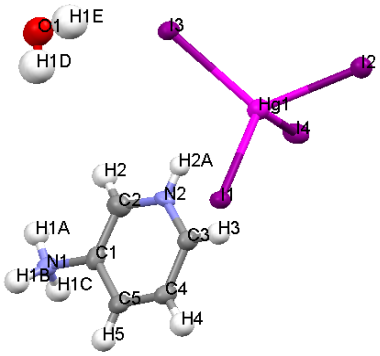
Alpha(α)=90º, Beta(β)=93.663(2)º, Gamma(γ)=90º

Space Group: $P2_1/n$

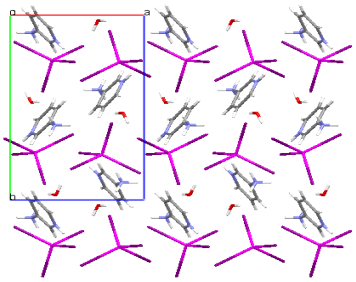
The asymmetric unit of **3ampHgI·H_2O** contains an isolated 3-ammoniopyridinium cation, an isolated tetrahedral tetraiodomercurate anion and an isolated water molecule. The 3-aminopyridinium cation adopts a planar geometry and is protonated at both the N2 (pyridine portion) and N1 (amino portion). The unit cell of **3ampHgI·H2O** contains four 3-ammoniopyridinium cations, four HgI_4^{2-} anions and four water molecules as shown in **Figure 29(a.).**

The structure consists of alternating organic and inorganic layers. The 3-ammoniopyridinium cations are separated by a layer of isolated and severely distorted tetrahedral HgI_4^{2-} anions, with I1-Hg1-I2 at 107.22º, I1-Hg1-I3 at 110.37º, I1-Hg1-I4 at 116.85º, I2-Hg1-I4 at 102.52º and I2-Hg1-I3 at 114.78º (see **Figure 29(b.)**). Charge assisted hydrogen-bonds of the type **pyrNH···X** and **amineNH···X** and occur between atoms I1 and H2A (2.911Å) and I3 and H1B (2.837Å) respectively. H1A also has a bifurcated hydrogen bond with I2 and I4, viz 2.949Å and 3.116Å. The water molecule acts as both a hydrogen bond donor and a hydrogen bond acceptor. **Water-H···X-M-Anion** interactions occur between I2 and H1D (3.071Å). **Cation-N-H···O-Water** interactions involving the ammonio nitrogen, forming an **amineNH···O** type interaction of 1.833Å between atoms O1 and H1C (see **Figure 29(d)**).

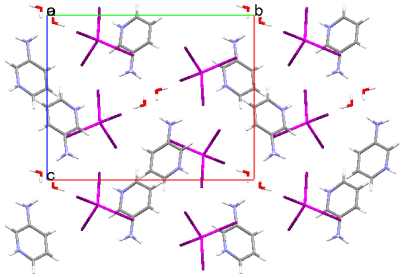
Adjacent cations are stacked rotated relative to each other (see **Figure 29(e.)**) with a centroid to centroid distance of 5.374Å, which is significantly larger than 3.8Å (cut-off distance for accepted pi-pi interactions). All intermolecular distances are similar to the reported crystal structure number **7, 3ampHgBr·H_2O** (Ali *et al*, 2008; TOBCOD). See **Table 7** on page 27**.**



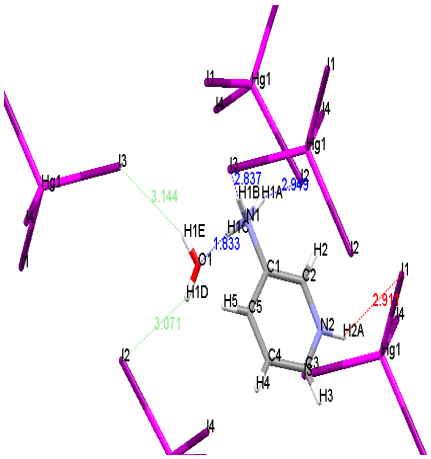
(a.)



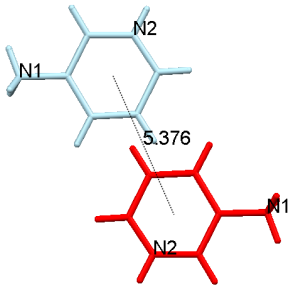
(b.)



(c.)



(d.)



(e.)

Figure 29: (a.) Asymmetric unit of **3ampHgI·H₂O. (b.)** Crystal structure of **3ampHgI·H₂O**, viewed down the *c*-axis. Space group $P2_1/n$. **(c.)** Structure viewed down the *a*-axis. **(d.)** Charge assisted intermolecular interactions in the crystal structure of **3ampHgI·H₂O**. **(e.)** Cation orientation.

3.11 Bis(4-aminopyridinium) tetrachlorozincate(II)

Chemical Formula: $(C_5H_7N_2^+)_2\ ZnCl_4^{2-}$

Unit cell parameters: *a*=7.1525(3)Å, *b*=14.9902(12)Å, *c*=14.9993(2)Å

Alpha(α)=90º, Beta(β)=90º, Gamma(γ)=90º

Space Group: $P2_12_12_1$

The asymmetric unit of **4ampZnCl** contains two crystallographically independent 4-aminopyridinium cations and one isolated tetrahedral tetrachlorozincate anion. The planar 4-aminopyridinium cations are protonated at N2 and N4 (pyridine portion) as opposed to N1 and N3 (amino portion). The unit cell of **4ampZnCl** contains eight 4-aminopyridinium cations and four $ZnCl_4^{2-}$ anions (see **Figure 30(a.)**).

The 4-aminopyridinium organic cations pack in the organic layer and alternate with a layer of isolated and slightly distorted tetrahedral $ZnCl_4^{2-}$ anions, with Cl-Zn1-Cl2 at 106.26°, Cl1-Zn1-Cl3 at 111.98°, Cl1-Zn1-Cl4 at 105.82°, Cl3-Zn1-Cl4 at 107.07° and Cl2-Zn1-Cl3 at 115.79°. (see **Figure 30(b.)).** Non-covalent interactions include charge assisted hydrogen-bonds of the type **pyrNH···X** and **amineNH···X** and between atoms Cl4 and H2 (2.514Å) and atoms Cl3 and H1B (2.472Å) respectively. In this structure the **amineNH···X** is shorter, hence stronger than the **pyrNH···X** type of interaction (see pink highlighted sections in **Table 14** on page 76.)

Pairs of cations are packed rotated relative to each other (see **Figure 30(e.)**). The centroid-to centroid distance between the cations containing atoms N1 and N2 is 4.565Å, which is significantly larger than the aromatic interaction cut-off distance of 3.8Å (Janiac, 2000). Pairs of cations containing atoms N3 and N4 display a centroid-to-centroid distance of 4.600Å.

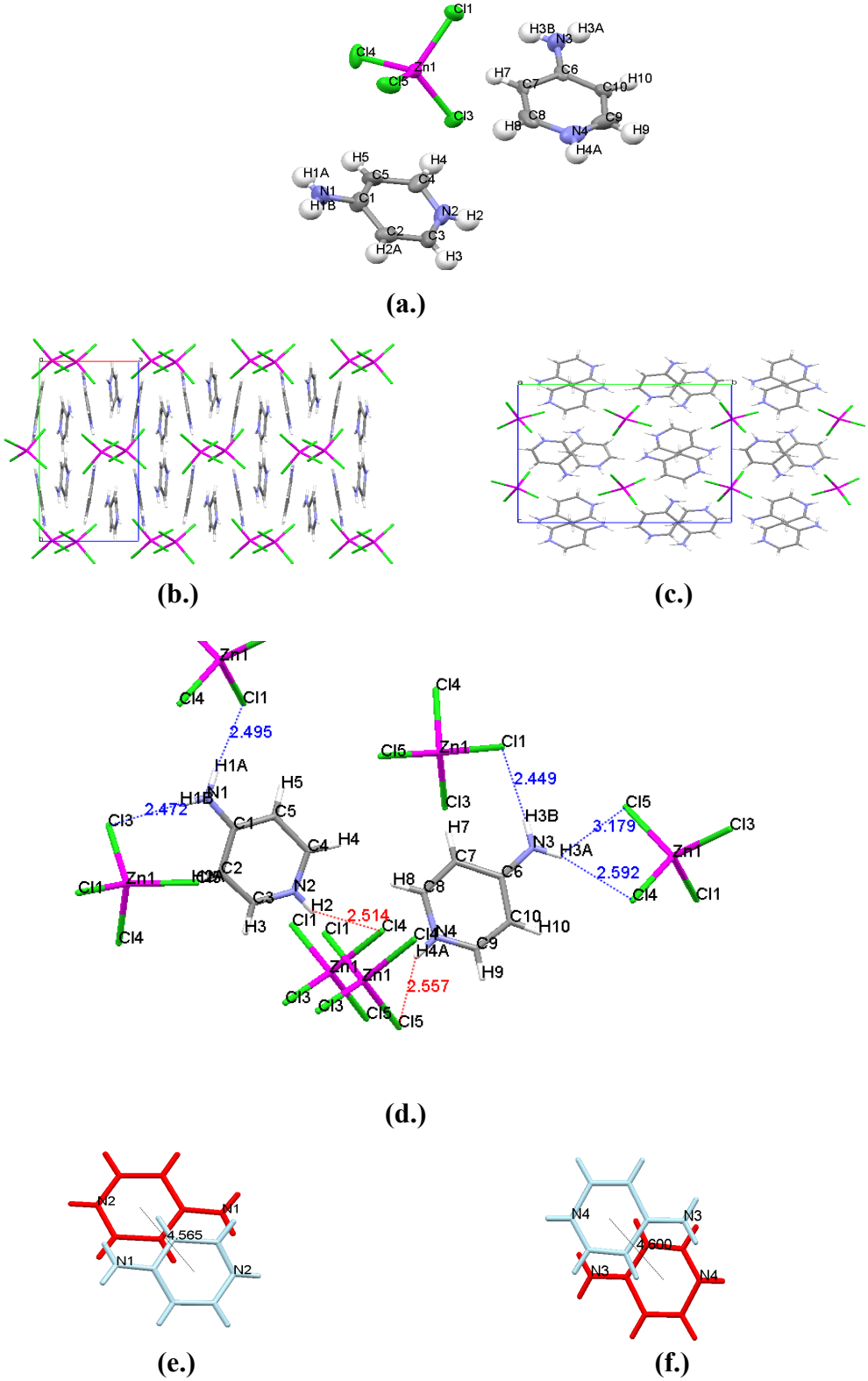


Figure 30: (a.) Asymmetric unit of **4ampZnCl. (b.)** Crystal structure of **4ampZnCl**, viewed down the *c*-axis. Space group $P2_12_12_1$. Isostructural to **4ampZnBr** and **4ampZnI. (c.)** Structure viewed down the *a*-axis. **(d.)** Intermolecular interactions. **(e.)** and **(f.)** Cation orientation.

3.12 Bis(4-aminopyridinium) tetrabromozincate(II)

Chemical Formula: $(C_5H_7N_2^+)_2\ ZnBr_4^{2-}$

Unit cell parameters: *a*=7.3747(7)Å, *b*=15.4569(13)Å, *c*=15.4716(13)Å

Alpha(α)=90º, Beta(β)=90º, Gamma(γ)=90º

Space Group: $P2_12_12_1$

This structure is isostructural to **bis(4-aminopyridinium) tetrachlorozincate(II)** and will not be discussed in detail. The asymmetric unit and other structural characteristics are shown in **Figure 31.**

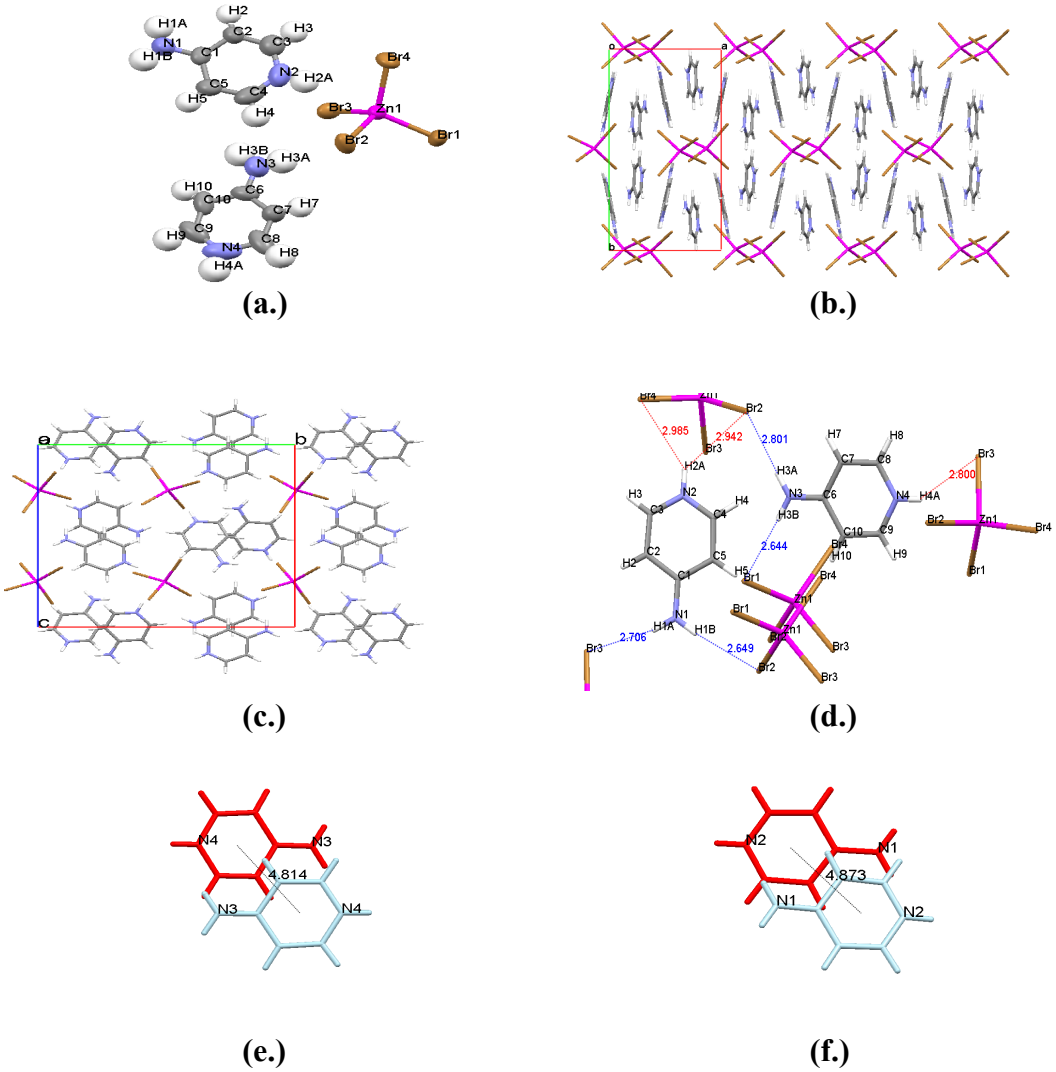


Figure 31: (a.) Asymmetric unit of **4ampZnBr. (b.)** Crystal structure of **4ampZnBr**, viewed down the *c*-axis. Space group $P2_12_12_1$. Isostructural to **4ampZnCl** and **4ampZnI**. **(c.)** Structure viewed down *a*-axis. **(d.)** Intermolecular interactions. **(e.)** and **(f.)** Cation orientation.

3.13 Bis(4-aminopyridinium) tetraiodozincate(II)

Chemical Formula: $(C_5H_7N_2^+)_2\ ZnI_4^{2-}$

Unit cell parameters: *a*=7.5844(4)Å, *b*=16.0413(7)Å, *c*=16.0410(5)Å

Alpha(α)=90º, Beta(β)=90º, Gamma(γ)=90º

Space Group: $P2_12_12_1$

This structure is isostructural to that of **bis(4-aminopyridinium tetrachlorozincate(II)** and will not be discussed in detail. The asymmetric unit and other structural characteristics are shown in **Figure 32.**

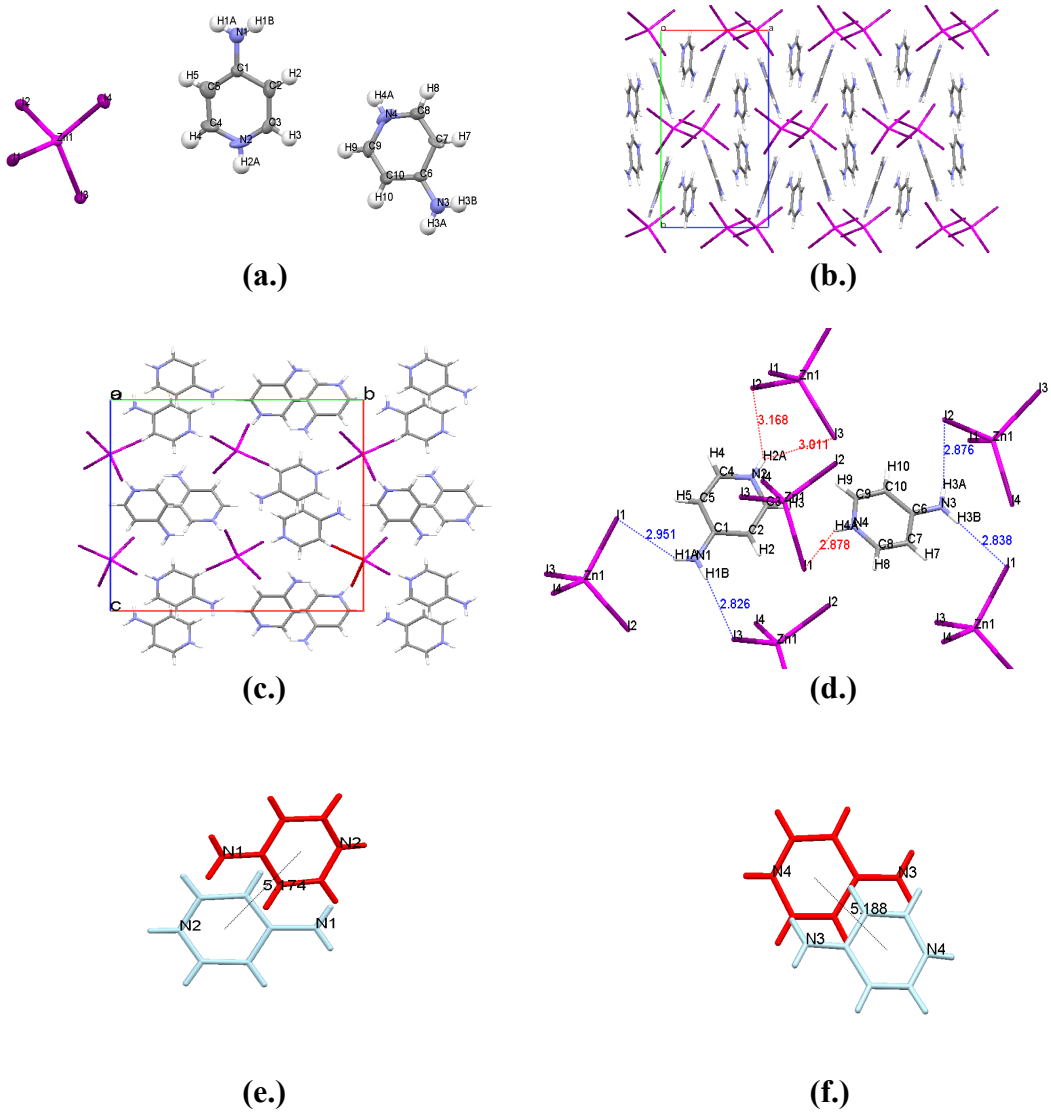


Figure 32: (a.) Asymmetric unit of **4ampZnI. (b.)** Crystal structure of **4ampZnI**, viewed down the c-axis. Space group $P2_12_12_1$. Isostructural to **4ampZnCl** and **4ampZnBr**. **(c.)** Structure viewed down *a*-axis. **(d.)** Intermolecular interactions. **(e.)** and **(f.)** Cation orientation.

3.14 Catena-(bis(4-aminopyridinium) bis(μ$_2$-chloro) dichlorocadmium(II) monohydrate)

Chemical Formula: $(C_5H_8N_2^+)_4Cd_2Cl_8^{4-}\cdot H_2O$

Unit cell parameters: *a*=7.496(5)Å, *b*=24.413(5)Å, *c*=12.453(5)Å

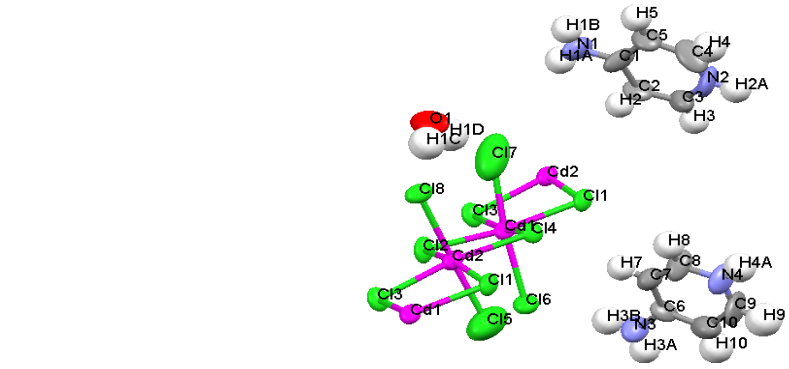
Alpha(α)=90º, Beta(β)=101.93(4)º, Gamma(γ)=90º

Space Group: $P2_1/c$

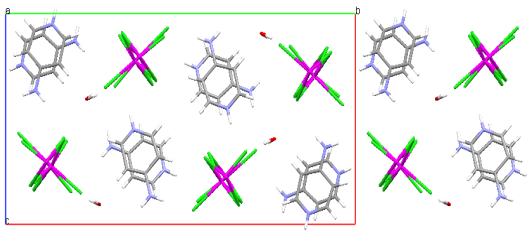
The asymmetric unit of **4ampCdCl·H$_2$O** contains two crystallographically independent 4-aminopyridinium cations, one $Cd_2Cl_8^{4-}$ unit and an isolated water molecule (see **Figure 33(a.)**). The 4-aminopyridinium cations are protonated at N2 and N4 (pyridine portion) as opposed to N1 and N3 (amino portion). The metal atom adopts an octahedral geometry, with neighbouring metal atoms sharing two bridging equatorial chloro ligands. The result of the face sharing is an infinite, one-dimensional perhalometallate polymeric anion. The unit cell of **4ampCdCl·H$_2$O** contains eight 4-aminopyridinium cations, four $Cd_2Cl_8^{4-}$ units and four water molecules (see **Figure 33(b.)**).

The structure is layered in that there is a layer of 4-aminopyridinium organic cations separated by a layer of polymeric one-dimensional perchlorocadmate anions (see **Figure 33(c.)**). Charge assisted hydrogen-bonds of the type **pyrNH···X** and **amineNH···X** occur between atoms Cl7 and H4A (2.009Å) and Cl6 and H3B (2.478Å) respectively. Furthermore water acts only as a hydrogen bond donor, such that a **Water-H···X-M-Anion** interaction occurs between Cl7 and H1D (1.809Å). There are no **Cation-N-H···O-Water** interactions (see **Figure 33(d.)**).

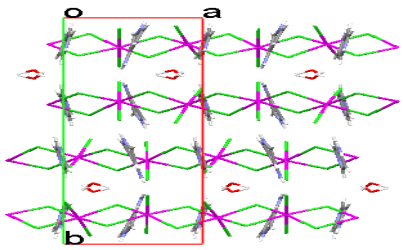
Pairs of cations are stacked rotated relative to each other. Only one type of stack is observed and occurs between N1 and N2, and N3 and N4 cations, with a centroid-to-centroid distance of 3.741Å (see **Figure 33(e.)**).



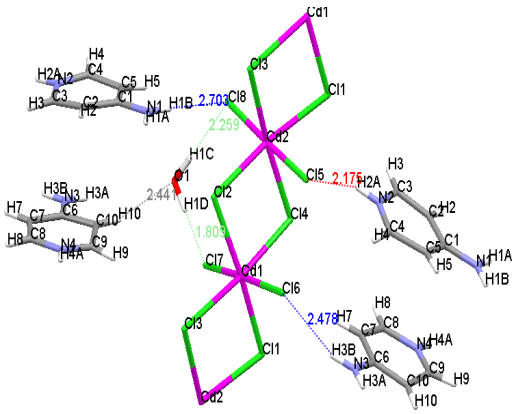
(a.)



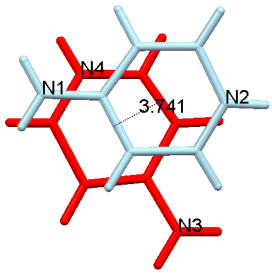
(b.)



(c.)



(d.)



(e.)

Figure 33: (a.) Asymmetric unit of **4ampCdCl·H₂O. (b.)** Crystal structure of **4ampCdCl·H₂O,** viewed down the *a*-axis. **(c.)** Structure viewed down *c*-axis. **(d.)** Charge assisted intermolecular interactions in the crystal structure of **4ampCdCl·H₂O**. **(e.)** Cation stacking, rotated relative to each other.

3.15 Bis(4-aminopyridinium) tetrabromocadmate(II) monohydrate

Chemical Formula: $(C_5H_8N_2^+)_2CdBr_4^{2-}\cdot H_2O$

Unit cell parameters: *a*=6.8746(12)Å, *b*=14.082(2)Å, *c*=18.842(3)Å

Alpha(α)=90º, Beta(β)=90º, Gamma(γ)=90º

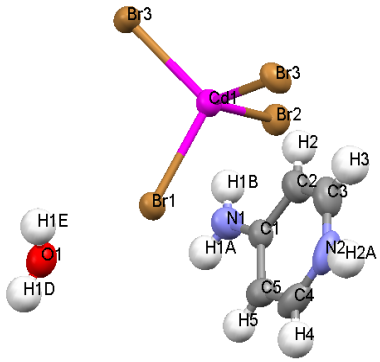
Space Group: *Pbcm*

Note that the crystal structure of **4ampCdBr·H_2O** has already been published and is present in the CSD, and is listed as structure number **8, 4ampCdBr·H_2O** (Hatano *et al*, 2008; POGHEZ) in the literature survey. However, the reported structure was incomplete because hydrogen atoms were not indicated on the oxygen atoms, resulting in incomplete water molecules. In the current study structure the positions of all the hydrogen atoms were determined.

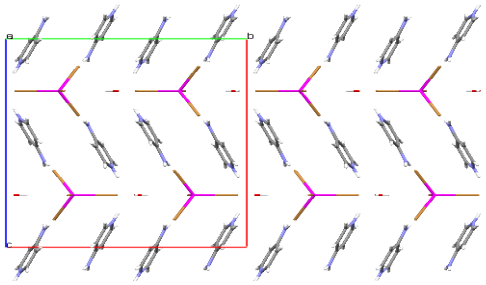
The asymmetric unit of **4ampCdBr·H_2O** contains one 4-aminopyridinium cation, one $CdBr_4^{2-}$ unit and an isolated water molecule. The cadmium atom is located at the position (0.482773, 0.720776, 0.250000) with the rest of the anion being generated by symmetry operators. The 4-aminopyridinium cation is protonated at N2 (pyridine portion) as opposed to N1 (amino portion). The unit cell of **4ampCdBr·H_2O** contains eight 4-aminopyridinium cations, four $CdBr_4^{2-}$ anions and four water molecules.

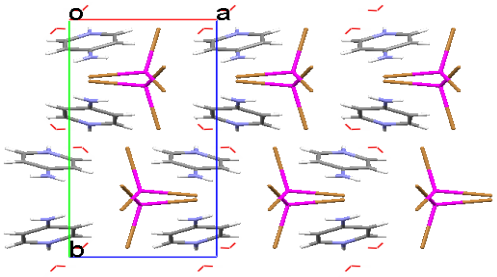
The structure is layered, with the organic layer containing the 4-aminopyridinium cations and water molecules and the inorganic layer the slightly distorted tetrahedral $CdBr_4^{2-}$ anions with Br1-Cd1-Br2 at 109.61º, Br1-Cd1-Br3 at 106.44º, Br2-Cd1-Br3 at 109.84º and Br3-Cd1-Br3 at 114.49º (see **Figure 34(c.)**). Interactions between the inorganic and organic parts are dominated by charge assisted hydrogen-bonds of the type **amineNH···X** and occur between Br3 and H1B (2.781Å) and Br3 and H1A (2.808Å) respectively. The water molecule acts as both a hydrogen bond donor and a hydrogen bond acceptor. **Water-H···X-M-Anion** occurs between Br2 and H1D (2.733Å). **Cation-N-H···O-Water**, occurs at the pyridine nitrogen, forming **pyrNH···O** interaction of 1.988Å between H2A and O1 (see **Figure 34(d.)**).

Adjacent cations are stacked head to tail (see **Figure 34(e.)**) with a centroid to centroid distance of 3.821Å, which is slightly larger than 3.8Å (cut-off distance for accepted π-π interactions).

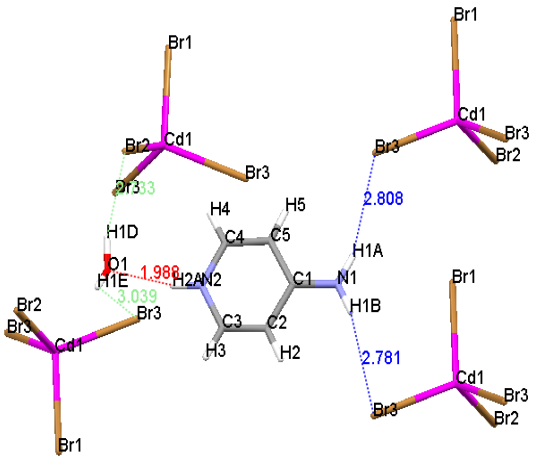


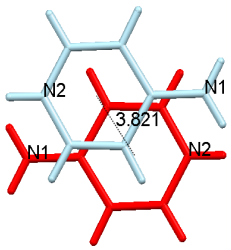
(a.)





(b.) **(c.)**





(d.) **(e.)**

Figure 34: (a.) Asymmetric unit of **4ampCdBr·H_2O** (full anion showed for clarity). **(b.)** Crystal structure of **4ampCdBr·H_2O**, viewed down the *a*-axis. Space group *Pbcm*. Isostructural to **4ampCdI·H_2O, 4ampHgCl·H_2O, 4ampHgBr·H_2O** and **4ampHgI·H_2O.** **(c.)** Structure viewed down *c*-axis. **(d.)** Charge assisted intermolecular interactions. **(e.)** Cation orientation.

3.16 Bis(4-aminopyridinium) tetraiodocadmate(II) monohydrate

Chemical Formula: $(C_5H_8N_2^+)_2CdI_4^{2-}\cdot H_2O$

Unit cell parameters: *a*=7.3983(3)Å, *b*=14.7586(7)Å, *c*=18.7562(10)Å

Alpha(α)=90º, Beta(β)=90º, Gamma(γ)=90º

Space Group: *Pbcm*

This structure is isostructural to **bis(4-aminopyridinium) tetrabromocadmate(II) monohydrate** and will not be discussed in detail. The asymmetric unit and other structural characteristics are shown in **Figure 35.**

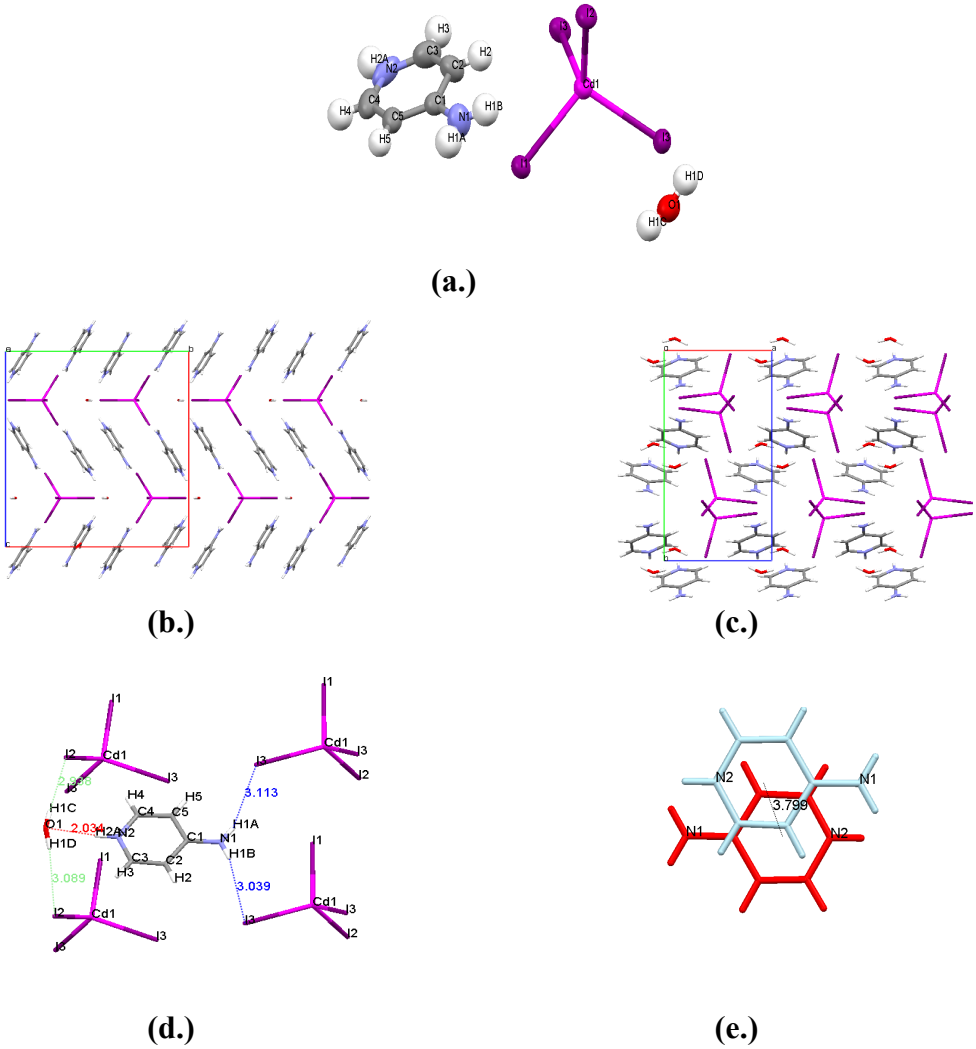


Figure 35: (a.) Asymmetric unit of **4ampCdI·H₂O. (b.)** Crystal structure of **4ampCdI·H₂O**, viewed down the *a*-axis. Space group *Pbcm.* Isostructural to **4ampCdBr·H₂O, 4ampHgCl·H₂O, 4ampHgBr·H₂O** and **4ampHgI·H₂O. (c.)** Structure viewed down *c*-axis. **(d.)** Charge assisted intermolecular interactions. **(e.)** Cation orientation.

3.17 Bis(4-aminopyridinium) tetrachloromercurate(II) monohydrate

Chemical Formula: $(C_5H_8N_2^+)_2HgCl_4^{2-}\cdot H_2O$

Unit cell parameters: *a*=6.5735(5)Å, *b*=13.6799(10)Å, *c*=18.7593(14)Å

Alpha(α)=90º, Beta(β)=90º, Gamma(γ)=90º

Space Group: *Pbcm*

This structure is isostructural to **bis(4-aminopyridinium) tetrabromocadmate(II) monohydrate** and will not be discussed in detail. The asymmetric unit and other structural characteristics are shown in **Figure 36.**

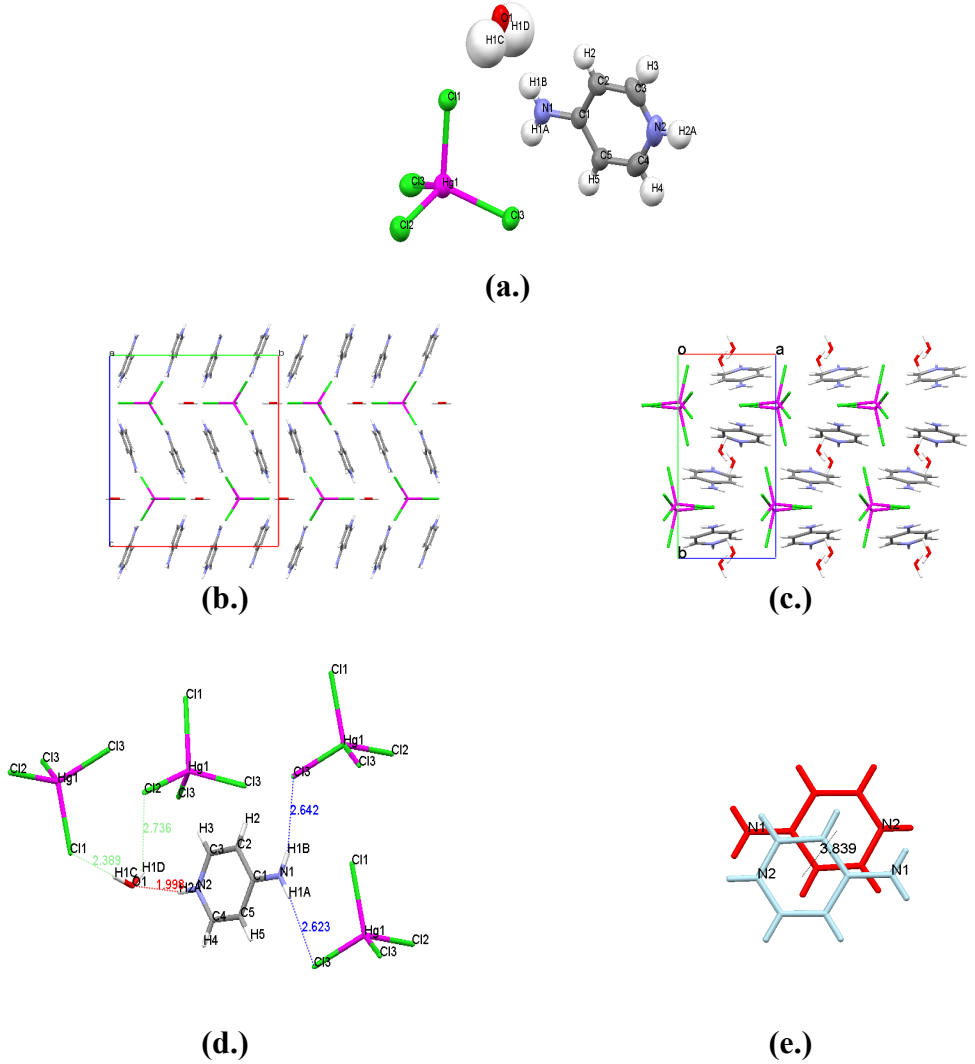


Figure 36: (a.) Asymmetric unit of **4ampHgCl·H₂O. (b.)** Crystal structure of **4ampHgCl·H₂O**, viewed down the *a*-axis. Space group *Pbcm.* Isostructural to **4ampCdBr·H₂O, 4ampCdI·H₂O, 4ampHgBr·H₂O** and **4ampHgI·H₂O. (c.)** Structure viewed down *c*-axis. **(d.)** Charge assisted intermolecular interactions. **(e.)** Cation orientation.

3.18 Bis(4-aminopyridinium) tetrabromomercurate(II) monohydrate

Chemical Formula: $(C_5H_8N_2^+)_2HgBr_4^{2-}\cdot H_2O$

Unit cell parameters: *a*=6.8625(3)Å, *b*=14.0041(6)Å, *c*=18.8161(9)Å

Alpha(α)=90º, Beta(β)=90º, Gamma(γ)=90º

Space Group: *Pbcm*

This structure is isostructural to **bis(4-aminopyridinium) tetrabromocadmate(II) monohydrate** and will not be discussed in detail. The asymmetric unit and other structural characteristics are shown in **Figure 37.**

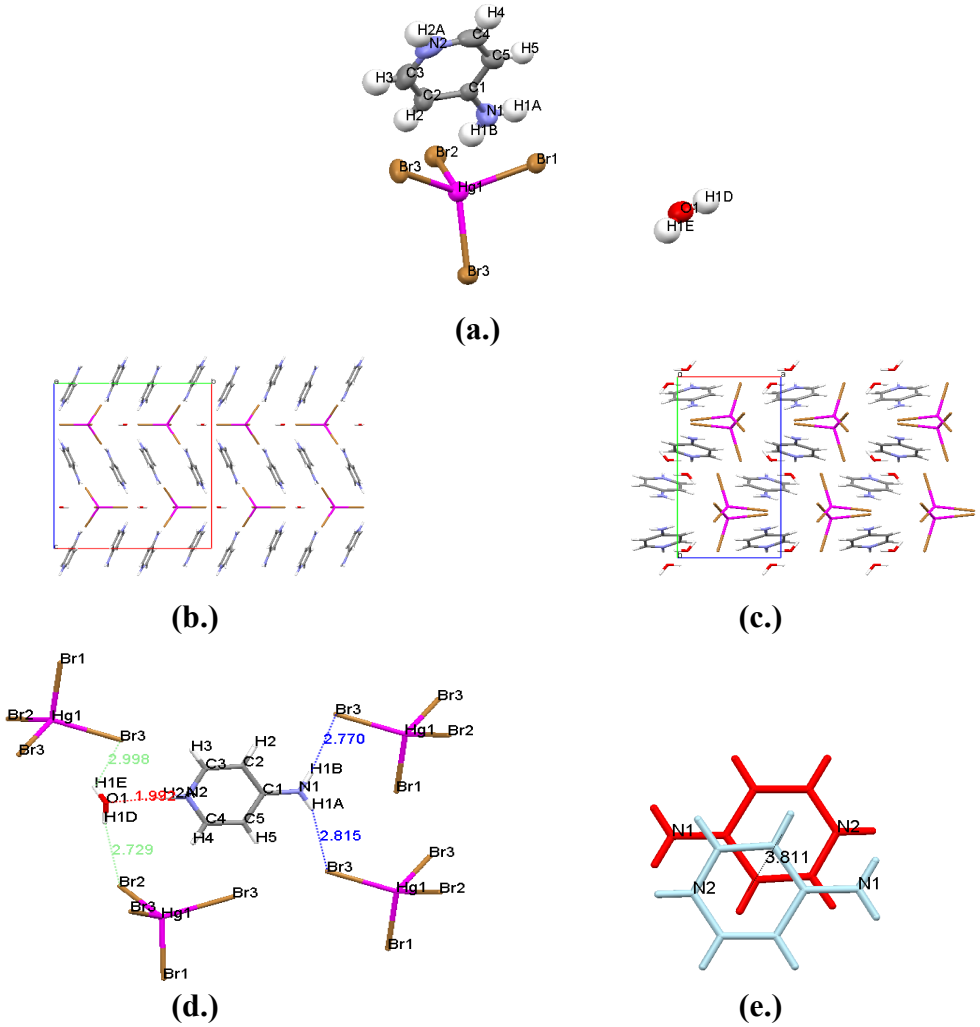


Figure 37: (a.) Asymmetric unit of **4ampHgBr·H₂O. (b.)** Crystal structure of **4ampHgBr·H₂O**, viewed down the *a*-axis. Space group *Pbcm*. Isostructural to **4ampHgCl·H₂O, 4ampCdBr·H₂O, 4ampCdI·H₂O** and **4ampHgI·H₂O. (c.)** Structure viewed down the *c*-axis. **(d.)** Charge assisted intermolecular interactions. **(e.)** Cation orientation.

3.19 Bis(4-aminopyridinium) tetraiodomercurate(II) monohydrate

Chemical Formula: $(C_5H_8N_2^+)_2HgI_4^{2-}\cdot H_2O$

Unit cell parameters: *a*=7.2736(4)Å, *b*=14.4831(7)Å, *c*=18.5793(8)Å

Alpha(α)=90º, Beta(β)=90º, Gamma(γ)=90º

Space Group: *Pbcm*

This structure is isostructural to **bis(4-aminopyridinium) tetrabromocadmate(II) monohydrate** and will not be discussed in detail. The asymmetric unit and other structural characteristics are shown in **Figure 38.**

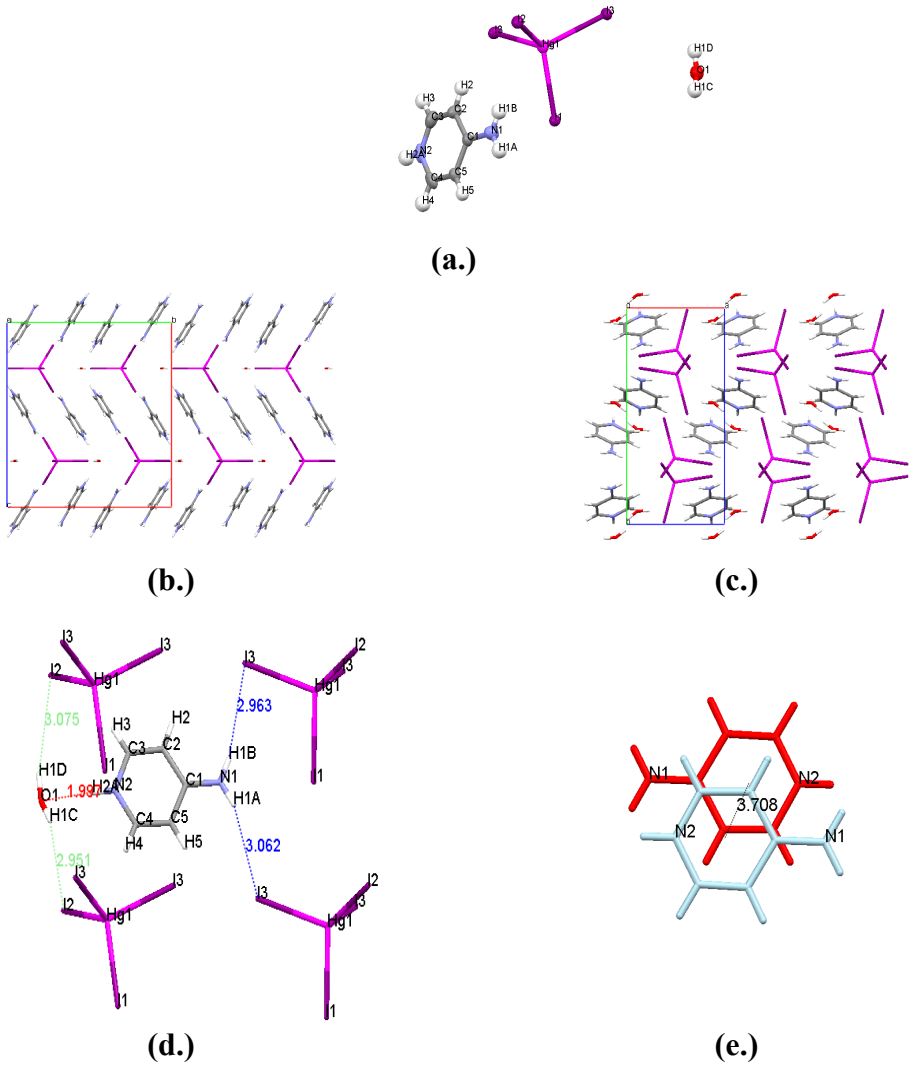


Figure 38: (a.) Asymmetric unit of **4ampHgI·H₂O. (b.)** Crystal structure of **4ampHgI·H₂O** , viewed down the *a*-axis. Space group *Pbcm*. Isostructural to **4ampHgCl·H₂O, 4ampHgBr·H₂O, 4ampCdBr·H₂O** and **4ampCdI·H₂O. (c.)** Structure viewed down c-axis. **(d.)** Charge assisted intermolecular interactions. **(e.)** Cation orientation.

Table 12: Selected Cg-Cg and Non-Covalent Intermolecular Distances of the the type d(H···A) for 2-aminopyridinium hybrids. Colour indicates isostructurality.

Hybrid	Perhallometallate Anion Geometry	Cg-Cg Distance (Å)	Shortest Cation-N-H···X-M-Anion Distance (Å)	
			pyrNH···X	amineNH···X
2ampZnCl	Isolated $ZnCl_4^{2-}$, distorted Tetrahedral	4.250	2.608	2.431
2ampZnBr	Isolated $ZnBr_4^{2-}$, distorted Tetrahedral	3.731	2.800	2.636
2ampZnI	Isolated ZnI_4^{2-}, distorted Tetrahedral	3.546 and 3.689	2.807	3.017
2ampCdI	Isolated CdI_4^{2-}, distorted Tetrahedral	4.188 and 3.514	2.784	3.003
2ampHgCl	Isolated $HgCl_4^{2-}$, distorted Tetrahedral	3.704	2.837 and 2.900 are bifurcated	2.448
2ampHgBr	Isolated $HgBr_4^{2-}$, distorted Tetrahedral	3.876 and 4.132	2.772	2.593; 2.804 and 3.017 are bifurcated
2ampHgI	Isolated HgI_4^{2-}, distorted Tetrahedral	3.515 and 4.168	2.757	2.987

Table 13: Selected Cg-Cg and Non-Covalent Intermolecular Distances of the the type d(H···A) for 3-aminopyridinium and 3-ammoniopyridinium hybrids. Isostructurality is indicated by colour. White blocks indicate no isostructural equivalent.

Hybrid	Perhallometallate Anion Geometry	Cg-Cg Distance (Å)	Shortest Cation-N-H···X-M-Anion Distance (Å)		Shortest Water-H···X-M-Anion Distance (Å)	Shortest Cation-N-H···O-Water Distance (Å)	
			pyrNH···X	amineNH···X		pyrNH···O	amineNH···O
3ampZnCl	Isolated $ZnCl_4^{2-}$, distorted Tetrahedral	3.672 and 3.892	2.454; 2.653 and 2.672 are bifurcated	2.553	No Water	No water	No water
3ampZnBr·H$_2$O	Isolated $ZnBr_4^{2-}$, distorted Tetrahedral	5.271	2.479	2.554; 2.683 and 2.964 are bifurcated	2.345	None	1.893
3ampHgI·H$_2$O	Isolated HgI_4^{2-}, distorted Tetrahedral	5.376	2.911	2.837; 2.949 and 3.116 are bifurcated	3.071	None	1.833

Table 14: Selected Cg-Cg and Non-Covalent Intermolecular Distances of the the type d(H···A) for 4-aminopyridinium hybrids. Colour indicates isostructurality.

Hybrid	Perhallometallate Anion Geometry	Cg-Cg *Distance* (Å)	Shortest Cation-N-H···X-M-Anion Distance (Å)	
			pyrNH···X	amineNH···X
4ampZnCl	Isolated $ZnCl_4^{2-}$; distorted Tetrahedral	4.565 and 4.600	2.514	2.449
4ampZnBr	Isolated $ZnBr_4^{2-}$; distorted Tetrahedral	4.814	2.803; 2.936 and 2.987 are bifurcated	2.640
4ampZnI	Isolated ZnI_4^{2-}; distorted Tetrahedral	5.175	2.878; 3.011 and 3.166 are bifurcated	2.827

Table 15: Selected Cg-Cg and Non-Covalent Intermolecular Distances of the the type d(H···A) for hydrated 4-aminopyridinium hybrids. Colour indicates isostructurality. White blocks indicate no isostructural equivalent.

Hybrid	Perhallometallate Anion Geometry	Cg-Cg Distance (Å)	Shortest Cation-N-H···X-M-Anion Distance (Å)		Shortest Water-H···X-M-Anion Distance (Å)	Shortest Cation-N-H···O-Water Distance (Å)	
			pyrNH···X	amineNH···X		pyrNH···O	amineNH···O
4ampCdCl·H$_2$O	Polymeric $Cd_2Cl_8^{4+}$	3.741	2.009	2.478	1.809	None	None
4ampCdBr·H$_2$O	Isolated $CdBr_4^{2-}$, distorted Tetrahedral	3.821	none	2.781	2.733; 3.039 and 3.039 are bifurcated	1.988	None
4ampCdI·H$_2$O	Isolated CdI_4^{2-}, distorted Tetrahedral	3.799	None	3.039	2.938	2.034	None
4ampHgCl·H$_2$O	Isolated $HgCl_4^{2-}$, distorted Tetrahedral	3.839	None	2.623	2.389	1.988	None
4ampHgBr·H$_2$O	Isolated $HgBr_4^{2-}$, distorted Tetrahedral	3.811	None	2.770	2.729	1.992	None
4ampHgI·H$_2$O	Isolated HgI_4^{2-}, distorted Tetrahedral	3.708	None	2.963	2.951	1.997	None

4. Discussion

4.1 Keeping the Cation Constant

In this section the structures have been grouped into classes of isostructurality where class 2, class 3 and class 4 indicate structures containing the 2, 3 and 4 aminopyridinium cations respectively. In the case that a particular class of structures shared the same space group but were not isostructural then that class was further divided into Class 2A, Class 2B and so forth.

4.1.1 2-Aminopyridinium Series

4.1.1.1 Trends in 2-Aminopyridinium Series

In this family of compounds, seven structures were determined in this study while five more high quality structures have been reported in the literature. In all twelve structures, the pyridine N is protonated, hence forming the 2-aminopyridinium cation and all structures are anhydrous. The cations all adopt a planar geometry, while the anions in ten of the twelve structures viz. **2ampZnCl, 2ampZnBr, 2ampZnI, 2ampCdI, 2ampHgCl, 2ampHgBr, 2ampHgI, 2ampCuCl** (**1** in the literature survey) (Kumar *et al*, 2005; YAPNAS01)**, 2ampCuBr** (**2** in the literature survey) (Luque *et al*, 1997; RIPWIW) and **2ampCoCl** (**3** in the literature survey) (Jebas *et al*, 2006; DELPOA) display an isolated tetrahedral geometry which is distorted in the case of **2ampCuCl** and **2ampCuBr (1** and **2** in the literature survey). **Class 2A1**, **Class 2A2** and **Class 2C** each contain isostructurality.

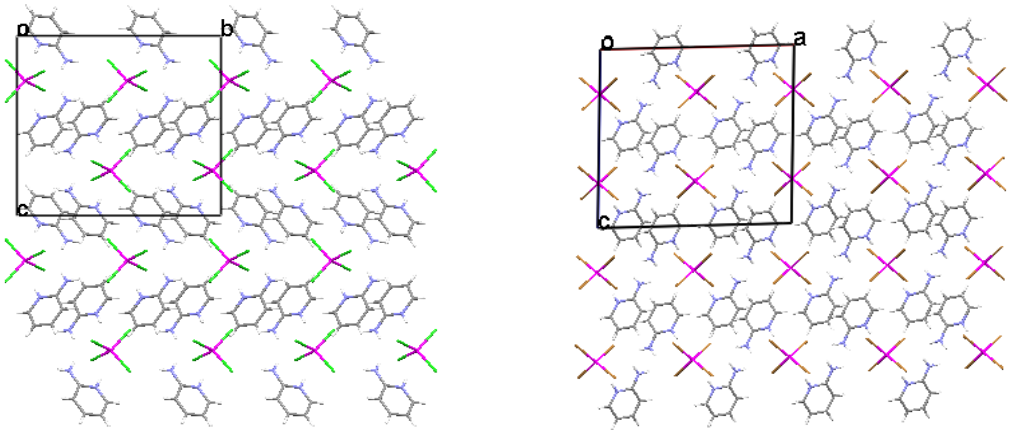
4.1.1.2 Class 2A

Space Group: *C*2/*c*
General Formula: $(C_5H_7N_2)_2MX_4$

Observed for four compounds: **2ampZnCl, 2ampZnBr, 2ampHgCl and 2ampCoCl** (number **3,** from the literature survey (Jebas, 2006; DELPOA)).Even though it may

initially seem, from the unit cell parameters (see **Table 16** on page 80), that these structures are all isostructural, this class may be divided into two subsets, **Class 2A1** and **Class 2A2**. The structures **2ampCoCl** (number **3,** from the literature survey (Jebas, 2006; DELPOA)) and **2ampZnCl** are isostructural and form **Class 2A1** (indicated in yellow in **Table 16**), while the structures **2ampHgCl** and **2ampZnBr** are isostructural and form **Class 2A2** (indicated in gray in **Table 16**). **Class 2A1** show a slight increase in all unit cell parameters as the metal atom is changed from the smaller Co atom (ionic radius of 0.58Å) (Shannon, 1976) to the slightly larger Zn atom (ionic radius of 0.60Å) (Shannon, 1976) while the chloro ligands remain constant. In **Class 2A2** all the unit cell parameters increase as the metal changes for Hg to Zn, and the ligands from chloro to bromo in going from structure **2ampHgCl** to **2ampZnBr**, hence the increase in ligand size outweighs the decrease in metal size. This most probably happens due to the fact that there are four ligands but only one metal atom per anion.

The structures in **Class 2A1** and **2A2** are very similar, but there are subtle differences. For the structures in **Class 2A1**, when viewed down the *a*-axis, pair of cations adopt alternating orientations in consecutive organic layers, but for the structures in **Class 2A2**, the all the cation pairs show the same orientation in all the layers, when viewed down the *b*-axis. See **Figure 39** below. In addition, the cation orientation differs in the two types of classes.



(a.) **(b.)**

Figure 39: (a.) Structure **2ampZnCl** (**Class 2A1**), viewed down the *a*-axis, showing alternating orientation of cation pairs. **(b.)** Structure **2ampZnBr** (**Class 2A2**), viewed down the *b*-axis, illustrating the same orientation adopted by cation pairs.

Table 16: Unit cell parameters of selected 2-aminopyridinium containing structures (* No standard deviation reported). Colour indicates isostructurality.

Name	Space Group	*a* (Å)	*b* (Å)	*c* (Å)	α (°)	β (°)	γ (°)	Volume (Å^3)	Packing Efficiency
2ampCoCl (3)	*C*2/*c*	8.2152(3)	14.0713(5)	13.5731(5)	90	95.190(2)	90	1562.598*	8 cations, 4 anions
2ampZnCl	*C*2/*c*	8.3104(6)	14.115(17)	13.8427(10)	90	93.641(6)	90	1620.5(3)	8 cations, 4 anions
2ampHgCl	*C*2/*c*	15.0298(8)	7.4925(4)	14.7577(9)	90	92.229(5)	90	1660.6(2)	8 cations, 4 anions
2ampZnBr	*C*2/*c*	15.3064(11)	7.7064(6)	14.7911(10)	90	92.313(6)	90	1743.3(2)	8 cations, 4 anions

4.1.1.3 Class 2B

Space Group: *C*2/*c*

General Formula: $(C_5H_7N_2)_2MX_4$

Observed for one compound: **2ampZnI**

4.1.1.4 Class 2C

Space Group: *P*$\bar{1}$

General Formula: $(C_5H_7N_2)_2MX_4$

Observed for two compounds: **2ampCdI, 2ampHgI**

4.1.1.5 Class 2D

Space Group: $P2_1/c$

General Formula: $(C_5H_7N_2)_2MX_4$

Observed for one compound: **2ampHgBr**

4.1.1.6 Class 2E

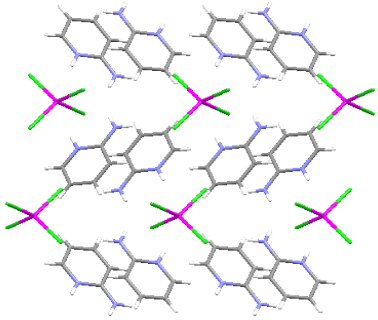
Space Group:

General Formula: $(C_5H_7N_2)_2MX_4$

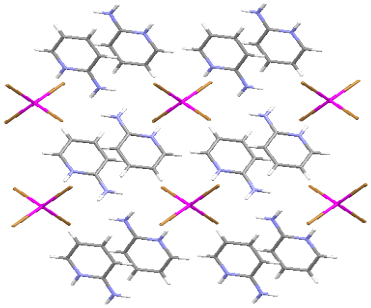
Observed for two compounds: **2ampCuCl** (Kumar *et al*, 2005; YAPNAS01), **2ampCuBr** (Luque *et al*, 1997; RIPWIW) (**1** and **2** in the literature survey)

4.1.1.7 2-Aminopyridinium Crystal Packing Trends

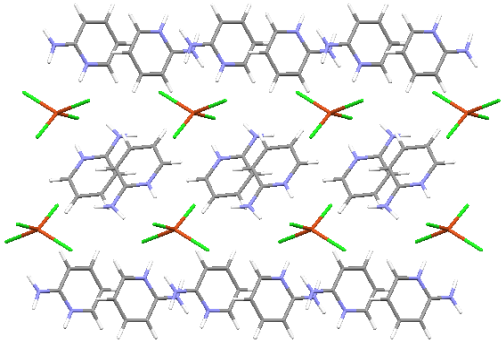
Layered structures consisting of organic layers containing 2-aminopyridinium cations and isolated tetrahedral anions comprising the inorganic layers, are formed, as illustrated in **Figure 40** on page 82.



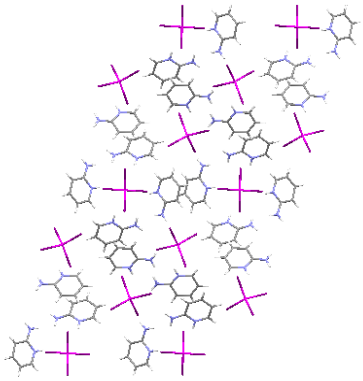
(a.)



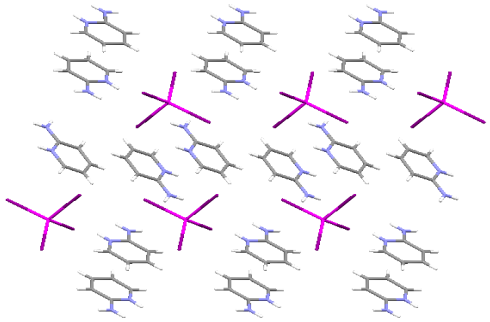
(b.)



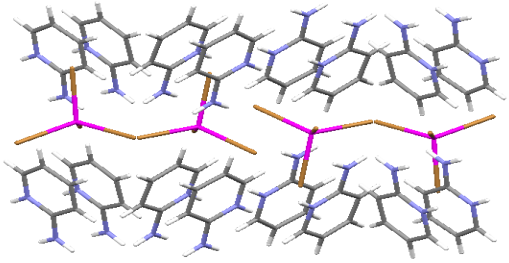
(c.)



(d.)



(e.)



(f.)

Figure 40: (a.) Structure of **2ampZnCl**, viewed down the *a*-axis. Isostructural to **2ampCoCl** (Jebas *et al*, 2006; DELPOA) number **3** in the literature survey. **(b.)** Structure of **2ampZnBr**, viewed down the *b*-axis, isostructural to **2ampHgCl**. **(c.)** Structure of **2ampCuCl** (Kumar *et al*, 2005; YAPNAS01), viewed down the *a*-axis. Isostructural to **2ampCuBr** (Luque *et al*, 1997; RIPWIW) and **3ampCuCl** (Kumar *et al*, 2005; PATMUT) (**1, 2** and **6** in the literature survey). **(d.)** Structure of **2ampZnI**, viewed down the *b*-axis. **(e.)** Structure of **2ampCdI,** viewed down the *a*-axis, isostructural to **2ampHgI**. **(f.)** Structure of **2ampHgBr**.

4.1.1.8 2-Aminopyridinium Cation Pair Packing

Six of the ten structures that display isolated tetrahedral anions each contain two crystallographically independent cations and hence display two different types of cation pair orientations, as shown in **Figure 41** on pages 84-85 viz. **2ampCuCl** (Kumar *et al*, 2005; YAPNAS01)**, 2ampCuBr** (Luque *et al*, 1997; RIPWIW)**, 2ampZnI, 2ampCdI, 2ampHgBr** and **2ampHgI**.

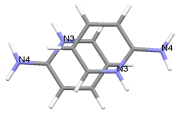
2ampCuCl (Kumar *et al*, 2005; YAPNAS01) and **2ampCuBr** (Luque *et al*, 1997; RIPWIW) share the same cation orientation for both pairs of cation packing. In both these structures the cation pairs consist of the same cation and exhibit a head-to-tail orientation. The first pair is slipped such that the head of one cation partially overlaps with the head of the other cation see **Figure 41 (a.)** and **(b.)** on pages 84. This cation orientation is also observed for **2ampZnBr** and **2ampHgCl**. The second pair is slipped such that the tail portion of one cation overlaps with the head portion of the other cation, so that no actual ring overlap occurs.

Similarly **2ampCdI** and **2ampHgI** share the same cation orientation for both cations pairs. Both orientations are head-to-tail, with each cation pair consisting of the same cation**.** In this case however one pair of cations is packed with an almost perfect head-to-tail overlap such that the head of one cation almost completely overlaps the head of the other cation (slippage distance of 0.435Å and 0.374Å for **2ampCdI** and **2ampHgI** respectively). The second pair is slipped such that the tail of one cation overlaps with the head of the other cation, so that no actual ring overlap occurs.

On the other hand **2ampZnI** contains three crystallographically independent cations and two different cation orientations. The first orientation contains the same cation and is head-to-tail. The second orientation contains the remaining two crystallographically independent cations, rotated relative to each other but with the pyridine N's facing opposite directions.

2ampHgBr contains two crystallographically independent cations and two different cation orientations. The first orientation containing the same cation is head-to-tail, with

a partial ring overlap. The second orientation contains both the crystallographically independent cations, facing the same direction, with pyridine N's facing the same direction, such that there is no ring overlap. **2ampCoCl** (Jebas *et al*, 2006; DELPOA) and **2ampZnCl** contain the same cation orientation, having only one crystallographically independent cation. The cation orientation is head-to-tail, with no ring overlap hence no significant aromatic interactions .



Cation Pair 1

Cg-Cg: 3.767Å

Slippage: 1.385Å

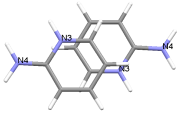


Cation Pair 2

Cg-Cg: 4.230Å

Slippage: 2.579Å

(a.) 2ampCuCl



Cation Pair 1

Cg-Cg: 3.852Å

Slippage 1.560Å

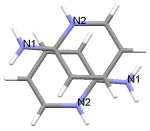


Cation Pair 2

Cg-Cg: 4.312Å

Slippage 2.742Å

(b.) 2ampCuBr



Cg-Cg 3.731Å

Slippage 1.661Å

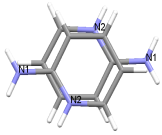
(c.) 2ampZnBr



Cg-Cg 3.704Å

Slippage 1.533Å

(d.) 2ampHgCl



Cation Pair 1

Cg-Cg 3.514Å

Slippage 0.435Å



Cation Pair 2

Cg-Cg 4.188Å

Slippage 2.321Å

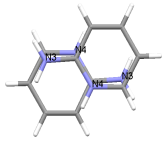
(e.) 2ampCdI



Cation Pair 1

Cg-Cg 3.515Å

Slippage 0.374Å

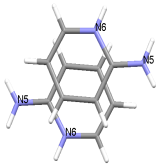


Cation Pair 2

Cg-Cg 4.168Å

Slippage 2.330Å

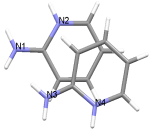
(f.) 2ampHgI



Cation Pair 1

Cg-Cg 3.456Å

Slippage 1.127Å

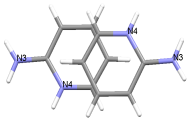


Cation Pair 2

Cg-Cg 3.689Å

Slippage 1.472Å

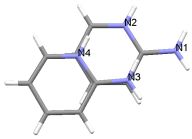
(g.) 2ampZnI



Cation Pair 1

Cg-Cg 3.876Å

Slippage 1.735Å

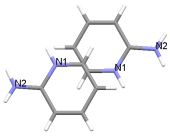


Cation Pair 2

Cg-Cg 4.132Å

Slippage 2.163Å

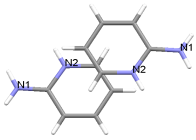
(h.) 2ampHgBr



Cg-Cg 4.228Å

Slippage 2.639Å

(i.) 2ampCoCl



Cg-Cg 4.250Å

Slippage 2.593Å

(j.) 2ampZnCl

Figure 41: Cation pair orientation in **(a.) 2ampCuCl** (Kumar *et al*, 2005; YAPNAS01). **(b.) 2ampCuBr** (Luque *et al*, 1997; RIPWIW). **(c.) 2ampZnBr. (d.) 2ampHgCl. (e.) 2ampCdI. (f.) 2ampHgI. (g.) 2ampZnI. (h.) 2ampHgBr. (i.) 2ampCoCl** (Jebas *et al*, 2006; DELPOA). **(j.) 2ampZnCl.**

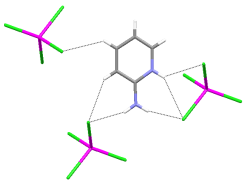
4.1.1.9 2-Aminopyridinium Synthons

A common synthon is observed for **2ampZnBr,** and cation 1 in the following structures **2ampHgI**, **2ampCuCl** (Kumar *et al*, 2005; YAPNAS01) and **2ampCuBr** (Luque *et al*, 1997; RIPWIW). The synthon is exhibited for four out of ten structures containing the 2-aminopyridinium cation and isolated tetrahedral anion. See **Figure 42** on pages 87-88. The synthon involves one 2-aminopyridinium cation and three tetrahalometallate anions. The pyridinium nitrogen together with the amino nitrogen on the cation forms two different charge assisted hydrogen bonds with two halogeno ligands on the same anion. The amino nitrogen then forms a second charge assisted hydrogen bond with a halogeno ligand on a second anion. A halogeno ligand on the third anion then interacts with a hydrogen atom bonded to a carbon neighbouring the pyridinium nitrogen.

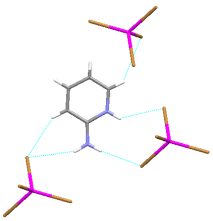
Similarly a common synthon is observed for **2ampHgCl**, cation 1 in both **2ampCuCl** (Kumar *et al*, 2005; YAPNAS01) and **2ampCuBr** (Luque *et al*, 1997; RIPWIW). The synthon is observed for three out of the ten structures containing the 2-aminopyridinium cation and isolated tetrahedral anion. This time, the third anion forms a hydrogen bond interaction with the carbon in the meta position to the amine nitrogen, not neighbouring the pyridinium nitrogen.

The third type of synthon is observed for **2ampZnBr**, **2ampCoCl** (Jebas *et al*, 2006; DELPOA) and cation 1 in **2ampHgBr**. This synthon consists of four anions and one 2-aminopyridinium cation. The pyridinium nitrogen together with the amino nitrogen on the cation forms two different charge assisted hydrogen bonds with two halogeno ligands on the same anion. The amino nitrogen then forms a second charge assisted hydrogen bond with a halogeno ligand on a second anion. A halogeno ligand on the third anion then interacts with a hydrogen atom bonded to a carbon neighbouring the pyridinium nitrogen. A halogeno ligand on the forth anion then interacts with a hydrogen atom bonded to a carbon in the meta position to the amine nitrogen, not neighbouring the pyridinium nitrogen.

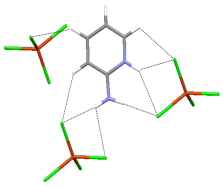
The remaining synthons consist of combinations of the above charge assisted intermolecular interactions.



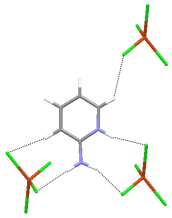
(a.) 2ampHgCl



(b.) 2ampZnBr

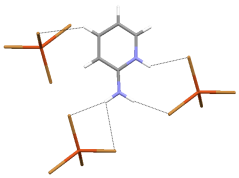


Cation 1

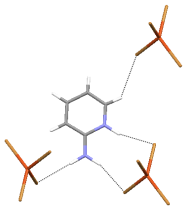


Cation 2

(c.) 2ampCuCl

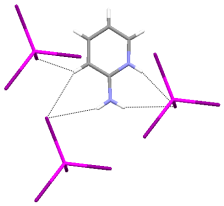


Cation 1

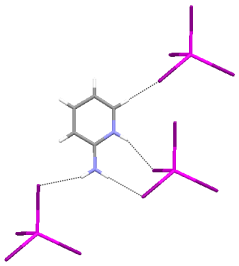


Cation 2

(d.) 2ampCuBr

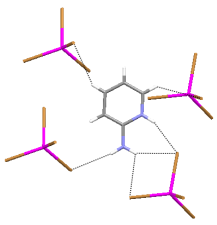


Cation 1

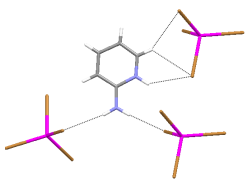


Cation 2

(e.) 2ampHgI

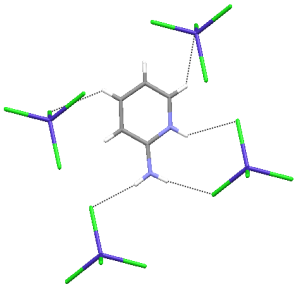


Cation 1

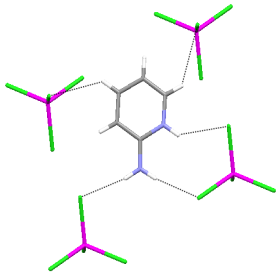


Cation 2

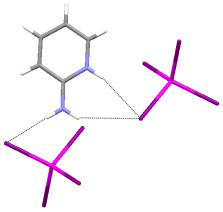
(f.) 2ampHgBr



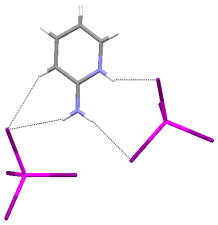
(g.) 2ampCoCl



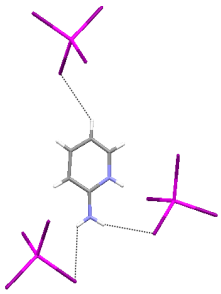
(h.) 2ampZnCl



Cation 1

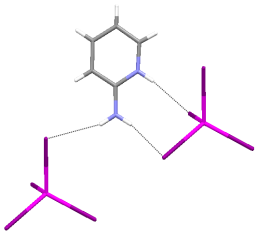


Cation 2

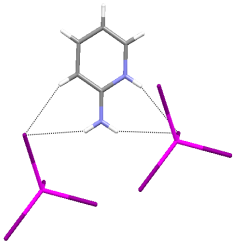


Cation 3

(i.) 2ampZnI



Cation 1



Cation 2

(j.) 2ampCdI

Figure 42: Identified synthons in **(a.) 2ampHgCl. (b.) 2ampZnBr. (c.) 2ampCuCl** (Kumar *et al*, 2005; YAPNAS01). **(d.) 2ampCuBr** (Luque *et al*, 1997; RIPWIW). **(e.) 2ampHgI. (f.) 2ampHgBr. (g.) 2ampCoCl** (Jebas *et al*, 2006; DELPOA). **(h.) 2ampZnCl. (i.) 2ampZnI. (j.) 2ampCdI.**

4.1.2 3-Aminopyridinium and 3-Ammoniopyridinium Series

The 3-aminopyridinium series contains three different classes of structures. The relevant intermolecular interactions are listed in **Table 7** on page 29 and **Table 13** on page 75.

4.1.2.1 Trends in 3-Aminopyridinium and 3-Ammoniopyridinium Series

In this family of compounds, only three structures were determined in this study while two more high quality structures have been reported in the literature. In three of the total number of five structures namely **3ampZnBr·H_2O**, **3ampHgI·H_2O** and **3ampHgBr·H_2O** (Ali, 2008; TOBCOD) both the pyridine N and the amine N of the 3-aminopyridine base are protonated, hence forming the 3-ammoniopyridinium cation as opposed to the 3-aminopyridinium cation. As discussed previously the second protonation occurs much more easily in the 3-aminopyridinium cation than in the other members of the *n*-aminopyridinium series. Interestingly, the same three structures also contain water molecules. The two structures in this family in which only the pyridine N atom is protonated are anhydrous. These are **3ampZnCl** and **3ampCuCl** (Kumar *et al*, 2005; PATMUT) number **6** in literature survey. In all the structures the cation adopts a planar geometry, and in all the structures the anion displays an isolated tetrahedral geometry which is distorted in the case of **3ampCuCl** (Kumar *et al*, 2005; PATMUT). The structures **3ampHgI·H_2O** and **3ampHgBr·H_2O** (Ali, 2008; TOBCOD) (number **8** in literature survey) are isostructural.

4.1.2.2 Class 3A

Space Group: *P*$\bar{1}$

General Formula: $(C_5H_7N_2)_2MX_4$

Observed for one compound: **3ampZnCl**

4.1.2.3 Class 3B

Space Group: $P2_1/c$

General Formula: $(C_5H_7N_2)_2MX_4·H_2O$

Observed for one compound: **3ampZnBr·H_2O**

4.1.2.4 Class 3C

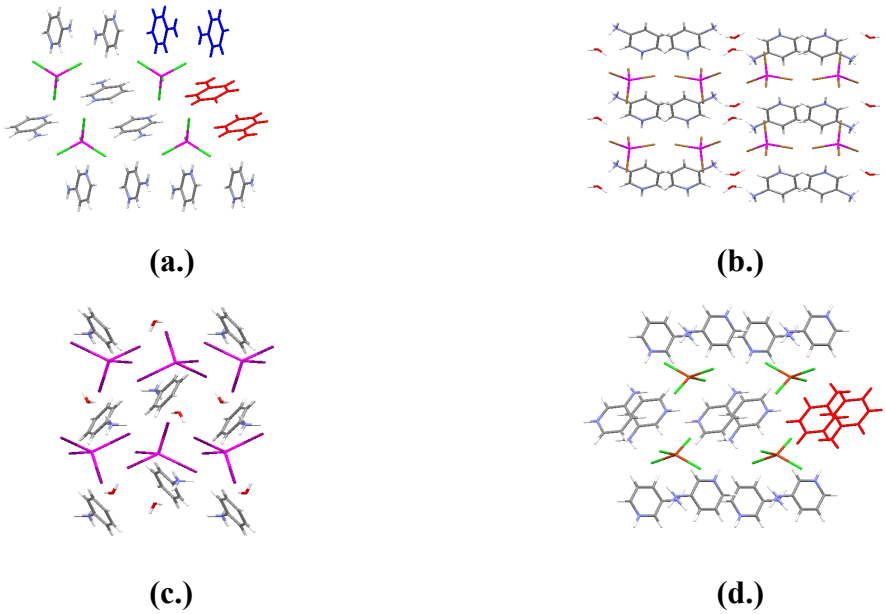
Space Group: $P2_1/n$

General Formula: $(C_5H_7N_2)_2MX_4{\cdot}H_2O$

Observed for two compounds: **3ampHgI·H_2O** and **3ampHgBr·H_2O** (Ali, 2008; TOBCOD) number **7** in the literature survey

4.1.2.5 3-Aminopyridinium and 3-Ammoniopyridinium Crystal Packing Trends

Layered structures consisting of organic layers containing the 3-aminopyridinium or 3-ammoniopyridinium cations, and isolated tetrahedral anions comprising the inorganic layers, are formed, as illustrated below in **Figure 43.** Note that **3ampZnCl (a.)** and **3ampCuCl (d.)** (Kumar *et al*, 2005; PATMUT) have similar alternating organic layers (highlighted by blue and red cation pairs), however the cation pairs in **3ampCuCl** (Kumar *et al*, 2005; PATMUT) are interdigitated and this in not observed in **3ampZnCl**.



(a.) **(b.)**

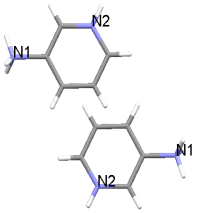
(c.) **(d.)**

Figure 43: Layered structures observed for the 3-aminopyridinium and 3-ammoniopyridinium family. **(a.) 3ampZnCl** viewed down the *a*-axis. **(b.) 3ampZnBr·H_2O** viewed down the *b*-axis. **(c.) 3ampHgI·H_2O**, viewed down the *c*-axis. Isostructural to **3ampHgBr·H_2O** (Ali, 2008; TOBCOD). **(d.) 3ampCuCl**, viewed down the *a*-axis (Kumar *et al*, 2005; PATMUT).

4.1.2.6 3-Aminopyridinium and 3-Ammoniopyridinium Cation Pair Packing

In the three structures containing the 3-ammoniopyridinium cation, pairs of cations show a very large slippage distance relative to each other, as illustrated on page 92 in **Figure 44 (a.) – (c.)**. For these structures **3ampHgBr·H_2O** (Ali, 2008; TOBCOD) and **3ampHgI·H_2O** (isostructural structures) the cation pair show a head-to-tail orientation with the pyridine N's facing in opposite directions, while in the **3ampZnBr·H_2O** structure the cations in the pair are rotated relative to each other, with the pyridine N's facing in the same direction, while the ammonium parts form an angle of approximately 100°. In summary, for these three structures the centroid-to-centroid distance as well as the degree of slippage is too large for any aromatic interactions to occur. The slippage and centroid-to-centroid distances are 4.230Å and 5.193Å for **3ampHgBr·H_2O** (Ali, 2008; TOBCOD), 4.458Å and 5.376Å for **3ampHgI·H_2O** and 4.139Å and 5.271Å for **3ampZnBr·H_2O** respectively.

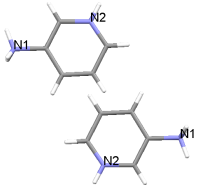
The **3ampZnCl** and **3ampCuCl** (Kumar *et al*, 2005; PATMUT) structures both have two crystallographically independent cations, and hence display two different types of cation pair orientations, as shown on page 92 in **Figure 44 (d.) – (e.)**. In both these structures the cation pairs consist of the same cation and exhibit a head-to-tail orientation with different degrees of slippage in the cation pair. The slippage in these structures is less than in those containing the 3-ammoniopyridinium cation.



(a.) 3ampHgBr·H_2O

Cg-Cg 5.193Å

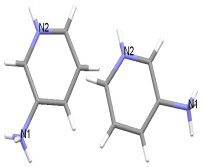
Slippage 4.230Å



(b.) 3ampHgI·H_2O

Cg-Cg 5.376Å

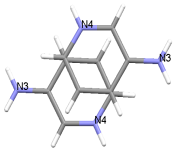
Slippage 4.458Å



(c.) 3ampZnBr·H_2O

Cg-Cg 5.271Å

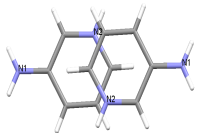
Slippage 4.139Å



Cation Pair 1

Cg-Cg 3.672Å

Slippage 1.392Å

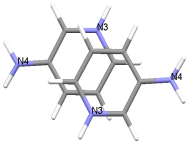


Cation Pair 2

Cg-Cg 3.892Å

Slippage 1.813Å

(d.) 3ampZnCl



Cation Pair 1

Cg-Cg 3.779Å

Slippage 1.383Å



Cation Pair 2

Cg-Cg 4.224Å

Slippage 2.568Å

(e.) 3ampCuCl

Figure 44: Cation pair orientation in **(a.) 3ampHgBr·H_2O** (Ali, 2008; TOBCOD). **(b.) 3ampHgI·H_2O. (c.) 3ampZnBr·H_2O. (d.) 3ampZnCl** and **(e.) 3ampCuCl.**

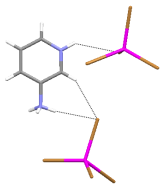
4.1.2.7 3-Aminopyridinium and 3-Ammoniopyridinium Synthons

A common synthon is observed for **3ampHgI·H₂O**, **3ampHgBr·H₂O** (Ali, 2008; TOBCOD) and for both cations in **3ampZnCl**. This synthon is exhibited by four out of the seven cations under investigation, and appears in structures containing the 3-ammoniopyridinium cation and structures with the 3-aminopyridinium cation.

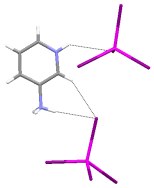


Cation 1 **Cation 2**

(a.) 3ampZnCl



(b.) 3ampHgBr·H₂O



(c.) 3ampHgI·H₂O

Figure 45: Identified synthons in **(a.) 3ampZnCl, (b.) 3ampHgBr·H₂O** (Ali, 2008; TOBCOD) and **(c.) 3ampHgI·H₂O.**

As illustrated above in **Figure 45**, the synthon involves one 3-aminopyridinium or 3-ammoniopyridinium cation and two tetrahalometallate anions. The pyridinium nitrogen on the cation forms a charge-assisted hydrogen bond with one of the halogeno ligands on one of the anions. At the same time one of the amine hydrogen atoms, as well as a hydrogen atom neighbouring both the amine group and the pyridinium N, interacts with the second anion, forming a bifurcated interaction. This synthon is not observed in the structures of **3ampZnBr·H₂O** and **3ampCuCl** (Kumar *et al*, 2005; PATMUT).

4.1.3 4-Aminopyridinium Series

The 4-aminopyridinium series contains three different classes of structures. The relevant intermolecular interactions are listed in **Table 8** (page 30), **Table 14** (page 76) and **Table 15** (page 77)**.**

4.1.3.1 Trends in 4-Aminopyridinium Series

In this family of compounds, all nine structures were determined. One of the nine has been previously reported, **4ampCdBr·H_2O** (Hatano *et al*, 2008; POGHEZ) and a tenth structure suitable for comparison has been reported in the literature **4ampCoCl** (Jebas *et al*, 2009; HOSVIV). The pyridine N in all ten structures is protonated, thus forming the 4-aminopyridinium cation. **Class 4A** structures are anhydrous (**4ampZnCl, 4ampZnBr, 4ampZnI** and **4ampCoCl** (Jebas *et al*, 2009; HOSVIV) number **17** in the literature survey), while **Class 4B** (**4ampCdCl·H_2O**) and **Class 4C** structures (**4ampCdBr·H_2O** (Hatano *et al*, 2008; POGHEZ) number **8** in the literature survey)**, 4ampCdI·H_2O, 4ampHgCl·H_2O, 4ampHgBr·H_2O** and **4ampHgI·H_2O**) are hydrated. In all ten structures the cation adopts a planar geometry. Nine of the ten contain isolated tetrahedral anions, all of which are slightly distorted. The only polymeric anion in this series is observed for **4ampCdCl·H_2O.**

4.1.3.2 Class 4A

Space Group: $P2_12_12_1$
General Formula: $(C_5H_7N_2)_2MX_4$
Observed for four compounds: **4ampZnCl, 4ampZnBr, 4ampZnI** and **4ampCoCl** (Jebas *et al*, 2009; HOSVIV) number **17** in the literature survey.

4.1.3.3 Class 4B

Space Group: $P2_1/c$
General Formula: $(C_5H_7N_2)_2M_2X_8·H_2O$
Observed for one compound: **4ampCdCl·H_2O**

4.1.3.4 Class 4C

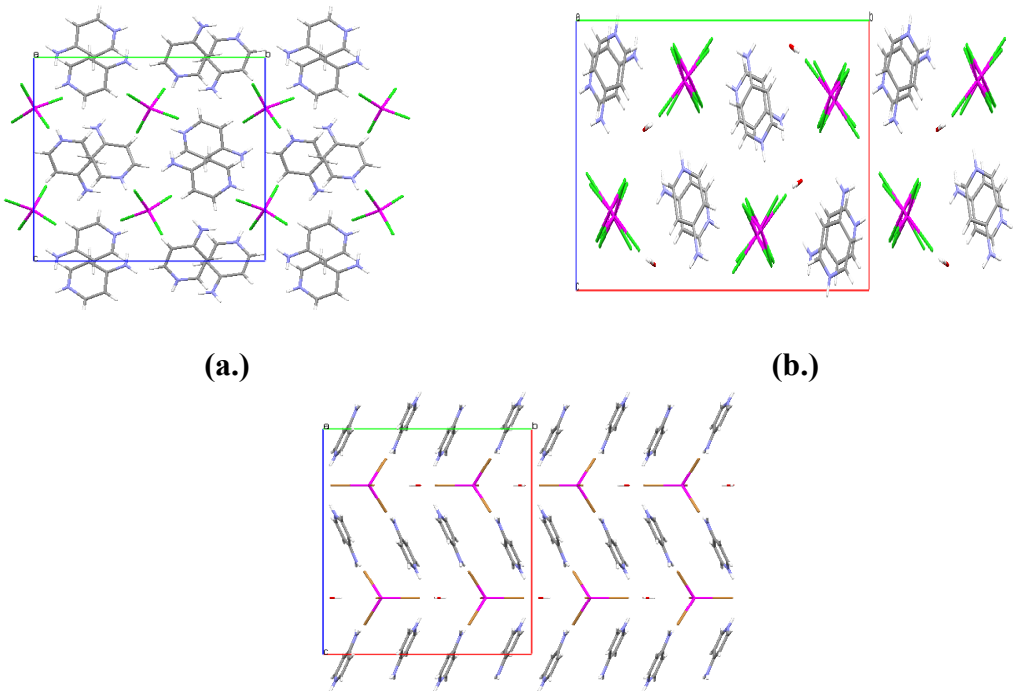
Space Group: *Pbcm*

General Formula: $(C_5H_7N_2)_2MX_4 \cdot H_2O$

Observed for five compounds: **4ampCdBr·H_2O** (Hatano *et al*, 2008; POGHEZ) number **8** in the literature survey)**, 4ampCdI·H_2O, 4ampHgCl·H_2O, 4ampHgBr·H_2O** and **4ampHgI·H_2O.**

4.1.3.5 4-Aminopyridinium Crystal Packing Trends

Layered structures consisting of organic layers containing the 4-aminopyridinium cations and isolated tetrahedral anions (with the exception of **4ampCdCl·H_2O**) comprising the inorganic layers, are formed, as illustrated below in **Figure 46**.



(a.) **(b.)**

(c.)

Figure 46: Layered structures observed for the 4-aminopyridinium family. **(a.)** **4ampZnCl**, viewed down the *a*-axis, observed for **Class 4A** structures. **(b.)** **4ampCdCl·H_2O**, viewed down the *a*-axis, observed for **Class 4B** structures. **(c.)** **4ampCdBr·H_2O**, viewed down the *a*-axis, observed for **Class 4C** structures.

4.1.3.6 4-Aminopyridinium Cation Pair Packing

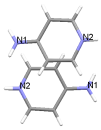
In the nineteen structures containing the 4-aminopyridinium cation, four structures contain two crystallographically independent cations and isolated tetrahedral anions (**4ampZnCl, 4ampZnBr, 4ampZnI** and **4ampCoCl** (Jebas *et al*, 2009; HOSVIV)).

4ampZnCl, 4ampZnBr, 4ampZnI and **4ampCoCl** (Jebas *et al*, 2009; HOSVIV) contain the same type of cation packing. See **Figure 47** on pages 97-98. In each of these structures the slippage distance and the centroid-to-centroid distances are too large for any significant aromatic interactions too occur. In all four of these structures the cation pair consists of the same cation and exhibits a head-to-tail orientation, such that no actual ring overlap occurs.

The remaining structures each contain one crystallographically independent 4-aminopyridinium cation. **4ampCdBr·H_2O** (Hatano *et al*, 2008; POGHEZ) reported in the literature is isostructural to **4ampCdBr·H_2O** synthesized for this project. The same cation orientation is observed for **4ampCdI·H_2O, 4ampHgCl·H_2O, 4ampHgBr·H_2O** and **4ampHgI·H_2O.** The cation pairs exhibit a head-to-tail orientation with partial ring overlap. In each case the slippage and centroid-to-centroid distances are bordering 3.8Å.

4ampCuCl·H_2O (Halvorson *et al*, 1990; SEZLEO) and **4ampCuBr·H_2O** (Román, 1996; ZUDKUE) do not exhibit any significant aromatic interactions, although their cation packing is the same. In both cases the cation pair orientation is head-to-tail with no ring overlap.

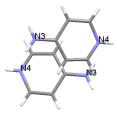
The last cation pair of interest is from **4ampCdCl·H_2O. 4ampCdCl·H_2O** contains two crystallographically independent cations but only type of cation orientation. The cation pair consists of both crystallographically independent cations rotated relative to each other with partial ring overlap.



Cation Pair 1

Cg-Cg 4.565Å

Slippage 2.904Å

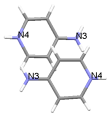


Cation Pair 2

Cg-Cg 4.600Å

Slippage 2.905Å

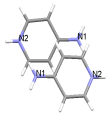
(a.) 4ampZnCl



Cation Pair 1

Cg-Cg 4.814Å

Slippage 3.187Å

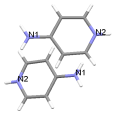


Cation Pair 2

Cg-Cg 4.873Å

Slippage 3.258Å

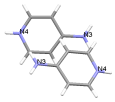
(b.) 4ampZnBr



Cation Pair 1

Cg-Cg 5.174Å

Slippage 3.681Å

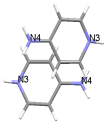


Cation Pair 2

Cg-Cg 5.188Å

Slippage 3.649Å

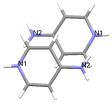
(c.) 4ampZnI



Cation Pair 1

Cg-Cg 4.565Å

Slippage 2.889Å

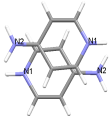


Cation Pair 2

Cg-Cg 4.630Å

Slippage 2.982Å

(d.) 4ampCoCl

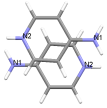


(e.) 4ampCdBr·H_2O

Cg-Cg 3.799Å

Slippage (9) 1.668Å

(Hatano *et al*, 2008; POGHEZ)

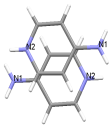


(f.) 4ampCdBr·H_2O

Cg-Cg 3.821Å

Slippage 1.674Å

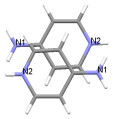
(Current Study)



(g.) 4ampCdI·H_2O

Cg-Cg 3.799Å

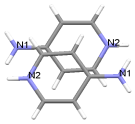
Slippage 1.652Å



(h.) 4ampHgCl·H_2O

Cg-Cg 3.839Å

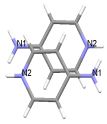
Slippage 1.752Å



(i.) 4ampHgBr·H_2O

Cg-Cg 3.811Å

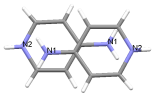
Slippage 1.692Å



(j.) 4ampHgI·H_2O

Cg-Cg 3.708Å

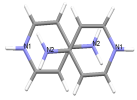
Slippage 1.613Å



(k.) 4ampCuCl·H_2O

Cg-Cg 4.200Å

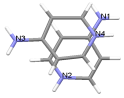
Slippage 2.525Å



(l.) 4ampCuBr·H_2O

Cg-Cg 4.302Å

Slippage 2.669Å



(m.) 4ampCdCl·H_2O

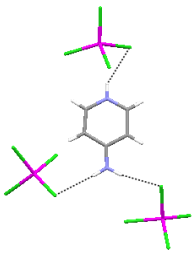
Cg-Cg 3.741Å

Slippage 1.351Å

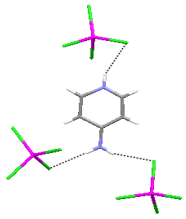
Figure 47: Cation pair orientation in **(a.) 4ampZnCl, (b.) 4ampZnBr, (c.) 4ampZnI, (d.) 4ampCoCl** (Jebas *et al*, 2009; HOSVIV), **(e.) 4ampCdBr·H_2O** (Hatano *et al*, 2008; POGHEZ), **(f.) 4ampCdBr·H_2O** (current study), **(g.) 4ampCdI·H_2O, (h.) 4ampHgCl·H_2O, (i.) 4ampHgBr·H_2O, (j.) 4ampHgI·H_2O, (k.) 4ampCuCl·H_2O** (Halvorson *et al*, 1990; SEZLEO), **(l.) 4ampCuBr·H_2O** (Román, 1996; ZUDKUE) and **(m.) 4ampCdCl·H_2O.**

4.1.3.7 4-Aminopyridinium Synthons

A common synthon is observed for all structures in the 4-aminopyridinium series. See **Figure 48** on pages 99-100. In **4ampZnCl, 4ampZnBr** and **4ampZnI** the synthon involves one 4-aminopyridinium cation and three tetrahalometallate anions. The pyridinium nitrogen on the cation forms a charge assisted hydrogen bond with one of the halogeno ligands on one of the anions. At the same each of the two amine hydrogen atoms form charge assisted hydrogen bonds with the halogeno ligands on the remaining two anions. A similar synthon is observed for **4ampCdCl**. The only difference is that anion is polymeric not tetrahedral. The same synthon is observed for **4ampCdBr, 4ampCdI, 4ampHgCl, 4ampHgBr** and **4ampHgI** because there are three hydrogen acceptors present in the same positions and there is one cation present with the same three hydrogen donors forming charge assisted hydrogen bonds. The hydrogen atom on the pyridinium nitrogen forms a charge assisted interaction with an oxygen atom from a water molecule. The two amine hydrogen atoms then form charge assisted hydrogen bonds with the halogeno ligands on the remaining two anions.

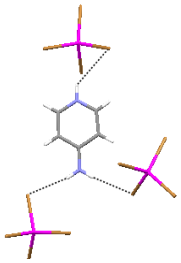


Cation 1

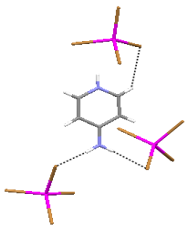


Cation 2

(a.) 4ampZnCl

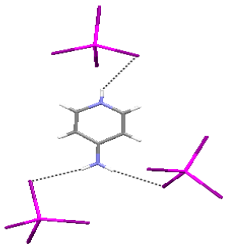


Cation 1

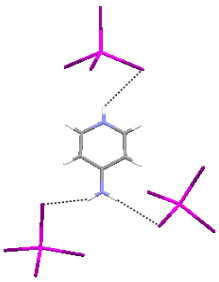


Cation 2

(b.) 4ampZnBr

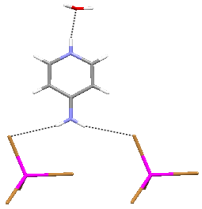


Cation 1

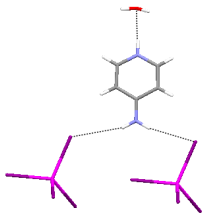


Cation 2

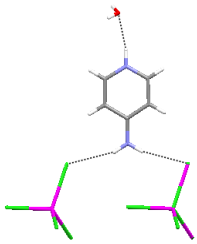
(c.) 4ampZnI



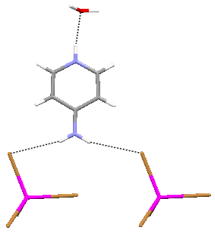
(d.) 4ampCdBr·H_2O



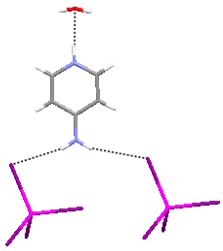
(e.) 4ampCdI·H_2O



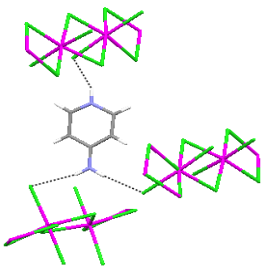
(f.) 4ampHgCl·H_2O



(g.) 4ampHgBr·H_2O



(h.) 4ampHgI·H_2O



(i.)4ampCdCl·H_2O

Figure 48: Identified synthons in **(a.) 4ampZnCl, (b.) 4ampZnBr, (c.) 4ampZnI, (d.) 4ampCdBr·H_2O, (e.) 4ampCdI·H_2O, (f.) 4ampHgCl·H_2O, (g.) 4ampHgBr·H_2O, (h.) 4ampHgI·H_2O** and **(i.) 4ampCdCl·H_2O.**

4.2 Comparison Across Cation Families

4.2.1 Cation Protonation

In the case of the 2-aminopyridinium and 4-aminopyridinium containing structures, only the pyridine N atom is protonated, as explained in **section 1.5.1**, while in the case of 3-aminopyridine containing structures, three out of the five structures contain the 3-ammoniopyridinium cation, where both pyridine and amine N atoms are protonated, while the other two contain the 3-aminopyridinium cation where only the pyridine N atoms are protonated.

4.2.2 Water Incorporation

In all the hydrated structures the water molecules participate in the hydrogen bonding network. Water molecules were available to be incorporated into all the structures during the crystallization process. However only 3-ammoniopyridinium and 4-aminopyridinium structures that contain cadmium and mercury are hydrated. This means that none of the 2-aminopyridinium, 3-aminopyridinium or zinc containing 4-aminopyridinium structures contain water. There is no space available for water in the 2-aminopyridinium and 3-aminopyridinium structures because the hydrogen bond donors (pyridine and amine N-H) in the cation, are too close to each other. However in 3-ammoniopyridinium structures the extra hydrogen atom on the amine N compensates for this cramped space. In 4-aminopyridinium structures there is enough space available to allow for water to be incorporated into the structure because the hydrogen bond donors are on opposite sides of the cation (pyridine and amine N-H on opposite sides of the cation). Why then are the zinc containing 4-aminopyridinium structures anhydrous and the cadmium and mercury containing 4-aminopyridinium structures hydrated? Considering the ionic radii of zinc, cadmium and mercury (0.60Å, 0.78Å and 0.96Å respectively (Shannon, 1976)) one may conclude that the zinc perhalometallate anions dominate the intermolecular bonding to the protonated N atoms because the intramolecular bonds in $ZnCl_4^{2-}$, $ZnBr_4^{2-}$ and ZnI_4^{2-} are shorter (hence stronger) compared to the corresponding mercury and cadmium perhalometallate anions. So when the halogeno ligand forms intermolecular interactions with the cation (N-H), the other side

of the halogen is bonded very closely to the zinc atom thus causing more congestion around the hydrogen bond donors allowing less space available for the water molecules.

4.2.3 Anions and Cations

For all the nineteen novel structures determined and the seventeen structures reported in the literature, twenty seven structures display an isolated tetrahedral or distorted isolated tetrahedral anion. Only the tetrahalocuprate anions typically display symmetrically distorted tetrahedral geometries. This occurs in the case of Cu due to Jahn-Teller distortion, which is not present when the metal is Zn, Cd or Hg. The effect of the Jahn-Teller distortion is to flatten the tetrahedron by increasing two of the X-Cu-X angles, leaving it somewhere between a tetrahedral and a square-planar geometry.

Only two structures among the total number of thirty six structures exhibit a polymeric anion. Firstly, for the novel structure **4ampCdCl·H_2O** a polymeric, one dimensional anion is formed. See **Figure 49** below. This anion is the only example of all the structures under investigation where the metal atom displays an octahedral coordination geometry, and it consists of edge sharing axial ligands. A search of the Cambridge Structural Database (September 2009 Update) did not reveal any other perhalocadmate structures with this anion geometry. This geometry was also not reported in the analysis of perhalocadmate polyhedra performed by Serezhkina *et al* (Serezhkina *et al*, **2000**).

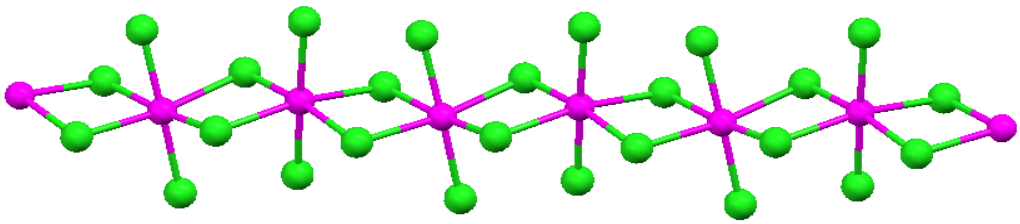


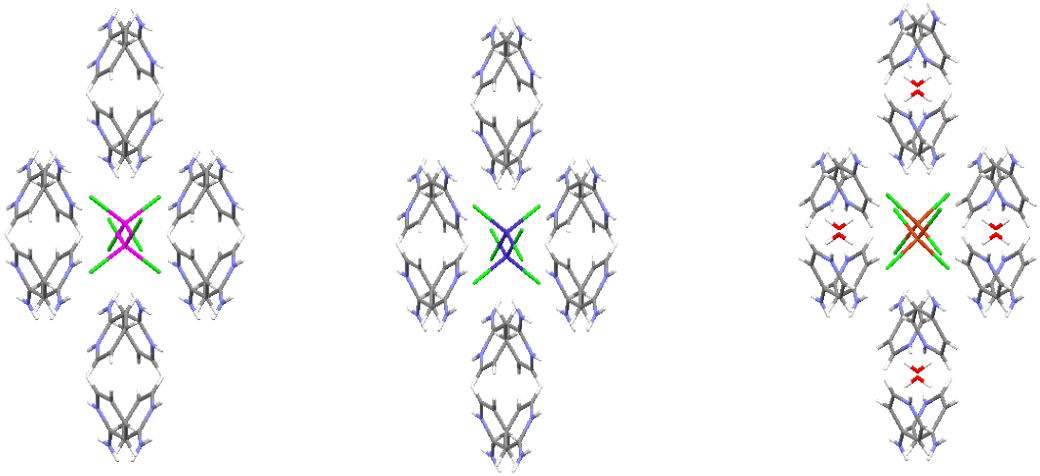
Figure 49: Polymeric anion observed for **4ampCdCl·H_2O**.

In the case of **4ampCuBr** two different types of anions occur in the same structure, namely an isolated tetrahedral anion as well as a one-dimensional polymer consisting of edge-sharing tetrahedra. In all the structures the cations have a planar geometry. The topic of the protonation of the cations has been discussed in detail in **Section 1.5.1**.

4.2.4 Crystal Packing Comparison

4.2.4.1 2-Aminopyridinium and 4-Aminopyridinium Families

The water containing crystal structures of bis(4-aminopyridinium) tetrachlorocuprate(II) monohydrate (**4ampCuCl·H_2O** (Halvorson *et al*, 1990; SEZLEO) **9** in literature survey) and 4-aminopyridinium tetrabromocopper(II) monohydrate (**4ampCuBr·H_2O** (Román, 1996; ZUDKUE) **10** in the literature survey) are isostructural to the **Class 2A1** structures (**2ampZnCl** and **2ampCoCl** (Jebas *et al*, 2006; DELPOA) **3** in the literature survey), and remarkably similar to the **Class 2A2** structures which contain the 2-aminopyridinium cation and no water molecules, as shown below in **Figure 50**. In all these structures the anions display a tetrahedral or distorted tetrahedral geometry, but the pyridine N atom position on the cation differs. The fact that very similar structures are formed even though the cations are different indicates that the hydrogen bonding interactions between the amine groups, the functional groups common to the 2-aminopyridinium and 4-aminopyridinium cations, as well as space-filling considerations play important roles in dictating the packing of the moieties.



(a.) **(b.)** **(c.)**

Figure 50: (a.) Crystal structure of **2ampZnCl**, viewed down the *c*-axis (Class 2A1)**. (b.)** Crystal structure of **2ampCoCl**, viewed down the *c*-axis (Jebas *et al*, 2006; DELPOA). **(c.)** Crystal structure of **4ampCuCl·H_2O**, viewed down the *c*-axis (Halvorson *et al*, 1990; SEZLEO), isostructural to (**4ampCuBr·H_2O** (Román, 1996; ZUDKUE), showing the incorporation of water molecules.

The unit cell parameters of the four structures **2ampCoCl** (Jebas *et al*, 2006; DELPOA), **2ampZnCl, 4ampCuCl** (Halvorson *et al*, 1990; SEZLEO) and **4ampCuBr** (Román, 1996; ZUDKUE) are listed in **Table 17** on page 106 and shown graphically in **Figure 51** below.

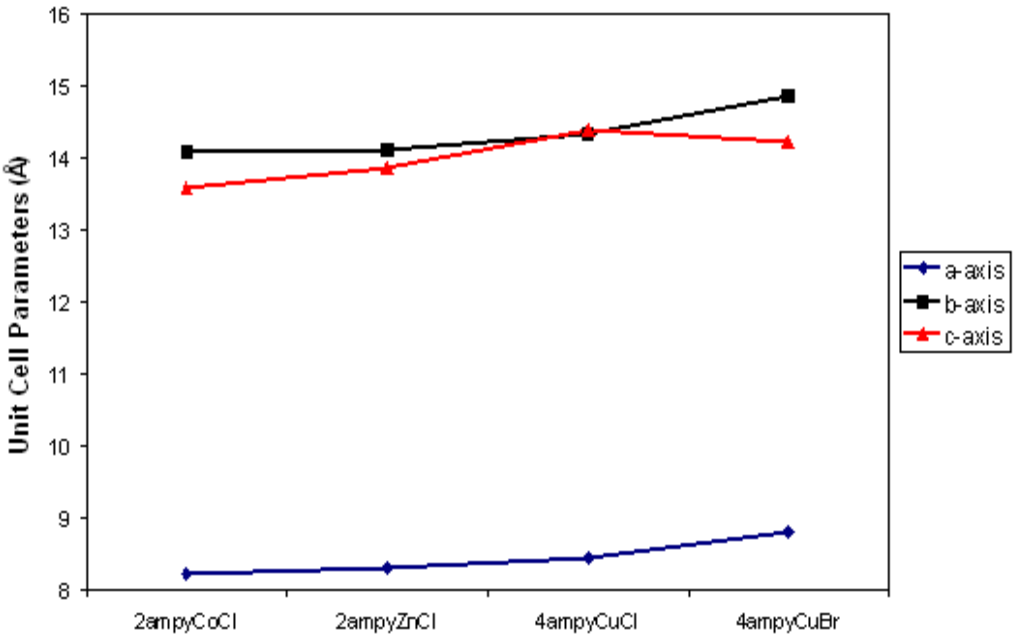


Figure 51: Unit cell parameters of isostructural compounds in the 2-aminopyridinium and 4-aminopyridinium family.

All of the structures crystallize in the space group *C*2/*c*, and the unit cell volumes of the hydrated structures are slightly larger than those of the anhydrous structures due to the incorporation of water molecules into the structure, when the ionic radii of the metal and halogen atoms are taken into account. In all the structures the tetrahalometallate anions are contained in channels formed by cations, as shown below in **Figure 52**.

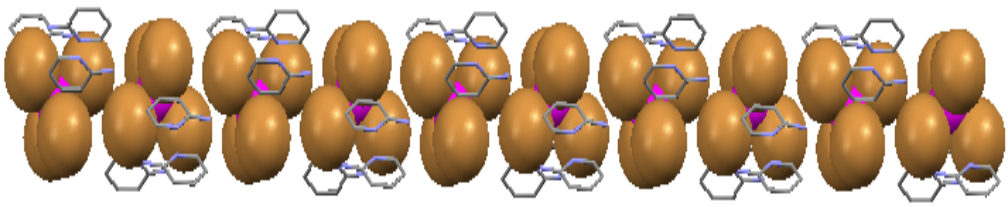


Figure 52: Anions packing in channel formed by 2-aminopyridinium cation in the structure **2ampZnBr**. Isostructural to **2ampHgCl.**

In the 4-aminopyridinium series the inside surface of the channel is formed by amine groups and aromatic C-H groups, and in the 2-aminopyridinium family the channel surface contains the amine groups and the protonated pyridine N. Hydrogen bonding interactions occur between the amine groups (and the pyridine N atoms in the case of the 2-aminopyridinium cation) and the anions.

In the hydrated 4-aminopyridinium structures the water molecules are contained in channels with the inside channel surface formed by the protonated ring N atom (see **Figure 50 (c.)**), and the water molecules are involved in hydrogen bonding interactions with this donor. In the related 2-aminopyridinium structures the inside surface of the channels is created by the aromatic C-H groups (see **Figure 50 (a.) and (b.)**). This explains why water molecules are not incorporated into the 2-aminopyridinium structures; due to the absence of a strong hydrogen bonding donor in the channel, water molecules cannot hydrogen bond to the channel, and thus are not incorporated into the channel. From a crystal engineering perspective this is a good example of the control the choice of cation delivers with regard to the incorporation or exclusion of water molecules from the structures.

For **class 2A** type structures the **amineNH···X** is shorter, hence stronger than the **pyrNH···X** type of interaction. By comparison with **4ampCuCl·H_2O** (Halvorson *et al*, 1990; SEZLEO) and **4ampCuBr·H_2O** (Román, 1996; ZUDKUE) **9** and **10** in the literature survey, it is found that only the **amineNH···X** is present (2.582Å and 2.561Å for **9** and **10** respectively), because the pyridine nitrogen atoms are hydrogen bonded to the water molecule, forming **pyrNH···O** hydrogen bonds (2.040Å and 1.840Å for **9** and **10** respectively).

Table 17: Unit cell parameters of selected 2-aminopyridinium and 4-aminopyridinium containing structures (* No standard deviation reported). Colour indicates isostructurality.

Name	Space Group	*a* (Å)	*b* (Å)	*c* (Å)	α (°)	β (°)	γ (°)	Volume (Å^3)	Packing Efficiency
2ampCoCl (3)	*C*2/*c*	8.2152(3)	14.0713(5)	13.5731(5)	90	95.190(2)	90	1562.598*	8 cations, 4 anions
2ampZnCl	*C*2/*c*	8.3104(6)	14.1150(17)	13.8427(10)	90	93.641(6)	90	1620.5(3)	8 cations, 4 anions
4ampCuCl·H_2O (9)	*C*2/*c*	8.457(2)	14.318(2)	14.382(2)	90	95.82(1)	90	1732.5*	8 cations, 4 anions, 2 waters
4ampCuBr·H_2O (10)	*C*2/*c*	8.797(1)	14.860(1)	14.216(1)	90	96.94(2)	90	1844.75*	8 cations, 4 anions, 2 waters
2ampHgCl	*C*2/*c*	15.0298(8)	7.4925(4)	14.7577(9)	90	92.229(5)	90	1660.6(2)	8 cations, 4 anions
2ampZnBr	*C*2/*c*	15.3064(11)	7.7064(6)	14.7911(10)	90	92.313(6)	90	1743.3(2)	8 cations, 4 anions

4.2.4.2 Packing Trends Across Families

A common packing characteristic observed in a number of structures is the tendency of many *n*-aminopyridinium tetrahalometallate structures with tetrahedral anions to pack in organic and inorganic layers, with the organic layer containing pairs of cations that often interact via aromatic interactions. Some of the structures are shown below in **Figure 53**. This is observed for twenty seven out of thirty six structures (including structures from the literature survey).

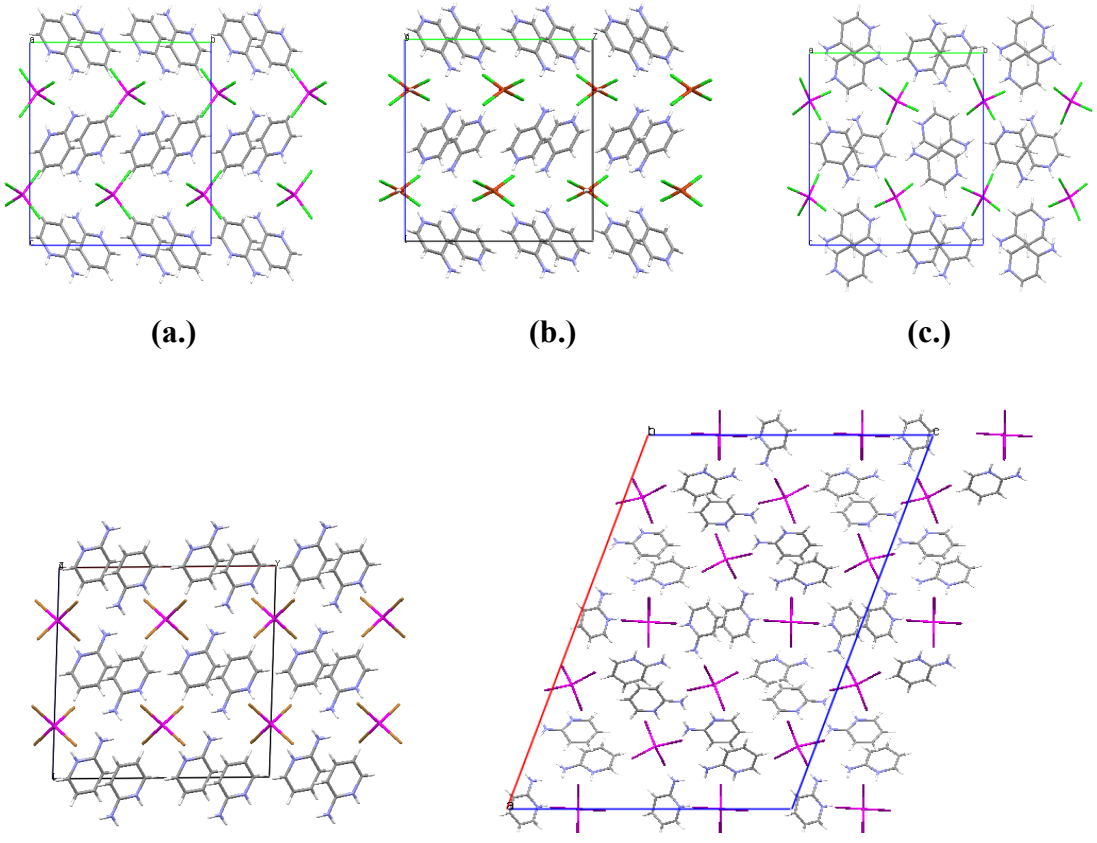


Figure 53: Layered structures with cation pairs in **(a.) 2ampZnCl**, viewed down the *c*-axis. **(b.) 4ampCuCl·H_2O** (Halvorson *et al*, 1990; SEZLEO), viewed down the *a*-axis. **(c.) 4ampZnCl**, viewed down the *a*-axis. **(d.) 2ampZnBr** viewed down the *b*-axis and **(e.) 2ampZnI** viewed down the *b*-axis.

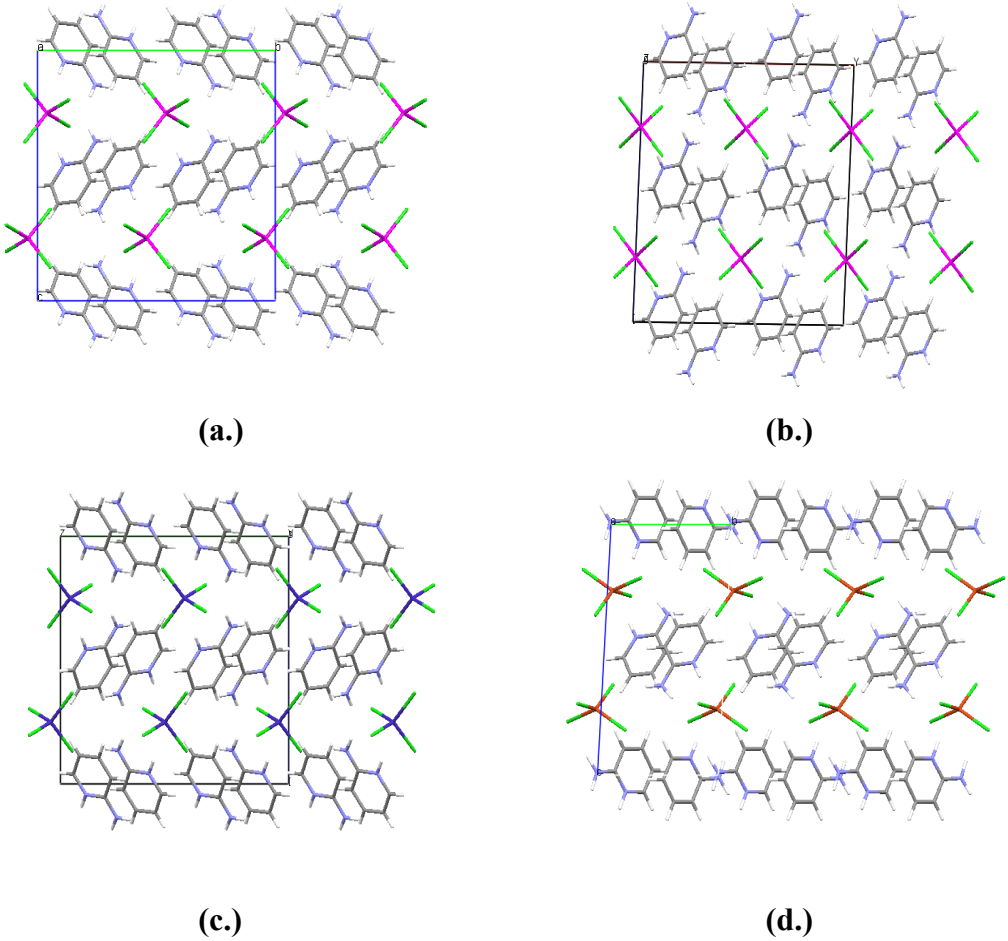
4.3 Effect of a Change in Metal Atom

The effect of changing the metal atom while keeping both the cation and halogen parts of the structures constant can be ascertained by looking at each cation family independently.

4.3.1 2-Aminopyridinium Family

In this family the following comparisons can be made:

4.3.1.1 2-Aminopyridinium Chlorometallate Structures: 2ampZnCl, 2ampHgCl, 2ampCoCl and 2ampCuCl



(a.) **(b.)**

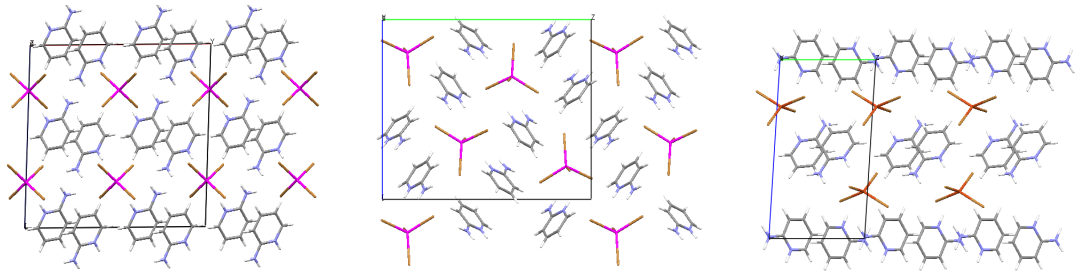
(c.) **(d.)**

Figure 54: Packing in 2-aminopyridinium tetrachlorometallate structures. **(a.) 2ampZnCl**, viewed down the *a*-axis. **(b.) 2ampHgCl**, viewed down the *b*-axis. **(c.) 2ampCoCl**, viewed down the *a*-axis (Jebas *et al*, 2006; DELPOA), **(d.) 2ampCuCl**, viewed down the *a*-axis (Kumar *et al*, 2005; YAPNAS01).

The structures **2ampZnCl**, **2ampHgCl** and **2ampCoCl** (Jebas *et al*, 2006; DELPOA) crystallize in the space group *C*2/*c* and contain tetrahedral anions while the **2ampCuCl** (Kumar *et al*, 2005; Yapnas01) structure crystallizes in the space group P$\bar{1}$ and displays a distorted tetrahedral anion. See **Figure 54** on page 108.

The **2ampZnCl** and **2ampCoCl** (Jebas *et al*, 2006; DELPOA) compounds are isostructural and differ from the **2ampHgCl** structure only in terms of the orientation of tilted cation pairs in consecutive organic layers. The **2ampCuCl** (Kumar *et al*, 2005; Yapnas01) structure has two types of organic layers, and one of these is similar to the tilted organic layers observed in the **2ampZnCl**, **2ampHgCl** and **2ampCoCl** (Jebas *et al*, 2006; DELPOA) structures. The second type of organic layer, however, contain cations that are parallel to the layer planes.

4.3.1.2 2-Aminopyridinium Bromometallate Structures: 2ampZnBr, 2ampHgBr and 2ampCuBr



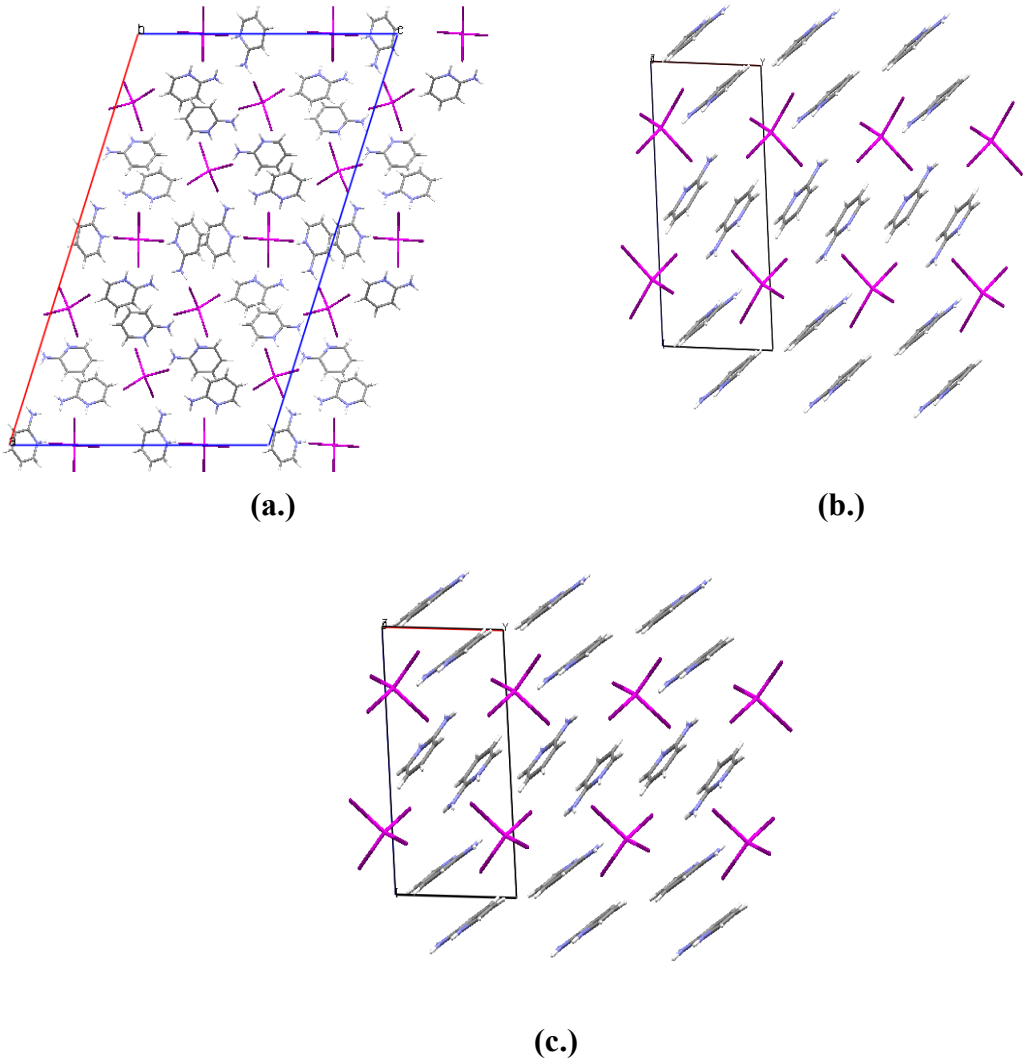
(a.) **(b.)** **(c.)**

Figure 55: Packing in 2-aminopyridinium tetrabromometallates. **(a.) 2ampZnBr**, viewed down the *b*-axis. **(b.) 2ampHgBr**, viewed down the *a*-axis. **(c.) 2ampCuBr**, viewed down the *a*-axis (Luque *et al*, 1997; RIPWIW).

None of the 2-aminopyridinium tetrabromometallate structures are isostructural, even though the anion geometry and the chemical formula is the same for all the structures. Two different types of organic layers occur in the **2ampCuBr** (Luque *et al*, 1997; RIPWIW) structure, one of which is related to the organic layer in the structure of **2ampZnBr**. See **Figure 55** above.

4.3.1.3 2-Aminopyridinium Iodometallate Structures: 2ampZnI, 2ampCdI and 2ampHgI

In this series the **2ampCdI** and **2ampHgI** structures are isostructural, exhibiting two different types of inorganic layers. A different layered structure is displayed by **2ampZnI**. It appears as if the increase in size in the metal atom in going from Zn to Cd and Hg causes a change from one type of structure to the other. No structures containing the 2-aminopyridinium cation and a tetraiodometallate anion have been reported in the literature. See **Figure 56** below.



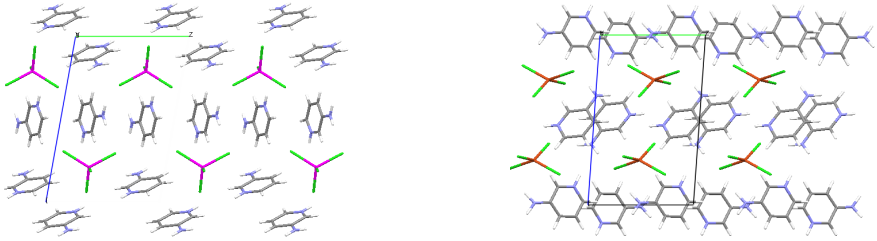
(a.) **(b.)**

(c.)

Figure 56: (a.) 2ampZnI viewed down the *b*-axis. **(b.) 2ampCdI** viewed down the *b*-axis **and (c.) 2ampHgI** viewed down the *b*-axis.

4.3.2 3-Aminopyridinium and 3-Ammoniopyridinium Family

4.3.2.1 3-Aminopyridinium Chlorometallate Structures: 3ampZnCl and 3ampCuCl

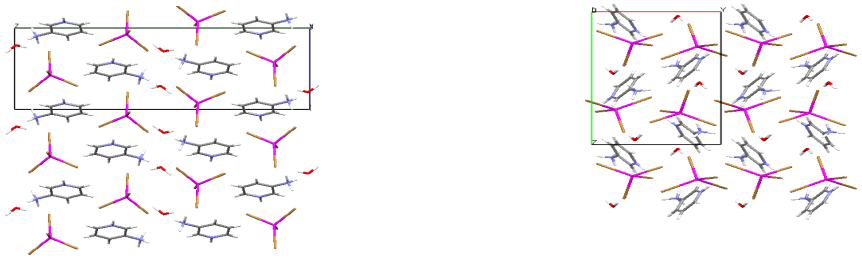


(a.) **(b.)**

Figure 57: Packing in **(a.) 3ampZnCl** viewed down the *a*-axis and **(b.) 3ampCuCl** viewed down the *a*-axis (Kumar *et al*, 2005; PATMUT)**.**

In both structures the 3-aminopyridinium cation is present, but the compounds are not isostructural, despite having the same chemical formula. Each structure shows two different types of organic layers. In the **3ampCuCl** structure (Kumar *et al*, 2005; PATMUT) the anions are distorted from the ideal tetrahedral geometry. See **Figure 57** above.

4.3.2.2 3-Ammoniopyridinium Bromometallate Structures: 3ampZnBr·H_2O and 3ampHgBr·H_2O



(a.) **(b.)**

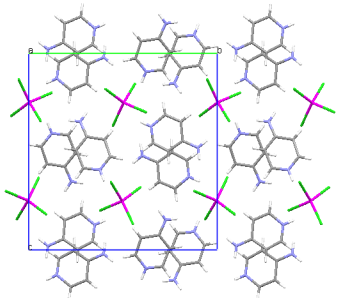
Figure 58: Packing in **(a.) 3ampZnBr·H_2O** viewed down the *a*-axis and **(b.) 3ampHgBr·H_2O** viewed down the *c*-axis (Ali *et al*, 2008; TOBCOD).

Both structures in **Figure 58** above crystallize as hydrates in layered structures, and contain the 3-ammoniopyridinium cation and tetrahedral anions, but are not isostructural. .

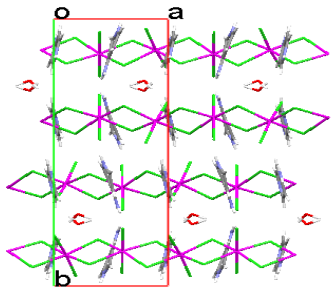
4.3.3 4-Aminopyridinium Family

4.3.3.1 4-Aminopyridinium Chlorometallate Structures: 4ampZnCl, 4ampCdCl·H_2O, 4ampHgCl·H_2O, 4ampCuCl·H_2O and 4ampCoCl

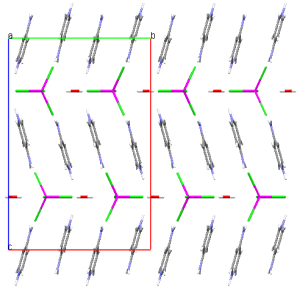
The structures **4ampZnCl** and **4ampCoCl** (Jebas *et al*, 2009; HOSVIV) are isostructural with tilted neighbouring cations and crystallizing in the space group $P2_12_12_1$. The remaining structures all contain water molecules but are not isostructural. **4ampHgCl·H_2O** contains tetrahedral anions, **4ampCuCl·H_2O** (Halvorson *et al*, 1990; SEZLEO) contains distorted tetrahedral anions and **4ampCdCl·H_2O** contains a polymeric $Cd_2Cl_8^{4-}$ anions. See **Figure 59** below.



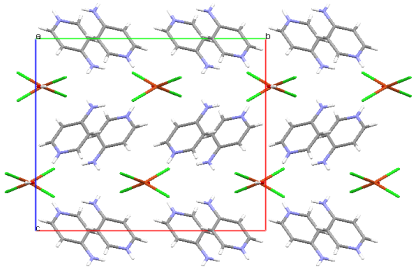
(a.) 4ampZnCl



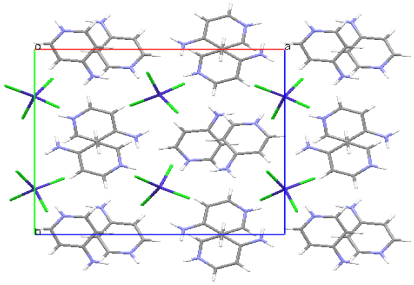
(b.) 4ampCdCl·H_2O



(c.) 4ampHgCl·H_2O



(d.) 4ampCuCl·H_2O

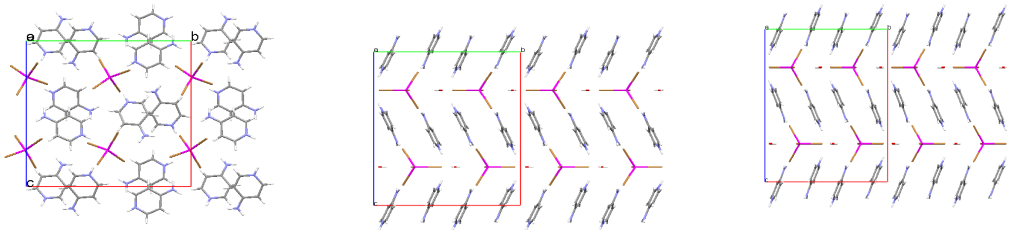


(e.) 4ampCoCl

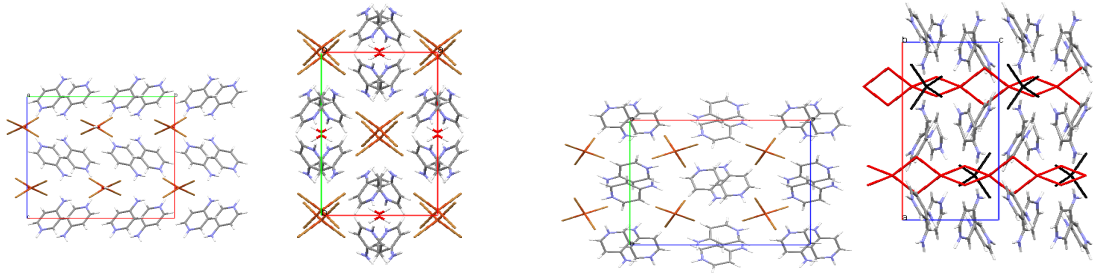
Figure 59: (a.) 4ampZnCl, viewed down the *a*-axis. **(b.) 4ampCdCl·H_2O**, viewed down the *c*-axis. **(c.) 4ampHgCl·H_2O**, viewed down the *a*-axis. **(d.) 4ampCuCl·H_2O**, viewed down the *a*-axis (Halvorson *et al*, 1990; SEZLEO) and **(e.) 4ampCoCl** viewed down the *c*-axis (Jebas *et al*, 2009; HOSVIV).

4.3.3.2 4-Aminopyridinium Bromometallate Structures: 4ampZnBr, 4ampCdBr·H_2O, 4ampHgBr·H_2O, 4ampCuBr and 4ampCuBr·H_2O

In the bromide set of structures (see **Figure 60** below) **4ampCdBr·H_2O** and **4ampHgBr·H_2O** are isostructural and crystallize in the space group ***Pbcm***. The hydrated **4ampCuBr·H_2O** (Román *et al*, 1996; ZUDKUE) bears very little similarity to the anhydrous structure **4ampCuBr** (Sertucha *et al*, 1998; LAHYAU). The hydrated form contains rings comprising four cations that surround pairs of water molecules. See **Figure 60: (d.) c-axis view.** The anhydrous form contains both polymeric and isolated tetrahedral anions. See **Figure 60: (e.) b-axis view.**



(a.) 4ampZnBr **(b.) 4ampCdBr·H_2O** **(c.) 4ampHgBr·H_2O**

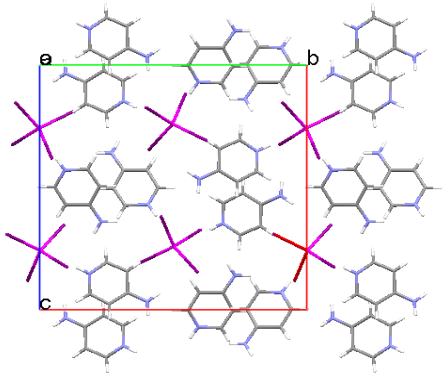


(*a*-axis) **(*c*-axis)** **(*c*-axis)** **(*b*-axis)**

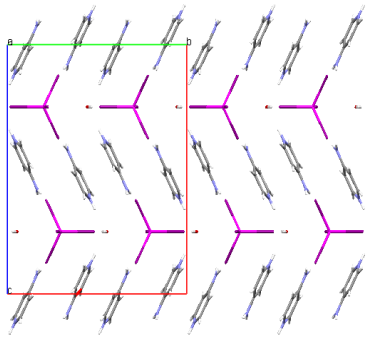
d.) 4ampCuBr·H_2O **(e.) 4ampCuBr**

Figure 60: (a.) 4ampZnBr, viewed down the *c*-axis. **(b.) 4ampCdBr·H_2O,** viewed down the *a*-axis. **(c.) 4ampHgBr·H_2O,** viewed down the *a*-axis. **(d.) 4ampCuBr·H_2O**, left: viewed down the *a*-axis, right: viewed down the *c*-axis (Román *et al*, 1996; ZUDKUE) and **(e.) 4ampCuBr**, left: viewed down the *c*-axis, right: viewed down the *b*-axis (Sertucha *et al*, 1998; LAHYAU).

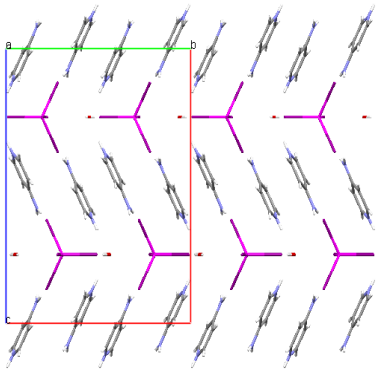
4.3.3.3 4-Aminopyridinium Iodometallate Structures: 4ampZnI, 4ampCdI·H_2O and 4ampHgI·H_2O



(a.) 4ampZnI



(b.) 4ampCdI·H_2O



(c.) 4ampHgI·H_2O

Figure 61: (a.) 4ampZnI, viewed down the *c*-axis. **(b.) 4ampCdI·H_2O,** viewed down the *a*-axis and **(c.) 4ampHgI·H_2O** viewed down the *a*-axis.

In the iodide subgroup, the metals show the same trend as with the bromides, for the zinc, cadmium and mercury analogues. See **Figure 61** above. The zinc analogue is anhydrous and crystallizes in the space group ***Pbcm*** and the cadmium and mercury analogues contain water, are isostructural and crystallize in the space group $\boldsymbol{P2_12_12_1}$.

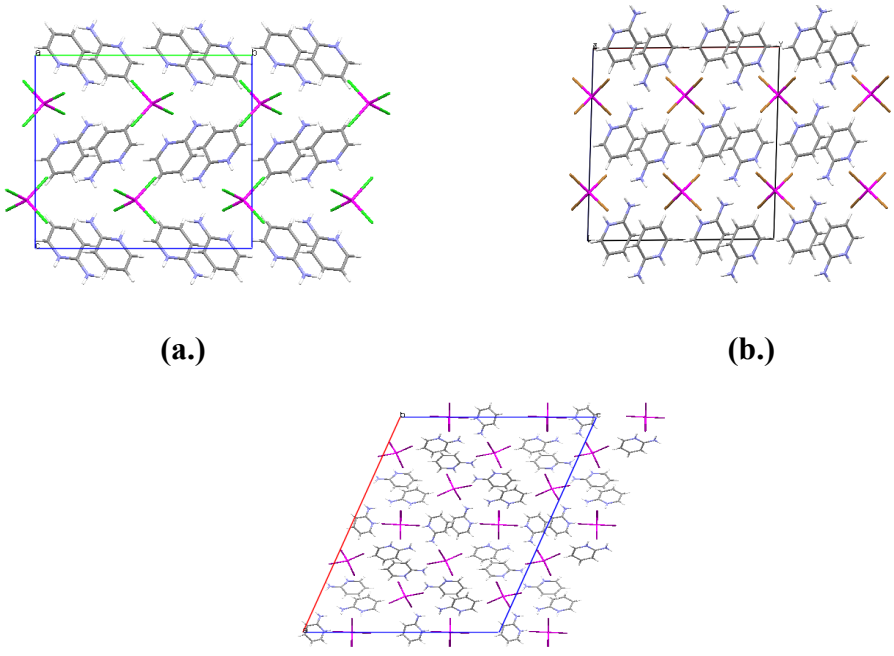
4.4 Effect of a Change in Halogeno Ligand

The effect of varying the halogeno ligand while keeping the metal and cation part of the structure constant is highlighted by comparing the following structures:

4.4.1 2-Aminopyridinium Family

4.4.1.1 2-Aminopyridinium Perhalozincate Structures: 2ampZnCl, 2ampZnBr, 2ampZnI

Although all the anhydrous structures in this subsection have the same chemical formula and contain isolated tetrahedral anions and pairs of cations, three different types of structures are formed. This may be due to the fact that the increase in halogeno ligand size result in the crystallization in different structures, or that the structures are different polymorphic forms. The **2ampZnCl** and **2ampZnBr** structures are similar, and differ in the orientation of cations in consecutive organic layers. In the **2ampZnI** structure neighbouring pairs of cations differ in their relative orientation. See **Figure 62** below.



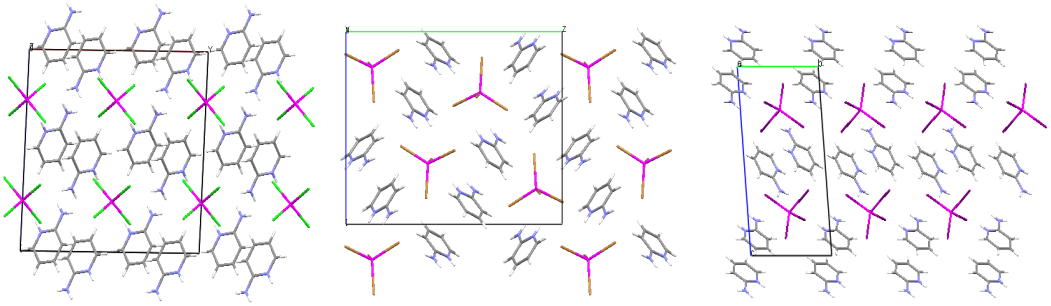
(a.) **(b.)**

(c.)

Figure 62: (a.) 2ampZnCl, viewed down the *a*-axis. **(b.) 2ampZnBr**, viewed down the *b*-axis and **(c.) 2ampZnI** viewed down the *b*-axis.

4.4.1.2 2-Aminopyridinium Perhalomercurate Structures: 2ampHgCl, 2ampHgBr, 2ampHgI

All three structures are anhydrous, have tetrahedral anions and the same chemical formula, however none of the structures are isostructural. This may indicate that the increase in halogeno ligand size cause the compounds to form different structures, or these may be different polymorphic forms. See **Figure 63** below**.**

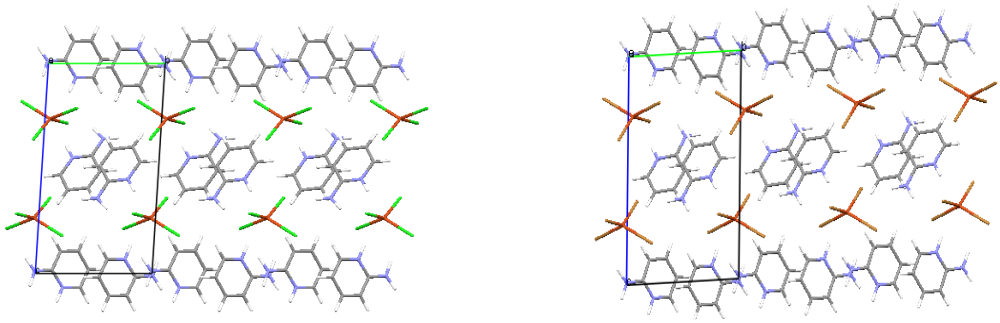


(a.) **(b.)** **(c.)**

Figure 63: (a.) 2ampHgCl, viewed down the *b*-axis. **(b.) 2ampHgBr** viewed down the *a*-axis and **(c.) 2ampHgI,** viewed down the *a*-axis.

4.4.1.3 2-Aminopyridinium Perhalocuprate Structures: 2ampCuCl, 2ampCuBr

The structures in this subgroup are isostructural and contain distorted tetrahedral anions. See **Figure 64** below.

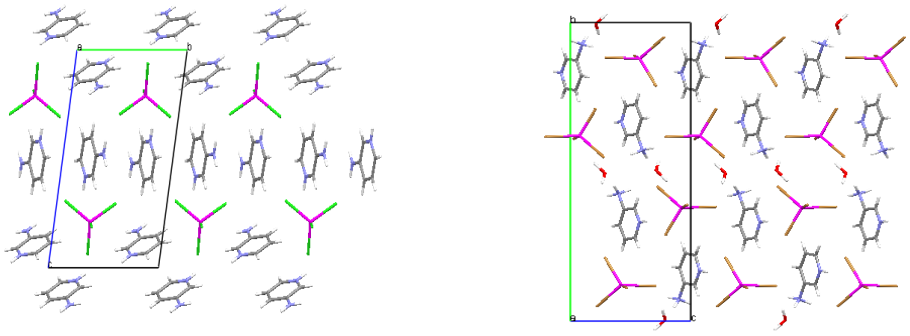


(a.) **(b.)**

Figure 64: (a.) 2ampCuCl, viewed down the *a*-axis (Kumar *et* al, 2005; YAPNAS01) and **(b.) 2ampCuBr**, viewed down the *a*-axis (Luque *et al*, 1997; RIPWIW).

4.4.2 3-Aminopyridinium and 3-Ammoniopyridinium Family

4.4.2.1 3-Aminopyridinium and 3-Ammoniopyridinium Perhalozincate Structures: 3ampZnCl, 3ampZnBr·H_2O



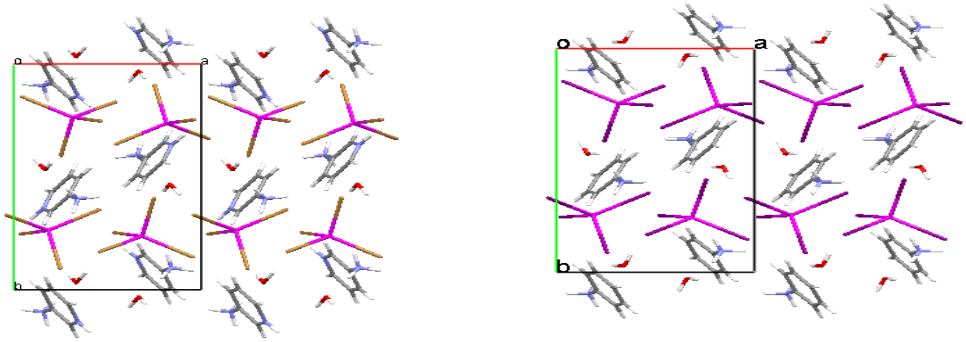
(a.) **(b.)**

Figure 65: (a.) 3ampZnCl, viewed down the *a*-axis and **(b.) 3ampZnBr·H_2O**, viewed down the *a*-axis.

In this group of structures the **3ampZnCl** structure is anhydrous and contains the 3-aminopyridinium cation while the **3ampyZnBr·H_2O** structure contains the 3-ammoniopyridinium cation and water molecules. See **Figure 65** above.

4.4.2.2 3-Ammoniopyridinium Perhalomercurate Structures: 3ampHgBr·H_2O, 3ampHgI·H_2O

The hydrated structures in this group are isostructural. See **Figure 66** below..

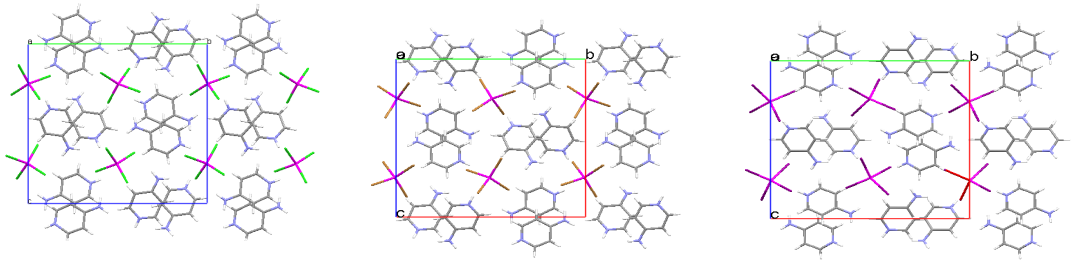


(a.) **(b.)**

Figure 66: (a.) 3ampHgBr·H_2O, viewed down the *c*-axis and **(b.) 3ampHgI·H_2O**, viewed down the *c*-axis.

4.4.3 4-Aminopyridinium Family

4.4.3.1 4-Aminopyridinium Perhalozincate Structures: 4ampZnCl, 4ampZnBr, 4ampZnI



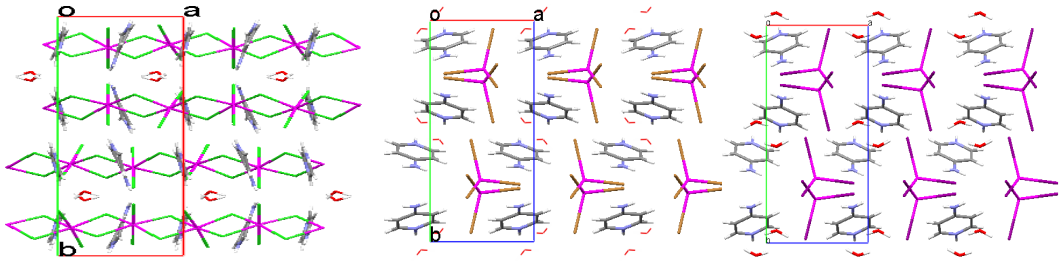
(a.) **(b.)** **(c.)**

Figure 67: (a.) 4ampZnCl, viewed down the *a*-axis. **(b.) 4ampZnBr**, viewed down the *a*-axis **(c.) 4ampZnI**, viewed down the *a*-axis.

All the structures in this subsection are anhydrous and isostructural. See **Figure 67** above.

4.4.3.2 4-Aminopyridinium Perhalocadmate Structures: 4ampCdCl·H_2O, 4ampCdBr·H_2O, 4ampCdI·H_2O

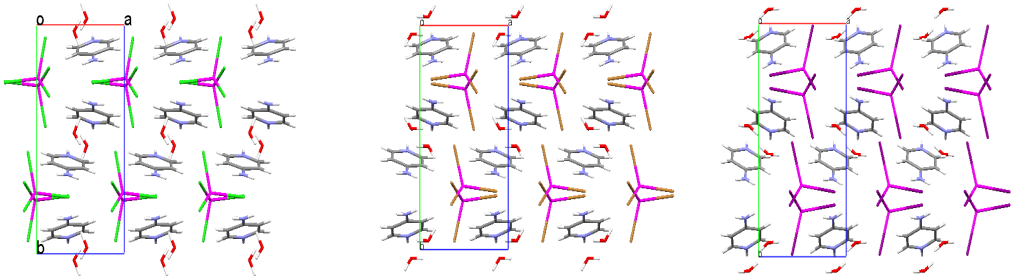
The cadmium subgroup of the 4-aminopyridinium family contains only hydrated structures. The bromo and iodo analogues are isostructural. The chloro analogue contains the only polymeric anion. See **Figure 68** below.



(a.) **(b.)** **(c.)**

Figure 68: (a.) 4ampCdCl·H_2O, viewed down the *c*-axis. **(b.) 4ampCdBr·H_2O**, viewed down the *c*-axis and **(c.) 4ampCdI·H_2O**, viewed down the *c*-axis.

4.4.3.3 4-Aminopyridinium Perhalomercurate Structures: 4ampHgCl·H_2O, 4ampHgBr·H_2O, 4ampHgI·H_2O



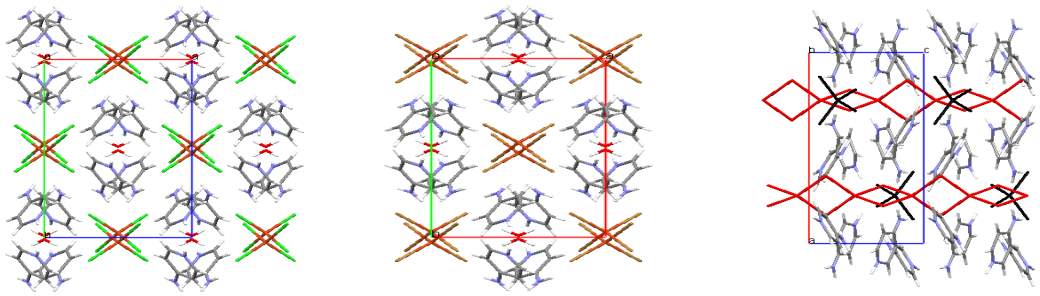
(a.) **(b.)** **(c.)**

Figure 69: (a.) 4ampHgCl·H_2O, viewed down the *c*-axis. **(b.) 4ampHgBr·H_2O**, viewed down the *c*-axis and **(c.) 4ampHgI·H_2O**, viewed down the *c*-axis.

In this subgroup all the structures are hydrates and isostructural. The anions move further apart with increasing ionic radii from chlorine to bromine to iodine. See **Figure 69** above.

4.4.3.4 4-Aminopyridinium Perhalocuprate Structures: 4ampCuCl·H_2O, 4ampCuBr·H_2O, 4ampCuBr

The hydrated chloro and bromo analogues are isostructural. The anhydrous bromo analogue contains a mixed anion geometry that consists of isolated tetrahedral anions and polymeric anions. See **Figure 70** below.



(a.) **(b.)** **(c.)**

Figure 70: (a.) 4ampCuCl·H_2O, viewed down the *c*-axis (Halvorson *et al*, 1990; SEZLEO). **(b.) 4ampCuBr·H_2O**, viewed down the *c*-axis (Román *et al*, 1996; ZUDKUE) and **(c.) 4ampCuBr**, viewed down the *c*-axis (Sertucha *et al*, 1998; LAHYAU).

4.5 Effect of Halogeno Ligands on Hydrogen Bonding Interactions

In this study, three halogeno ligands were used namely chloro, bromo and iodo. Since it is the halogeno ligand that acts as hydrogen bond acceptor and forms an intermolecular interaction with the hydrogen bond donor, it is worth while to take a look at how each halogen prefers to form these hydrogen bonds, and how the different ionic radii of the ligand affects the interaction.

Table 18: Ionic Radii of selected halogens (Brown, 2003).

Halogen	Ionic Radius (Å)
Cl^-	1.81
Br^-	1.96
I^-	2.20

4.5.1 Hydrogen Bonding Interactions in Chloro Ligand containing Structures

There are sixteen chloro ligand containing hybrids under investigation, six from this study and ten from the literature survey. The average **Cation-N-H···X-M-Anion** hydrogen bonding interaction distance of the type **pyrNH···X** is 2.492Å and the **amineNH···X** distance is 2.516Å.

Three of the structures in the chloro subgroup contain water molecules and all three contain the 4-aminopyridinium cation. For these hydrated structures the average **Water-H···X-M-Anion** distance is 2.218Å. Water hydrogen bonds only to the pyridine portion of the cation, and the average **pyrNH···O** distance is 2.014Å.

Ten of the total number of sixteen chloro ligand containing structures contain tetrahedral anions, five contain polymeric or octahedral anions and one contains a square planar anion.

4.5.2 Hydrogen Bonding Interactions in Bromo Ligand containing Structures

There are thirteen bromo ligand containing hybrids under investigation, six from this study and seven from the literature survey. The average **Cation-N-H···X-M-Anion** interaction distance of the type **pyrNH···X** is 2.674Å and for the **amineNH···X** interaction the distance is 2.689Å.

Seven out of the thirteen of the bromo ligand containing structures contain water molecules, and contain either the 3-aminopyridinium or 4-aminopyridinium cation. The average **Water-H···X-M-Anion** distance is 2.616Å. Water bonds either to the pyridine portion or amino portion, but not both. The average **pyrNH···O** hydrogen bonding distance is 1.915Å and the average **amineNH···O** distance is 1.846Å. However only two of the seven contain **amineNH···O** so one would think that **pyrNH···O** are slightly, if at all, preferred over **amineNH···O** interactions. Ten of the structures in the bromo ligand subgroup contain distorted tetrahedral anions, two contain octahedral or polymeric anions and one contains a mixture of tetrahedral anions and polymeric anions.

4.5.3 Hydrogen Bonding Interactions in Iodo Ligand containing Structures

There are seven iodo ligand containing hybrids under investigation, all seven from this study because no suitable comparisons were not found for the literature survey. The average **Cation-N-H···X-M-Anion** hydrogen bonding interaction distance of the type **pyrNH···X** is 2.904Å and for the interaction **amineNH···X** the distance is 2.921Å.

Three of the iodo ligand containing structures contain water molecules, and contain either the 3-aminopyridinium or 4-aminopyridinium cation. The average **Water-H···X-M-Anion** distance is 2.987Å. Water bonds either to the pyridine portion or amino portion, but not both. The average **pyrNH···O** hydrogen bonding distance is 2.016Å and the average **amineNH···O** hydrogen bonding distance is 1.833Å. However only one of the three contain **amineNH···O,** so one would think that **pyrNH···O** are slightly, if at all, preferred over **amineNH···O** interactions. All seven of the structures contain distorted tetrahedral anions.

4.5.4 Trends, When Keeping the Halogeno Ligand Constant

A summary of the above analysis is given in **Table 19** on page123. A parallel can be drawn from the ionic radii of the halogens and the hydrogen bonding interaction distance. That is as the ionic radii of the halogen increases, so does the length of the intermolecular interaction. Simply put; the size of the ionic radii has a direct impact on the length and therefore strength of intermolecular interaction. We know that ionic radii increase as follows: Cl < Br < I. The parallel is that the **Average Cation-N-H···X-M-Anion** and **Average Water-H···X-M-Anion** interaction increases as follows:

Average Cation-N-H···Cl-M-Anion < Average Cation-N-H···Br-M-Anion < Average Cation-N-H···I-M-Anion

and

Average Water-H···Cl-M-Anion < Average Water-H···Br-M-Anion < Average Water-H···I-M-Anion

Table 19: Summary of the effect of halogeno ligands on hydrogen bonding interactions.

Halogen	Perhallometallate Anion Geometry	Hydrated Hybrids	Average Cation-N-H···X-M-Anion Distance (Å)		Average Water-H···X-M-Anion Distance (Å)	Average Cation-N-H···O-Water Distance (Å)	
			pyrNH···X	amineNH···X		pyrNH···O	amineNH···O
Cl	10 out of 16 Tetrahedral, 5 Polymeric/Octahedral, 1 Square Planar	3 out of 16	2.492	2.516	2.218	2.014	No interaction
Br	10 out of 13 Tetrahedral, 2 Polymeric/ Octahedral, 1 mixture of Tetrahedral and Polymeric	7 out of 14	2.674	2.689	2.616	1.915	1.846
I	7 out 7 Tetrahedral	3 out of 7	2.904	2.921	2.987	2.016	1.833

5. Conclusion and Recommendations for Future Work

5.1 Conclusion

The crystallographic investigation of *n*-aminopyridinium perhalometallates is an important step in the understanding of hybrid crystal structures and how these structures prefer to pack. In crystallography the word hybrid means combining two different components, one organic, the other inorganic, in a single material, while each component retains many of it's original properties.

The results of this dissertation prove that making sense of a family of hybrids is not all that easy because of the give and take between intermolecular hydrogen bonding and the structural arrangement that yields the best fit. Nineteen of the proposed twenty-seven novel structures (70%) were successfully synthesized, characterized and studied in detail. Eighteen of the nineteen structures (95%) contained isolated tetrahedral anions that were slightly distorted. The remaining structure catena-(bis(4-aminopyridinium) bis(μ_2-chloro) dicadmium(II) monohydrate) contained a corrugated polymeric $Cd_2Cl_8^{4-}$ anion.

All nineteen hybrids contained layered structures, where there was an organic layer containing the *n*-aminopyridinium cations separated by an inorganic layer containing the perhalometallate anions. In each structure the cations packed in pairs, either head to tail or rotated relative to each other. It was discovered that cation pairs that illustrated significant π-π interactions (centroid to centroid cut-off distance of 3.8 Å) were arranged head-tail and contained a slippage distance of between 0.4 Å and 1.6 Å. The only exception was for that of catena-(bis(4-aminopyridinium) bis(μ_2-chloro) dicadmium(II) monohydrate) where the cations were rotated relative to each other and contained a centroid to centroid distance of 3.471Å and a slippage distance of 1.351Å.

In sixteen of the nineteen hybrids (89%), the pyridine N of the *n*-aminopyridinium cation was protonated as opposed the to the amine N. Two structures containing the 3-aminopyridine organic component formed the 3-ammoniopyridinium cation, where both the amine N and pyridine N were protonated as opposed to the 3-aminopyridinium cation where only the pyridine N was protonated.

Eight of the nineteen hybrid structures (42 %) contained water. The 42 % include the two 3-ammoniopyridinium structures and all the cadmium and mercury containing 4-aminopyridinium structures. This means that none of the 2-aminopyridinium, 3-aminopyridinium or zinc containing 4-aminopyridinium structures contained water. The availability of space at the hydrogen bond donor (protonated N) was the determining factor as to whether a structure would or would not contain water. Space was available when the hydrogen bond donors were further apart from each other as was the case with 4-aminopyridinium hybrids and when there was an additional hydrogen atom available at the hydrogen bond donor, as was the case with 3-ammoniopyridinium hybrids. The metal in the hybrid also played a role in the space available around the protonated N. Smaller metals tend to have stronger and shorter metal ligand bonds. This allows the perhalometallate anion to form shorter intermolecular interactions with the protonated N and hence occupy more space closer to the protonated N as compared to perhalometallate anions with larger metals. This is most likely the reason that the smaller and more compact zinc containing 4-aminopyridinium hybrids were anhydrous, whereas the larger cadmium and mercury containing hybrids were hydrated.

Six classes of isostructural hybrids were identified (including three structures reported in the literature), three classes from the 2-aminopyridinium series, one class from the 3-ammoniopyridinium series and two classes from the 4-aminopyridinium series: **Class 2A1**, **Class 2A2**, **Class 2C**, **Class 3C**, **Class 4A** and **Class 4C**. In **Class 2A1** **2ampZnCl** and **2ampCoCl** were isostructural, zinc and cobalt both being smaller metals and of similar size were therefore interchangeable.

In **Class 2A2** **2ampHgCl** and **2ampZnBr** were isostructural. In this case a larger metal Hg combined with a smaller halogen Cl was interchangeable with a smaller metal Zn combined with a larger halogen Br. In **Class 2C** **2ampCdI** was isostructural to **2ampHgI**, Cd and Hg being larger metals of similar size were interchangeable. In **Class 3C** **3ampHgI·H_2O** was isostructural to **3ampHgBr·H_2O**. In this case a larger halogen I was interchangeable with a smaller halogen Br. In **Class 4A** **4ampZnCl, 4ampZnBr, 4ampZnI** and **4ampCoCl** were isostructural. In this case the smaller metals Zn and Co were interchangeable irrespective of the halogen used. In **Class 4C** **4ampCdBr·H_2O**, **4ampCdI·H_2O**, **4ampHgCl·H_2O**, **4ampHgBr·H_2O** and **4ampHgI·H_2O** were

isostructural. The larger metals Cd and Hg were interchangeable irrespective of the halogen used. The 4-aminopyridinium series yielded the most robust synthon because all nine 4-aminopyridinium perhalometallates from this study yielded the same synthon, irrespective of the metal or halogen or whether water was present. 2-aminopyridinium yielded four different synthons and 3-aminopyridine containing structures yielded a synthon common to both the 3-aminopyridinium and 3-ammoniopyridinium structures.

5.2 Recommendations for Future Work

For future work, it is recommended that the outstanding hybrids be synthesized, characterised and studied to gain a more complete picture of how these *n*-aminopyridinium perhalometallates behave. It is also recommended that the degree of isostructurality be investigated, for the identified classes of structures that exhibit isostructurality. This may be carried out using calculations that involve the volume of the unit cell. It is also recommended that the series be expanded to ascertain whether the trends identified can actually be applied beyond the scope of this study.

6. References

Aakeröy, C. B.; Beatty, A. M.; Helfrich, B. A. *Angew. Chem. Int. Ed.* **2001**, *40*, 3240.

Adams, C. J.; Angeloni, A.; Orpen, A. G.; Podesta, T. J.; Shore, B. *Crystal Growth & Design* **2006**, *6*, 411.

Ali, B. F.; Al-Far, R. H.; Haddad, S. F. *Acta Cryst.* **2008**, *E64*, m751.

Aullo'n, G.; Bellamy, D.; Brammer, L.; Bruton, E. A.; Orpen, A. G. *Chem. Commun.* **1998**, 653.

Bordwell, F. G.; Singer, D. L.; Satish, A. V. *J. Am. Chem Soc.* **1993**, *115*, 3543.

Braga, D.; Grepioni, F. *Chem. Commun*. **2005**, 3635.

Brammer, L.; Swearingen, E. A.; Bruton, P. S. *Proc. Natl. Acad. Sci. USA.* **2002**, *99*, 4956.

Bruker **2005a**: APEX2. Version 2.0-1. Bruker AXS Inc., Madison, Wisconsin, USA.

Bruker **2005b**: SAINT+. Version 6.0 (includes XPREP and SADABS) Bruker AXS Inc., Madison, Wisconsin, USA.

Bruker **1999a**: SAINT+ Version 6.02 (includes XPREP and SADABS), Bruker AXS Inc., Madison, Wisconsin, USA.

Bruker **1999b**: SAINT+ Version 5.1 (includes XS, XL, XP, XSHELL), Bruker AXS Inc., Madison, Wisconsin, USA.

Bruno, I. J.; Cole, J. C.; Edingtion, P. R.; Kessler, M. K.; Macrae, C. F.; McCabe, P.; Pearson, J.; Taylor, R. MERCURY. *Acta Cryst*. **2002**, *B58*, 389.

Caballero, N. A.; Melendez, F. J.; Muñoz-Caro, C.; Niño, A. *Biophysical Chemistry.* **2006**, *124*, 155.

Campana, C. F. In *Bruker Analytical Application Notes*; Putnis, A., Introduction to Mineral Sciences; Cambridge University Press: Cambridge, UK, **1992**; Chapter 3, pp 41-80.

Clegg, W. In *Crystal Structure Determination*; Oxford Chemistry Primers; Oxford Science Publications, 2005; p 27.

Dann, S. E. In *Basic Concepts in Chemistry, Reactions and Characterization of Solids*; Royal Society of Chemistry; Wiley Interscience, 2002; pp 49-54.

Desiraju, G. R. *Angew. Chem. Int. Ed.* **1995**, *34,* 2311.

Desiraju, G. R. *Chem. Commun*. **1997**, 1457.

Desiraju, G. R. *Acc. Chem. Res.* **2002**, *35*, 565.

Farrugia, L. J. WinGX. *J. Appl. Cryst*. **1999**, *32*, 837.

Fossey, J.; Loupy, A.; Strzelecka, H. *Tetrahedron*, **1981**, *37*, 1935.

Gillon, A. L.; Lewis, G. R.; Orpen, A. G.; Rotter, S.; Starbuck, J.; Wang, X.; Rodríguez-Martín, Y.; Ruiz-Pérez, C. *J. Chem. Soc., Dalton Trans*. **2000**, 3897.

Gillon, A. L.; Orpen, A. G.; Starbuck, J.; Wang, X.; Rodríguez-Martín, Y.; Ruiz-Pérez, C. *Chem. Commun*. **1999**, 2287.

Halvorson, K. E.; Patterson, C.; Willett, R. D. *Acta Cryst.* **1990**, *B46*, 508.

Hashimoto, M.; Terao, H.; Fuess, H.; Svoboda, I.; Ehrenberg, H. *Bull. Chem. Soc. Jpn.* **2003**, *76*, 749.

Hatano, N.; Nakashima, M.; Horiuchi, K.; Terao, H.; Ishihara, H. *Z. Naturforsch.* **2008**, *63b*, 1181.

Ivanova, B. B.; Arnaudov, M. G.; Mayer-Figge, H. *Polyhedron.* **2005**, *24*, 1624.

Jakubas, R.; Ciunik, Z.; Bator, G. *Physical Review B.* **2003**, 67.

Janiak, C. *J.Chem.Soc.;Dalton Trans.* **2000**, 3005.

Jebas, S. R.; Balasubramanian, T.; Light, M. E. *Acta Cryst.* **2006**, *E62*, m1818.

Jebas, S. R.; Sinthiya, A.; Nayagam, B. R. D.; Schollmeyer, D.; Raj, A. C. *Acta Cryst.* **2009**, *E65*, m521.

Kulicka, B.; Jakubas, R.; Bator, G.; Ciunik, Z.; Medycki, W. *J. Phys.: Condens. Matter*. **2004**, *16*, 8155.

Kulicka, B.; Jakubas, R.; Pietraszko, A.; Medycki, W.; Świergiel, J. *Journal of Molecular Structure.* **2006**, *783*, 88.

Kumar, D. K.; Ballabh, A.; Jose, D. A. *Crystal Growth & Design.* **2005**, *5*, 651.

Lewis, G. R.; Orpen, A. G. *Chem. Commun*. **1998**, 1873.

Luque, A.; Sertucha, J.; Lezama, L.; Rojo, T.; Román, P. *J. Chem. Soc., Dalton Trans.* **1997**, 847.

Mitzi, D. B. In *Synthesis, Structure, and Properties of Organic-Inorganic Perovskites and Related Materials*; Karlin, K. D., Progress in Inorganic Chemistry; John Wiley & Sons Inc: NY, **1999**; Vol. 48, pp 2-4.

Mitzi, D. B.; Chrondroudis, K.; Kagan, C. *IBM J. Res. & Dev*. **2001**, *45*, 29.

Online Dictionary of Crystallography Isostructural Crystals. http://reference.iucr.org/dictionary/Isostructural_crystals (accessed September 27, 2011).

Ostojić, B. D.; Janjić, G. V.; Zarić, S. D. *Chem. Commun.* **2008**, 6546.

Oxford Diffraction Ltd. **2006**: CrysAlis CCD and CrysAlis RED, Version 1.171.29.9. Oxford Diffraction Ltd, Abingdon, Oxford, England.

Pidcock, E.; Motherwell, W. D. S. *Acta Cryst.* **2004**, *B60*, 725.

Rademeyer, M.; Lemmerer, A.; Billing, D. G. *Acta Cryst.* **2007**, *C63*, m289.

Read, R. J. *University of Cambridge*. All rights reserved. © **1999-2009** "The Phase Problem: Introduction to Phasing Methods" http://www-structmed.cimr.cam.ac.uk/Course/Basic_phasing/Phasing.html (accessed September 27, 2011)

Román, P.; Sertucha, J.; Luque, A.; Lezama, L.; Rojo, T. *Polyhedron.* **1996**, *15*, 1253.

Sanchez, C.; Julián, B.; Belleville, P.; Popall, M. *J.Mater.Chem.* **2005**, *15*, 3359.

Serezhkina, L. B.; Bakhhet'eva, L. M. *Zhurnal Neorganicheskoi KhimII.* **2000**, *45*, 489.

Sertucha, J.; Luque, A.; Lloret, F.; Román, P. *Polyhedron.* **1998**, *17*, 3875.

Shannon, R. D. *Acta Crystallogr.* **1976**, *A32*, 751.

Sheldrick, G. M., **1997**, University of Gottingen, Germany

Smith, J. G. In *Organic Chemistry*; McGraw Hill International Edition, **2006**; pp 621-623, 912.

Spek, A. L. PLATON. *J. Appl. Cryst*. **2000**, 36.

Steiner, T. *Angew. Chem. Int. Ed.* **2002**, *41*, 48.

Turro, N. J. *PNAS*. **2005**, *102*, 10765.

Appendix A: Crystallographic Codes

Name of Hybrid	Code
Bis(2-aminopyridinium) tetrachlorocuprate(II) (Kumar *et al*, 2005)	2ampCuCl
Bis(2-aminopyridinium) tetrabromocuprate(II) (Luque *et al*, 1997)	2ampCuBr
Bis(2-aminopyridinium) tetrachlorocobolt(II) (Jebas *et al*, 2006)	2ampCoCl
2-Aminopyridinium tetrachloroantimony(III) (Kulicka *et al*, 2004)	2ampSbCl
2-Aminopyridinium tetrabromoantimony(III) (Kulicka *et al*, 2004)	2ampSbBr
Bis(3-aminopyridinium) tetrachlorocuprate(II) (Kumar *et al*, 2005)	3ampCuCl
3-Ammoniopyridinium tetrabromidomercurate(II) monohydrate (Ali *et al*, 2008)	3ampHgBr·H_2O
Bis(4-aminopyridinium) tetrabromocadmium(II) monohydrate (Hatano *et al*, 2008)	4ampCdBr·H_2O
Bis(4-aminopyridinium) tetrachlorocuprate(II) monohydrate (Halvorson *et al*, 1990)	4ampCuCl·H_2O
4-Aminopyridinium tetrabromocopper(II) monohydrate (Román *et al*, 1996)	4ampCuBr·H_2O
Catena(tetrakis(4-aminopyridinium) tetrabromo-copper(ii) bis(bis(m~2~-bromo)-copper(i))) (Sertucha *et al*, 1998)	4ampCuBr
4-Aminopyridinium tetrachloroantimony(III) (Jakubas *et al*, 2003)	4ampSbCl(see-saw)
4-Aminopyridinium hexachloroantimonate(V) (Kulicka *et al*, 2006)	4ampSbCl(octahedron)
Catena-(4-aminopyridinium bis(m~2~-bromo)-dibromo-antimony(III)) (Hashimoto *et al*, 2003)	4ampSbBr
Bis(4-aminopyridinium) tetrachloropalladate(II) (Ivanova *et al*, 2005)	4ampPdCl
Bis(4-aminopyridinium) hexachloridostannate(IV) (Rademeyer *et al*, 2007)	4ampSnCl
Bis(4-aminopyridinium) tetrachloridocobaltate(II) (Jebas *et al*, 2009)	4ampCoCl
Bis(2-aminopyridinium) tetrachlorozincate(II)	2ampZnCl
Bis(2-aminopyridinium) tetrabromozincate(II)	2ampZnBr
Bis(2-aminopyridinium) tetraiodozincate(II)	2ampZnI
Bis(2-aminopyridinium) tetraiodocadmate(II)	2ampCdI
Bis(2-aminopyridinium) tetrachloromercurate(II)	2ampHgCl
Bis(2-aminopyridinium) tetrabromomercurate(II)	2ampHgBr
Bis(2-aminopyridinium) tetraiodomercurate(II)	2ampHgI
Bis(3-aminopyridinium) tetrachlorozincate(II)	3ampZnCl
Bis(3-ammoniopyridinium) tetrabromozincate(II) monohydrate	3ampZnBr·H_2O
Bis(3-ammoniopyridinium) tetraiodomercurate(II) monohydrate	3ampHgI·H_2O
Bis(4-aminopyridinium) tetrachlorozincate(II)	4ampZnCl
Bis(4-aminopyridinium) tetrabromozincate(II)	4ampZnBr
Bis(4-aminopyridinium) tetraiodozincate(II)	4ampZnI
Catena-(bis(4-aminopyridinium) bis(μ_2-chloro) dichlorocadmium(II) monohydrate)	4ampCdCl·H_2O
Bis(4-aminopyridinium) tetrabromocadmate(II) monohydrate	4ampCdBr·H_2O
Bis(4-aminopyridinium) tetraiodocadmate(II) monohydrate	4ampCdI·H_2O
Bis(4-aminopyridinium) tetrachloromercurate(II) monohydrate	4ampHgCl·H_2O
Bis(4-aminopyridinium) tetrabromomercurate(II) monohydrate	4ampHgBr·H_2O
Bis(4-aminopyridinium) tetraiodomercurate(II) monohydrate	4ampHgI·H_2O

a